AWARD NUMBER: W81XWH-16-1-0400

TITLE: Powering Up Mitichondrial Functions to Treat Mitochondrial Disease

PRINCIPAL INVESTIGATOR: Liming Pei, Ph.D.

CONTRACTING ORGANIZATION: Children's Hospital of Philadelphia
Philadelphia, PA 19104

REPORT DATE: October 2017

TYPE OF REPORT: Annual

PREPARED FOR: U.S. Army Medical Research and Materiel Command
Fort Detrick, Maryland 21702-5012

REPORT DOCUMENTATION PAGE

Form Approved
OMB No. 0704-0188

1. REPORT DATE	2. REPORT TYPE	3. DATES COVERED
October 2017	Annual	30 Sep 2016 - 29 Sep 2017

4. TITLE AND SUBTITLE

Powering Up Mitichondrial Functions to Treat Mitochondrial Disease

5a. CONTRACT NUMBER

5b. GRANT NUMBER
W81XWH-16-1-0400

5c. PROGRAM ELEMENT NUMBER

6. AUTHOR(S)
Douglas C. Wallace, Ph.D. and Liming Pei, Ph.D.

E-Mail: wallaced1@email.chop.edu and peil@email.chop.edu

5d. PROJECT NUMBER

5e. TASK NUMBER

5f. WORK UNIT NUMBER

7. PERFORMING ORGANIZATION NAME(S) AND ADDRESS(ES)
Children's Hospital of Philadelphia, The
3615 Civic Center Blvd
Philadelphia, PA 19104-4318

8. PERFORMING ORGANIZATION REPORT NUMBER

9. SPONSORING / MONITORING AGENCY NAME(S) AND ADDRESS(ES)

U.S. Army Medical Research and Materiel Command
Fort Detrick, Maryland 21702-5012

10. SPONSOR/MONITOR'S ACRONYM(S)

11. SPONSOR/MONITOR'S REPORT NUMBER(S)

12. DISTRIBUTION / AVAILABILITY STATEMENT

Approved for Public Release; Distribution Unlimited

13. SUPPLEMENTARY NOTES

14. ABSTRACT

We proposed that induction of the ERRα/γ signaling pathway can enhance mitochondrial function in both cell and animal models of mitochondrial disease. Our major findings include;

1) We recently compared in detail the different mitochondrial disease animal models (under review in Cell Metabolism). We found that the compound Ant1-/-ND6 mutant mouse model exhibited the earliest and strongest mitochondrial cardiomyopathy phenotype and therefore provided the best therapeutic window for our proposed intervention research strategy.
2) We discovered that GDF15 is a heart-derived hormone whose serum level correlates positively with the severity of mitochondrial cardiomyopathy (recently published with DOD grant support acknowledged), and it can be used as a biomarker in our studies.

15. SUBJECT TERMS
Mitochondria, mitochondrial disease, cardiomyopathy, estrogen-related receptor, transcriptional regulation, mitochondrial biogenesis, signaling, iPSCs, heart disease,

16. SECURITY CLASSIFICATION OF:			17. LIMITATION OF ABSTRACT	18. NUMBER OF PAGES	19a. NAME OF RESPONSIBLE PERSON
a. REPORT	b. ABSTRACT	c. THIS PAGE			USAMRMC
Unclassified	Unclassified	Unclassified	Unclassified	98	19b. TELEPHONE NUMBER *(include area code)*

Table of Contents

Page

1. **INTRODUCTION:** We recently identified that two transcription factors, ERRα and ERRγ, are critical transcriptional regulators of mitochondrial biogenesis and function. Loss of both cardiac ERRα and ERRγ in mice results in severe mitochondrial cardiomyopathy, heart failure and death within the first month of life. This is because that ERRα and ERRγ are both sufficient and required to induce the transcription of many genes crucial for normal mitochondrial function and biogenesis. Overexpression of ERRα and ERRγ increases mitochondrial biogenesis and function in cells. Therefore, we hypothesize that induction of the ERRα/ERRγ signaling pathway (with both genetic and pharmacological approaches) can enhance mitochondrial function in both cells and tissues, thus providing a general approach for treating a broad spectrum of mitochondrial diseases. We propose to test our hypothesis using novel animal models of mitochondrial disease we recently developed.
2. **KEYWORDS:** Mitochondria, mitochondrial disease, cardiomyopathy, estrogen-related receptor, transcriptional regulation, mitochondrial biogenesis, signaling, iPSCs, heart disease
3. **ACCOMPLISHMENTS:**

- **What were the major goals of the project?**

Specific Aim 1 (specified in proposal)	**Timeline**	**% complete**
Major Task 1	**Months**	
Subtask 1: Treat mitochondrial cardiomyopathy in ND6 mutant mice	1-36	30%; **Wallace lab** has generated mice; **Pei lab** is generating virus
Subtask 2: Treat mitochondrial cardiomyopathy in CO1 mutant mice	1-36	30% **Wallace lab** has generated mice; **Pei lab** is generating virus
Milestone(s) Achieved: Successful completion of subtasks 1 and 2.	36	

IACUC Approval	1	100% August 09, 2016 **Wallace and Pei**
Milestone Achieved: HRPO/ACURO Approval	1	100% October 24, 2016 **Wallace and Pei**
Specific Aim 2 (specified in proposal)		
Major Task 2		
Subtask 1: Treat mitochondrial cardiomyopathy in Ant1$_{-/-}$ mice	1-36	30% **Wallace lab** has generated mice; **Pei lab** is generating virus
Milestone(s) Achieved: Successful completion of subtask 1.	36	
Specific Aim 3 (specified in proposal)		
Major Task 3		
Subtask 1: Improve mitochondrial and cellular functions in human Ant1$_{-/-}$ patient iPSCs-derived cardiomyocytes	13-36	10% **Pei lab**
Milestone(s) Achieved: Successful completion of subtask 1	36	

What was accomplished under these goals?

1) Major activities: Overall we are on track to achieve our major research goals.

   - Aims 1 and 2: the **Wallace lab** recently compared in detail the different mitochondrial disease animal models (under review in Cell Metabolism, also see Appendices). Based on these latest results we decided to prioritize our research efforts on the compound Ant1-/-ND6 mutant mouse model, because this model exhibited the earliest and strongest mitochondrial cardiomyopathy phenotype and therefore provided the best therapeutic window for our proposed intervention research strategy. We devoted our

efforts in this model in Year 1. The **Wallace lab** have set up breeding colonies that have generated the first cohort of compound Ant1-/-ND6 mutant mice for our experiments. The **Pei lab** is generating the AAV9-ERRγ virus and the **Pei lab** expects to inject Ant1-/-ND6 mutant mice in the first 2 months of Year 2.

- Aim 3: **Pei lab** has initiated studies in Aim 3 using Ant1-/- iPSC. We have designed and adopted a new gene-editing approach to overexpress ERRγ in control and Ant1-/- iPSC and differentiated cardiomyocytes. This improved approach will also allow us to control the timing and scale of ERRγ overexpression.

2) Specific objectives: In addition to aforementioned progress in major activities, **Pei and Wallace** together have successfully achieved milestones of institute IACUC protocol and ACURO approvals on time.

3) Significant results and key outcomes:

- **Pei lab** has recently discovered that GDF15 is a heart-derived hormone that regulates body growth. Circulating GDF15 level correlates positively with the severity of mitochondrial cardiomyopathy and can be used as a serum biomarker for our mitochondrial disease studies. This work was recently published (see appendices) and the DOD grant support was acknowledged. We will take advantage of these new findings and monitor serum GDF15 level as an additional, more convenient and less invasive method to determine whether mitochondrial cardiomyopathy was ameliorated by ERR overexpression and activation (Aims 1 and 2).
- **Wallace lab** recently compared in detail the different mitochondrial disease animal models (under review in Cell Metabolism, also see Appendices). We found that the compound Ant1-/-ND6 mutant mouse model exhibited the earliest and strongest mitochondrial cardiomyopathy phenotype and therefore provided the best therapeutic window for our proposed intervention research strategy.

- **What opportunities for training and professional development has the project provided?**

- Training: Dr. Zhao has received one-on-one training in iPSC technology and gene editing.
- Professional Development: Dr. **Wallace**, **Pei,** Murdock, Hernandez, and Zhao all attended The TriMAD Regional Symposium in 2016. TriMAD is an annual conference which promotes cross-talk and collaboration between mitochondrial/metabolism and aging-centered research groups at the University of Pittsburgh, Penn State, and the University of Pennsylvania, and CHOP.

- **How were the results disseminated to communities of interest?**
- The **Pei lab** has published a manuscript showing that GDF15 is a heart-derived hormone that regulated body growth. (Wang T, McDonald C, Lupino K, Zhai X, Wilkins BJ, Hakonarson H, Pei L. 2017 EMBO Mol Med 2017 Aug;9(8): 1150-1164, see appendix)
- The **Wallace lab** has a manuscript in review at Cell Metabolism that described the cardiac phenotype of mice with combined mutations in mitochondrial and nuclear genes. (McManus M, Chen HW, Picard M, DeHaas HJ, Potluri P, Leipzig J, Towheed A, Angelin A, Sengupta P, Morrow R, Kauffman B, Vermulst M, Narula J, Wallace DC. 2017 Mitochondrial DNA Variation Dictates Expressivity and Progression of Nuclear DNA Mutations Causing Cardiomyopathy, in review)
- **What do you plan to do during the next reporting period to accomplish the goals?**

We plan to make significant progress in all research aims. For Aims 1 and 2, the **Wallace** lab will continue to breed and genotype the mitochondrial mutant mice needed, and to provide expertise in their care and evaluation. The **Pei** hopes to complete injecting AAV9-ERR to all Ant1-/-ND6 mutant mice, and the **Pei lab** will monitor their cardiac functions periodically as we proposed. For Aim 3 the **Pei lab** hopes to complete establishing the ERR overexpressing Ant1-/- iPSC and differentiated cardiomyocytes, and the **Pei lab** and **Wallace lab** will proceed with evaluating all different aspects of their mitochondrial and cardiac functions as we proposed.

4. **IMPACT:**

- **What was the impact on the development of the principal discipline(s) of the project?**

The **Pei lab** recently discovered that GDF15 is a heart-derived hormone that regulates body growth. Circulating GDF15 level correlates positively with the severity of mitochondrial cardiomyopathy and can be used as a serum biomarker for our

mitochondrial disease studies. This work was recently published (see appendices) and the DOD grant support was acknowledged. We will take advantage of these new findings and monitor serum GDF15 level as an additional, more convenient and less invasive method to determine whether mitochondrial cardiomyopathy was ameliorated by ERR overexpression and activation (Aims 1 and 2).

- **What was the impact on other disciplines?**

  The **Pei lab** recently discovered that GDF15 is a heart-derived hormone that regulates body growth. Pediatric heart disease induces GDF15 synthesis and secretion by cardiomyocytes. Circulating GDF15 in turn acts on the liver to inhibit growth hormone (GH) signaling and body growth. We demonstrate that blocking cardiomyocyte production of GDF15 normalizes circulating GDF15 level and restores liver GH signaling, establishing GDF15 as a bona fide heart-derived hormone that regulates pediatric body growth. Importantly, plasma GDF15 is further increased in children with concomitant heart disease and failure to thrive (FTT). Together these studies reveal a new endocrine mechanism by which the heart coordinates cardiac function and body growth. Our results also provide a potential mechanism for the well-established clinical observation that children with heart diseases often develop FTT. This work was recently published (see appendices) and the DOD grant support was acknowledged.

- **What was the impact on technology transfer?**
  - Nothing to Report
- **What was the impact on society beyond science and technology?**
  - Nothing to report

5. **CHANGES/PROBLEMS:**

- **Changes in approach and reasons for change**
- As detailed above, we have prioritized the compound Ant1-/-ND6 mutant mouse model based on our latest research results. This model exhibited the earliest and strongest mitochondrial cardiomyopathy phenotype and therefore provided the best therapeutic window for our proposed intervention research strategy. We devoted our efforts in this model in Year 1 and moving forward.
- **Changes that had a significant impact on expenditures**
- Nothing to report
- **Significant changes in use or care of human subjects, vertebrate animals, biohazards, and/or select agents**

- Nothing to report
- **Significant changes in use or care of human subjects**
- Nothing to report
- **Significant changes in use or care of vertebrate animals.**
- Nothing to report
- **Significant changes in use of biohazards and/or select agents**
- Nothing to report

6. **PRODUCTS:**

- **Publications, conference papers, and presentations**
- **Journal publications.**

Wang T, Liu J, McDonald, C, Lupino K, Zhai X, Wilkins BJ, Hakonarson H, **Pei L** (2017). GDF15 is a heart-derived hormone that regulates body growth. EMBO Molecular Medicine *9*, 1150-1164. PMID: 28572090. PMCID: PMC5538424. (published, DOD support acknowledged).

McManus MJ, Chen HW, Picard M, Potluri P, Leipzig J, Towheed A, Angelin A, Sengupta P, Morrow R, Kauffman B, Vermulst M, Narula J, Wallace DC. (in revision) Mitochondrial DNA Variation Dictates Expressivity and Progession of Nuclear DNA Mutations Causing Cardiomyopathy. Cell Metabolism in revision

- **Books or other non-periodical, one-time publications.** Nothing to report
- **Other publications, conference papers, and presentations.**
- **Liming Pei presentations**

*10/2016 The 6th Regional Translational Research in Mitochondrial, Aging, and Disease (TriMAD) Symposium. Philadelphia, PA. "Listen to your heart"
*05/2017 Keystone Symposia—Mitochondria, Metabolism and Heart. Santa Fe, NM. "A heart-derived hormone that regulates body growth"
*05/2017 Cold Spring Harbor Laboratory meetings—Mechanisms of Metabolic Signaling. Cold Spring Harbor, NY.
09/2017 Inaugural Canadian Mitochondrial Disease Conference Toronto, Canada. "Regulation of mitochondrial function by nuclear receptors"

10/2017 Institute for Diabetes and Obesity (IDO), Helmholtz Zentrum München, Munich, Germany "Listen to your heart – a heart-derived hormone that regulates body growth"

Doug Wallace presentations

Oct, 2016 "A Mitochondria Etiology of Complex Diseases", The 19th Annual John B. Little Symposium – Theme: "Using Innovative Approaches in Stress Response Research", Boston, MA

Nov, 2016 "A Mitochondria Etiology of Complex Diseases", The 11th Annual International Conference on Genomics, Shenzhen, China

Nov, 2016 "A Mitochondria Etiology of Complex Diseases", The Seminars in Neuroscience: Brain, Mind, and Society Lecturer Series, Vanderbilt University, Nashville, TX

Nov, 2016 "A Mitochondria Etiology of Complex Diseases", University of California, San Francisco, San Francisco, CA

Dec, 2016 "A Mitochondrial Etiology of Complex Diseases", 2nd Conference Functional Genomics and Beyond: Nature via Nurture, Qatar National Convention Center, Doha, Qatar

Jan, 2017 "A Mitochondrial Etiology of Ophthalmological Diseases", Basic Science Course in Ophthalmology at Columbia University, New York, NY

Feb, 2017 "A Mitochondrial Etiology of Common Complex Diseases", Wayne State Seminar, Detroit, MI

Feb, 2017 "A Mitochondria Etiology of Complex Diseases", Temple University School of Medicine, Philadelphia, PA

Mar, 2017 "A Mitochondria Etiology of Complex Diseases", Oregon Health & Science University, Combined Basic Science Seminar, Portland, OR

Mar, 2017 "A Mitochondria Etiology of Complex Diseases", East Carolina Diabetes and Obesity Institute, Greenville, NC

May, 2017 "Human Origins and Complex Diseases: A Mitochondrial Perspective", The 2017 Franklin Institute Life Science Symposium 'Mitochondria: Our Origins – Our Diseases', The College of Physicians of Philadelphia, PA

May, 2017 "A Mitochondrial Etiology of Common Complex Diseases", The Florida Hospital Research Forum, Orlando, FL

May, 2017 "A Mitochondrial Etiology of Common Complex Diseases", Clinical and Translational Science Institute (CTSI) Seminar at UCLA Luskin, Los Angeles, CA

June, 2017 "Mitochondrial DNA Variation: Its Origins and Impact on Health", 27th Marabou Nutrition Conference, Stockholm, Sweden

June, 2017 "Mitochondrial Physiology and Molecular Genetics of Human Origins and Diseases", MBL Physiology Lecture, Woods Hole, MA

July, 2017 "A Mitochondrial Eitology of Neuropsychiatric Disorders", Collaborate2Cure, Philadelphia, PA

Aug, 2017 "Mitochondrial in Human Evolution and Disease", University of Pennsylvania Perelman School of Medicine, Undergraduate Student Scholar Programs Symposium, Philadelphia, PA

Sept, 2017 "Mitochondrial DNA Variation in Human Evolution and Disease", Mitochondrial Evolutionary Genomics Conference Keynote Speaker, Ein Gedi, Israel

Sep, 2017 "The Mitochondrion: Our Origins – Our Diseases", 2017 Dr. Paul Janssen Award Symposium, New York City, NY

Sep, 2017 "A Mitochondrial Etiology of Metabolic and Degenerative Diseases", The Canada Mitochondrial Network and MitoCanada Foundation, Toronto, Canada

Oct, 2017 "The Mitochondrion: Our Origins – Our Diseases", Genetics and Complex Diseases, Harvard Chan School, Boston, MA

Oct, 2017 "A Mitochondrial Etiology of Complex Diseases", University of Pennsylvania Perelman School of Medicine, Department of Cardiovascular Institute Seminar Series, Philadelphia, PA

Oct, 2017 "Mitochondria: Our Origins-Our Diseases", Cornell University, Ithaca, NY

Oct, 2017 "Our Origins-Our Diseases: The Mitochondrial Perspective", Golden Sages Lecture, Bryn Mawr College, Bryn, Mawr, PA

Oct, 2017 "A Mitochondrial Etiology of Complex Diseases and Associated Inflammation", University of Pennsylvania Perelman School of Medicine, Penn Transplant Institute Research Lecture, Philadelphia, PA

Oct, 2017 "Mitochondria: Our Origins-Our Diseases", the 12th Annual International Conference in Genomics, Shenzhen, China

Nov, 2017 "Mitochondrial Variation in Metabolic and Degenerative Diseases, Cancer, & Aging", University of Chicago Cancer Biology Seminar Series, Chicago, IL

Nov, 2017 "Mitochondrial Genetic Variation in Human Evolution and Disease", Cleveland Clinic, Cleveland, OH

- **Website(s) or other Internet site(s)**

  www.mitomap.org

MITOMAP reports published and unpublished data on human mitochondrial DNA variation. Currently our variant tables report frequencies from 30589 human mitochondrial DNA sequences.

- **Technologies or techniques**

  nothing to report
- **Inventions, patent applications, and/or licenses**

  nothing to report
- **Other Products**

  nothing to report

7. **PARTICIPANTS & OTHER COLLABORATING ORGANIZATIONS**

- **What individuals have worked on the project?**

Name:	***Liming Pei, Ph.D.***
Project Role:	*No change*
Name:	***Juanjuan Zhao, Ph.D.***
Project Role:	*Postdoctoral fellow*
Nearest person month worked:	*11*
Contribution to Project:	*Dr Zhao has been responsible for designing and producing AAV9-ERR viruses and evaluate cardiac function both in animal (Aims 1 and 2) and cell (Aim 3) models of mitochondrial disease.*
Name:	***Katherine Lupino***
Project Role:	*Research technician*
Nearest person month worked:	*10*
Contribution to Project:	*Ms Lupino has provided technical support in maintain mouse colonies and cell cultures. Miss Lupino replaced Caitlin McDonald*

Name:	***Jian Liu, PhD***
Project Role:	*Postdoctoral fellow*
Nearest person month worked:	*1*
Contribution to Project:	*Dr. Jian Liu has been responsible for working with and assisting Dr. Juanjuan Zhao in designing and producing AAV9-ERR viruses and evaluate cardiac function both in animal (Aims 1 and 2) and cell (Aim 3) models of mitochondrial disease.*

- **Has there been a change in the active other support of the PD/PI(s) or senior/key personnel since the last reporting period?** See below

Research Support Liming Pei

Current Support

WW Smith Charitable Trust #H1407

Liming Pei (PI) 07/01/2015-06/30/2016 (10% effort)

Improve mitochondrial dynamics to treat cardiomyopathy

The major goal of this project is to conduct preliminary studies to explore whether improving mitochondrial dynamics can reverse mitochondrial dysfunction common in cardiomyopathy.

Role: Principal Investigator

This grant ended

NIH P30 DK019525

Mitchell Lazar (PI) 04/01/2015-03/31/2016 (5% effort)

CNS ERRγ in regulating energy balance in obesity and diabetes

The major goal of this project is to study how hypothalamic ERRγ impacts whole body energy balance and obesity.

Role: Principal Investigator on this subaward

This grant ended

NIH RO1 HL127110

Liming Pei (PI) 04/01/2016-03/31/2021 (40% effort)

Coordinated regulation of cardiac metabolism and functions by estrogen-related receptors

The major goal of this project is to study nuclear receptors ERRα and ERRγ in coordinating cardiac metabolism and functions.

Role: Principal Investigator

Note: There is no overlap between this NIH application and my FY15 DoD CDMRP PRMRP application.

This grant started

PR150585

Pei and Wallace Partner PI's 09/30/16 – 09/29/18 (35% effort)

Department of Defense

Powering Up Mitochondrial Function to Treat Mitochondrial Disease

This project is to determine whether induction of the ERR pathway can be employed as a novel approach to treat mitochondrial disease in a preclinical model.

Role: Co-PI

There is no scientific or budgetary overlap

What other organizations were involved as partners?

Nothing to Report

Published online: June 1, 2017

Research Article

SOURCE DATA | TRANSPARENT PROCESS | OPEN ACCESS

EMBO Molecular Medicine

GDF15 is a heart-derived hormone that regulates body growth

Ting Wang[1,2,†,‡], Jian Liu[1,2,†], Caitlin McDonald[1,2], Katherine Lupino[1,2], Xiandun Zhai[1,2,3], Benjamin J Wilkins[2,4], Hakon Hakonarson[5,6] & Liming Pei[1,2,4,*]

Abstract

The endocrine system is crucial for maintaining whole-body homeostasis. Little is known regarding endocrine hormones secreted by the heart other than atrial/brain natriuretic peptides discovered over 30 years ago. Here, we identify growth differentiation factor 15 (GDF15) as a heart-derived hormone that regulates body growth. We show that pediatric heart disease induces GDF15 synthesis and secretion by cardiomyocytes. Circulating GDF15 in turn acts on the liver to inhibit growth hormone (GH) signaling and body growth. We demonstrate that blocking cardiomyocyte production of GDF15 normalizes circulating GDF15 level and restores liver GH signaling, establishing GDF15 as a *bona fide* heart-derived hormone that regulates pediatric body growth. Importantly, plasma GDF15 is further increased in children with concomitant heart disease and failure to thrive (FTT). Together these studies reveal a new endocrine mechanism by which the heart coordinates cardiac function and body growth. Our results also provide a potential mechanism for the well-established clinical observation that children with heart diseases often develop FTT.

Keywords body growth; failure to thrive; GDF15; heart disease; heart-derived hormone

Subject Categories Cardiovascular System; Metabolism

DOI 10.15252/emmm.201707604 | Received 18 January 2017 | Revised 6 May 2017 | Accepted 11 May 2017

Introduction

A central question in physiology is how different organs communicate with each other to maintain whole-organism homeostasis. The classical endocrine system is well documented for its essential role in inter-organ communication. In addition, research in the past 20 years has revealed that certain non-glandular organs including adipose tissue, liver, skeletal muscle, intestine, and bone have secondary endocrine functions and secrete various hormones that regulate whole-body metabolism (Zhang *et al*, 1994; Deng & Scherer, 2010; Potthoff *et al*, 2012; Stefan & Haring, 2013; Liu *et al*, 2014; Wang *et al*, 2015a; Gribble & Reimann, 2016; Karsenty & Olson, 2016). In contrast, little is known regarding heart-derived hormones besides atrial natriuretic peptide (ANP) and brain natriuretic peptide (BNP) discovered more than 30 years ago (de Bold, 1985; Frohlich, 1985; Karsenty & Olson, 2016). Cardiac synthesis and secretion of ANP and BNP are increased in various heart diseases, and plasma level of BNP is used clinically to diagnose heart failure (Yancy *et al*, 2013). ANP and BNP in turn signal to target tissues such as kidneys and vascular smooth muscles and increase natriuresis (excretion of sodium in the urine) and decrease blood pressure, reducing the burden on the distressed heart. Identification of new heart-derived hormones and study of their biological functions will significantly advance our understanding of cardiac biology and whole-organism homeostasis.

Failure to thrive refers to poor physical growth of children, typically evaluated by height and body weight gain. FTT is seen in 5–10% of children in the U.S. primary care settings (Cole & Lanham, 2011). It is well established that pediatric heart diseases such as congenital heart disease often cause FTT, but the underlying mechanism is poorly understood (Menon & Poskitt, 1985; Poskitt, 1993; Forchielli *et al*, 1994; Nydegger & Bines, 2006). Intriguingly, FTT associated with pediatric heart disease often features lower circulating insulin-like growth factor 1 (IGF1) and IGF binding protein 3 (IGFBP3) levels (Barton *et al*, 1996; Dinleyici *et al*, 2007; Surmeli-Onay *et al*, 2011; Peng *et al*, 2013). GH-IGF1 signaling is a dominant mechanism regulating postnatal mammalian growth (Pilecka *et al*, 2007; Baik *et al*, 2011; Savage *et al*, 2011; Rotwein, 2012; Milman *et al*, 2016). GH secreted from the pituitary signals to the liver to stimulate the production of

1 Center for Mitochondrial and Epigenomic Medicine, Children's Hospital of Philadelphia, Philadelphia, PA, USA
2 Department of Pathology and Laboratory Medicine, Children's Hospital of Philadelphia, Philadelphia, PA, USA
3 Institute of Forensic Medicine, Henan University of Science and Technology, Luoyang, Henan, China
4 Department of Pathology and Laboratory Medicine, Perelman School of Medicine, University of Pennsylvania, Philadelphia, PA, USA
5 Center for Applied Genomics, Children's Hospital of Philadelphia, Philadelphia, PA, USA
6 Department of Pediatrics, Perelman School of Medicine, University of Pennsylvania, Philadelphia, PA, USA
*Corresponding author. Tel: +1 267 425 2118; E-mail: lpei@mail.med.upenn.edu
†These authors contributed equally to this work
‡Present address: Institute of Cell Metabolism, Shanghai Key Laboratory of Pancreatic Disease, Shanghai General Hospital, School of Medicine, Shanghai Jiaotong University, Shanghai, China

IGF1, IGFBP3, and IGFBP acid-labile subunit (IGFALS) via the JAK2-STAT5 pathway. Circulating IGF1 forms a ternary complex with IGFBP3 and IGFALS and is a major mediator of GH's effect on mammalian postnatal body growth (Czech, 1989; Pilecka *et al*, 2007; Baik *et al*, 2011; Savage *et al*, 2011; Rotwein, 2012). Mutations of almost every gene in this pathway cause severe to mild growth inhibition in humans and animals.

GDF15 (also known as MIC-1, NAG-1, PLAB, or PTGFB) is a distant member of the transforming growth factor beta (TGFβ) family of secreted proteins with pleiotropic functions (Bootcov *et al*, 1997; Yokoyama-Kobayashi *et al*, 1997; Paralkar *et al*, 1998; Bottner *et al*, 1999; Fairlie *et al*, 1999; Baek *et al*, 2001; Johnen *et al*, 2007; Unsicker *et al*, 2013). GDF15 has been shown to have a local cardioprotective role (Kempf *et al*, 2006; Xu *et al*, 2006), presumably due to its autocrine/paracrine function. Plasma GDF15 was found elevated in various heart diseases in many independent biomarker studies and in animal models (Wollert & Kempf, 2012; Baggen *et al*, 2017; Wollert *et al*, 2017). However, the organ source and biological function of increased circulating GDF15 in heart disease are little known.

Estrogen-related receptor alpha (ERRα) and gamma (ERRγ) are important transcriptional regulators of cellular metabolism especially mitochondrial functions (Huss & Kelly, 2005; Giguere, 2008; Villena & Kralli, 2008). Using cardiomyocyte-specific Myh6-Cre, we recently generated mice lacking *ERRα* and cardiac *ERRγ* (αKOγKO mice; genotype is $ERR\alpha^{-/-}ERR\gamma^{flox/flox}Myh6\text{-}Cre^{+}$). Control mice and those lacking *ERRα* or cardiac *ERRγ* alone exhibited normal cardiac metabolism and function, overall health and survival (Wang *et al*, 2015b). In contrast, αKOγKO mice developed lethal dilated cardiomyopathy and heart failure soon after birth (median life span of 14–15 days), featuring metabolic, contractile, and conduction dysfunctions. These results demonstrated that ERRα and ERRγ are essential for maintaining normal cardiac metabolism and function. Intriguingly, although loss of both *ERRα* and *ERRγ* occurred exclusively in cardiomyocytes (Wang *et al*, 2015b), αKOγKO mice exhibited secondary FTT as often observed in children with pediatric heart disease. Using these αKOγKO mice as a model of primary pediatric cardiomyopathy with secondary FTT, here we identify GDF15 as a heart-derived hormone that inhibits pediatric body growth. We show that GDF15 is both sufficient and required for inhibition of liver GH signaling in FTT associated with pediatric heart disease. In addition, we find that children with concomitant heart disease and FTT have elevated plasma GDF15. These results uncover a new endocrine mechanism by which the heart coordinates cardiac function and body growth. Our results also reveal a potential underlying mechanism of FTT associated with pediatric heart disease.

Results

Cardiac αKOγKO mice exhibit FTT with impaired liver GH signaling

Both male and female αKOγKO mice were significantly slower at gaining weight (slope of the weight curve) and were visibly smaller and shorter (height) from 5 to 7 days of age (Fig 1A and B, and data not shown), despite that weighing similar to controls around birth suggests little preterm growth defects. We hereafter chose body weight over bone or body length to determine body growth because body weight can be more accurately measured (0.01 gram precision with digital scale). Most internal organs except the heart of αKOγKO mice showed decreased absolute weight but maintained same relative weight (Appendix Fig S1A), indicating FTT-like whole-body growth inhibition rather than organ-specific developmental defects. We therefore used αKOγKO mice as a model to investigate the mechanism of FTT associated with pediatric heart disease.

The reduced body growth (about 30% less body weight) in αKOγKO mice is similar to that seen in animal and humans with defective GH-IGF1 signaling (Cui *et al*, 2007; Baik *et al*, 2011; Savage *et al*, 2011; Rotwein, 2012). We therefore measured their plasma GH and IGF1 concentrations. We found that αKOγKO mice had normal plasma GH (Fig 1C and D). In addition, expression of *Gh* in the pituitary and GH-releasing hormone (*Ghrh*) in the hypothalamus remained unchanged, indicating normal GH production and secretion (Appendix Fig S1B). Hypothalamic expression of appetite-regulating neuropeptide Y (*Npy*) and pro-opiomelanocortin (*Pomc*) was not changed either (Appendix Fig S1B). In contrast, plasma IGF1 level in αKOγKO mice was significantly decreased across multiple ages and was about 70% lower than controls by 16 days of age (Fig 1C and D). Normal plasma GH but significantly decreased IGF1 suggests that impaired liver GH signaling underlies FTT in αKOγKO mice. We therefore next examined the key components of liver GH signaling in αKOγKO mice. STAT5 phosphorylation was significantly reduced in αKOγKO mouse livers (Fig 1E and F, and Appendix Fig S1C) while upstream JAK2 phosphorylation remained unchanged (Fig 1F). Moreover, expression of STAT5 target genes *Igf1*, *Igfbp3,* and *Igfals* was all significantly decreased in αKOγKO mouse livers (Fig 1G). These result in reduced production and secretion of IGFBP3 (Fig 1H) in addition to IGF1 (Fig 1C and D). These results demonstrate that liver GH resistance underlies FTT in αKOγKO mice.

Circulating factors mediate impaired liver GH signaling in cardiac αKOγKO mice

In our αKOγKO mouse model, loss of both *ERRα* and *ERRγ* is restricted to cardiomyocytes, which was confirmed by unchanged *ERRγ* expression in every other tissue examined (Wang *et al*, 2015b). In addition, only αKOγKO mice exhibit primary pediatric cardiomyopathy and secondary FTT, while control littermates including *ERRα* KO mice retain normal cardiac function and liver GH signaling (Fig 1C–E and G). We asked how primary cardiac genetic defects affected liver GH signaling and caused secondary FTT. We considered the possibility that the heart was communicating its functional status to the liver via nervous or endocrine mechanisms. Unfortunately, the severe cardiomyopathy and early postnatal lethality (median life span of 14–15 days) in αKOγKO mice prevented us from using surgical procedures such as vagectomy or parabiosis to investigate these possibilities. As an alternative approach to test a potential endocrine mechanism, we treated wild-type (WT) mouse primary hepatocytes with plasma from αKOγKO or control littermate αHetγWT mice. Although αKOγKO mouse plasma contained the same amount of GH (Fig 1C and D, and Appendix Fig S2), it induced significantly less STAT5 phosphorylation in WT hepatocytes (Fig 2A), recapitulating *in vivo* observations (Fig 1E and F, and Appendix Fig S1C). This suggests that the

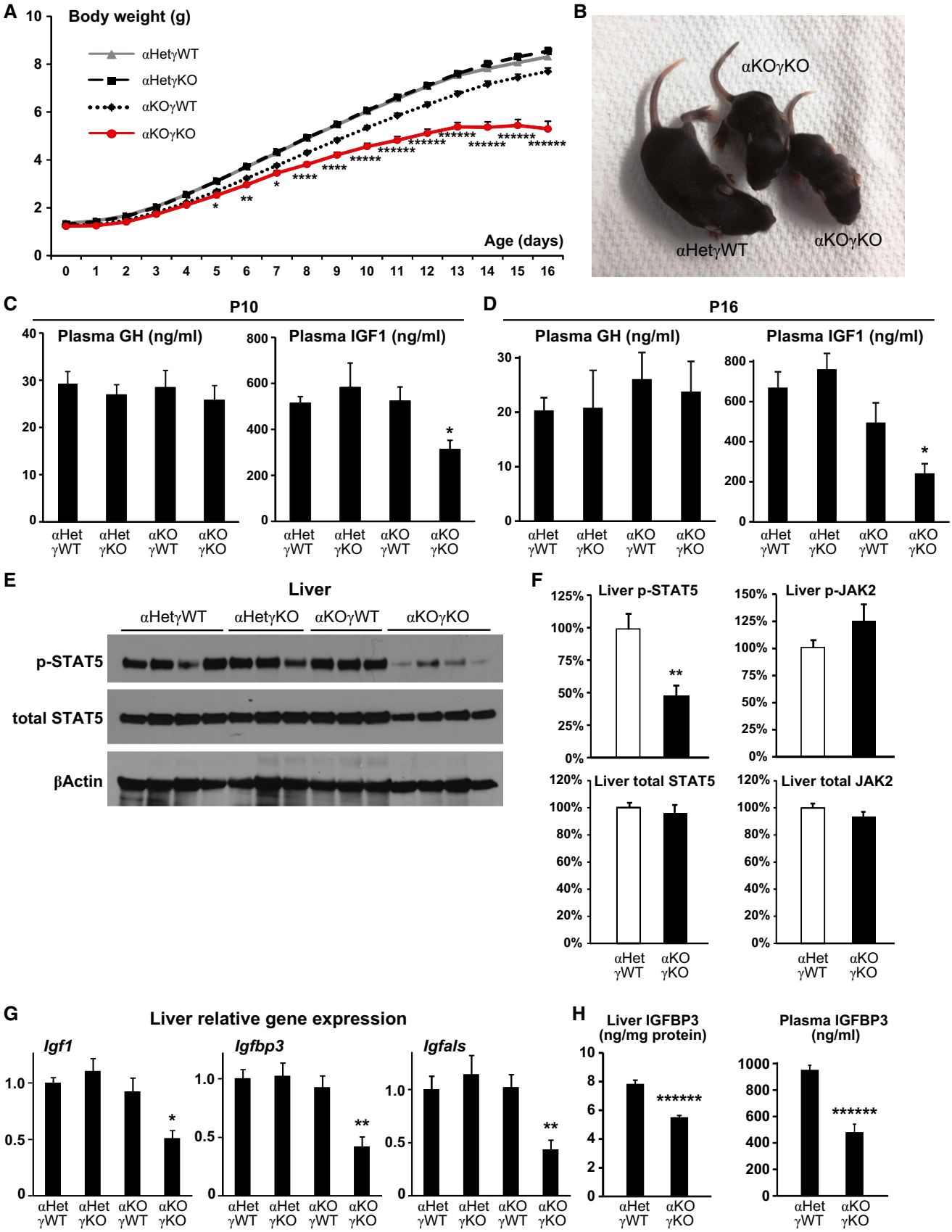
A
Body weight (g)
αHetγWT
αHetγKO
αKOγWT
αKOγKO
Age (days)
B
αKOγKO
αHetγWT
αKOγKO
C
P10
Plasma GH (ng/ml)
Plasma IGF1 (ng/ml)
D
P16
Plasma GH (ng/ml)
Plasma IGF1 (ng/ml)
αHet γWT
αHet γKO
αKO γWT
αKO γKO
E
Liver
αHetγWT
αHetγKO
αKOγWT
αKOγKO
p-STAT5
total STAT5
βActin
F
Liver p-STAT5
Liver p-JAK2
Liver total STAT5
Liver total JAK2
G
Liver relative gene expression
Igf1
Igfbp3
Igfals
H
Liver IGFBP3 (ng/mg protein)
Plasma IGFBP3 (ng/ml)

Figure 1.

Figure 1. Cardiac αKOγKO mice exhibit FTT with impaired liver GH signaling.

A Daily body weight of αKOγKO and littermate control mice. n = 55–145 mice per group with both genders included.

B Representative picture of 10-day-old αKOγKO and littermate control αHetγWT mice.

C, D Plasma GH and IGF1 concentrations in 10- (C, n = 7–10 mice per group) and 16-day-old mice (D, n = 9–11 mice per group) measured by ELISA.

E Phosphorylated (Tyr694) and total STAT5 in 10-day-old mouse livers determined by Western blot (n = 3–4 mice per group). β-Actin serves as a loading control.

F Relative levels of phosphorylated and total STAT5 and JAK2 in 13-day-old mouse livers (normalized to total protein content of individual mouse liver) were quantified by ELISA (n = 13 mice per group).

G Expression of STAT5 target genes *Igf1*, *Igfbp3*, and *Igfals* in 10-day-old mouse livers measured by qPCR (n = 7–8 mice per group).

H Liver (normalized to total protein content, n = 15–16 mice per group) and plasma (n = 9–10 mice per group) IGFBP3 concentrations in 13-day-old mice measured by ELISA.

Data information: *P < 0.05, **P < 0.01, ****P < 0.0001, *****P < 0.00001, and ******P < 0.000001 between αKOγKO and all other control genotypes by t-test. All values are mean + s.e.m.
Source data are available online for this figure.

αKOγKO mouse plasma contains altered amount of specific factors that regulate endogenous hepatocyte GH signaling.

To determine the chemical nature of such circulating factors, we used size fractionation to separate plasma into high molecular weight (HMW, > 3 KD) and low molecular weight (LMW, < 3 KD) fractions. We then recombined different HMW and LMW fractions of the littermate control αHetγWT and αKOγKO mouse plasma to treat WT mouse hepatocytes (Fig 2B). Reconstituted αKOγKO HMW and LMW fractions recapitulated its inhibitory effect on GH signaling. Intriguingly, αKOγKO HMW and αHetγWT LMW combination also inhibited STAT5 phosphorylation (behaving as the αKOγKO plasma). In contrast, αHetγWT HMW and αKOγKO LMW combination had no effect on STAT5 phosphorylation (behaving as the αHetγWT plasma). This result suggests that the putative GH signaling regulating factors exist in the HMW fraction of αKOγKO mouse plasma and are therefore most likely proteins rather than small chemicals or cellular metabolites.

GDF15 is a candidate heart-derived hormone that inhibits liver GH signaling and body growth

We employed two independent, unbiased strategies aiming to identify such heart-derived circulating factors that impact pediatric body growth. We used SOMAscan, an aptamer-based multiplexed proteomic platform which measures relative levels of more than 1,000 plasma proteins at one time (Gold *et al*, 2010), to identify proteins with altered plasma concentrations in the αKOγKO mice (Appendix Table S1). IGF1 appeared as the top decreased plasma protein in the SOMAscan assay, validating the power of this approach. To take account of proteins not covered by SOMAscan, we also performed RNA-Seq in αKOγKO and littermate control mouse hearts and identified genes with altered cardiac expression that encode secreted proteins (Chen *et al*, 2005; Appendix Table S2). We combined the candidates obtained from both approaches and focused on genes that showed significantly higher expression in the

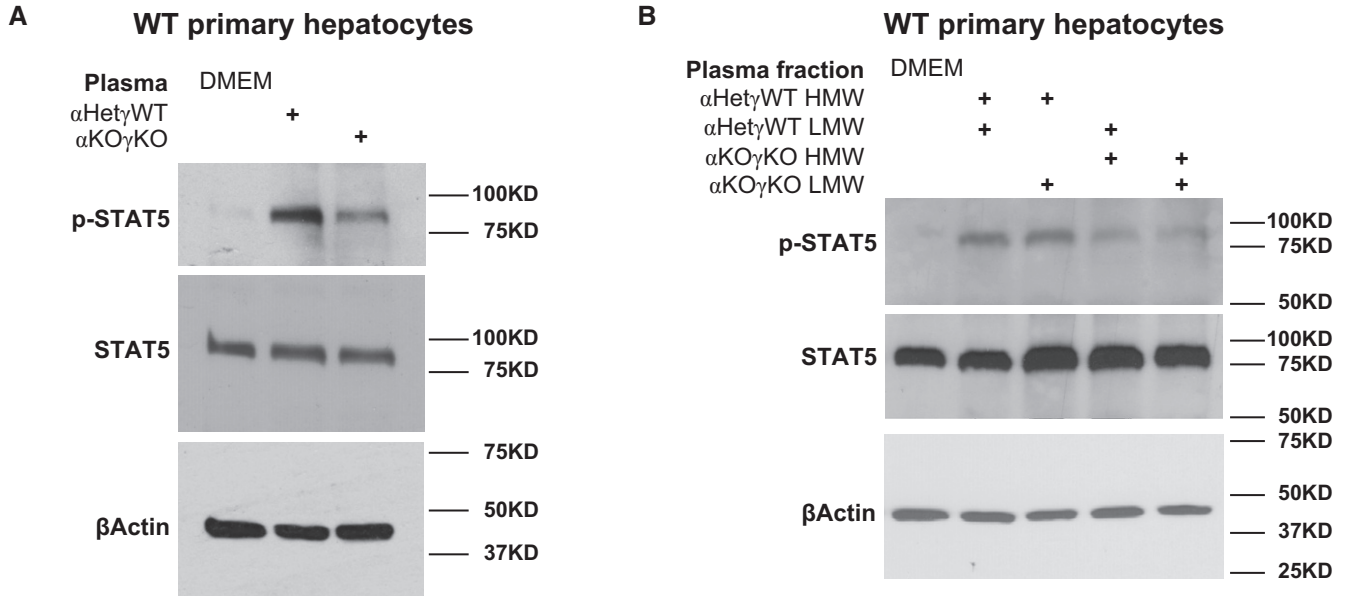

Figure 2. Circulating factors mediate impaired liver GH signaling in cardiac αKOγKO mice.

A, B Phosphorylated and total STAT5 in WT mouse primary hepatocytes treated with DMEM (control), 50% plasma in DMEM (A), or 50% plasma fractions in DMEM (B) for 1 h were determined by Western blot. β-Actin is used as loading control in all Western blots.

Source data are available online for this figure.

heart than in other tissues such as the liver (by qRT–PCR). In case of proteins with similar sequence/structure/functions such as BNP and ANP, we chose to prioritize testing one of them (e.g., BNP) first. With these criteria, we came up with eight prioritized candidates (Fig 3A). We then tested whether any of them impacted liver GH signaling in young WT mice *in vivo*, using a 96-well ELISA-based screen with plasma IGF1 as the readout. Only GDF15 significantly altered plasma IGF1 level, resulting in about 30% decrease 2 days after injection (Fig 3A). To determine whether GDF15 impacts postnatal body growth by interfering with liver GH signaling, we next performed daily GDF15 injections to WT mice from 3 days of age and monitored their daily body growth (Appendix Fig S3A). GDF15 was found to inhibit liver STAT5 phosphorylation without altering JAK2 phosphorylation (Fig 3B), decrease liver expression of STAT5 target genes *Igf1*, *Igfbp3,* and *Igfals* (Fig 3C), and reduce plasma IGF1 and IGFBP3 concentrations without affecting GH level (Fig 3D–F). Importantly, GDF15 consistently reduced body weight gain in multiple independent cohorts of WT mice as the result of this constant inhibition of liver GH signaling (Fig 3G). Individual organs such as kidneys were proportionally lighter with relative weight remaining constant (Appendix Fig S3B). GDF15 did not change hypothalamic *Npy* and *Pomc* expression (Appendix Fig S3C), suggesting that this growth-inhibiting effect is distinct from its appetite-suppressing function seen in adult mice (Johnen *et al*, 2007). This almost complete molecular and phenotypic recapitulation of the αKOγKO mice (Fig 1 and Appendix Fig S1) strongly suggests that GDF15 is a major mediator of the FTT phenotype in αKOγKO mice. In contrast, injection of BNP did not alter liver GH signaling, plasma IGF1 level, or body weight in WT mice (Appendix Fig S3D–G).

To determine whether GDF15 directly acts on the liver to alter GH signaling, we next tested whether GDF15 can inhibit GH signaling in primary hepatocytes from young WT mice. We found consistently that GDF15 inhibits hepatocyte GH signaling in a dose-dependent manner (Fig 3H). In particular, pathological concentration of GDF15 seen in the αKOγKO mouse plasma (2 ng/ml, see Fig 4C) was found to inhibit signaling of physiological level of GH based on STAT5 phosphorylation. The total cellular protein tyrosine phosphatase (PTP) activity remained unchanged (Appendix Fig S3H), suggesting that GDF15 does not affect the activity of potential PTPs known to deactivate STAT5 under these conditions (Chen *et al*, 2003; Rigacci *et al*, 2003). Together these results suggest that GDF15 directly acts on hepatocytes to inhibit GH signaling.

GDF15 is increased in pediatric heart disease and is synthesized in cardiomyocytes

GDF15 is believed to be synthesized in the cell as a pro-protein with the C-terminal mature peptide secreted (Appendix Fig S4A; Bauskin *et al*, 2000). We found that cardiac *Gdf15* expression in αKOγKO mice was similar to control at 3 days of age, but continued to quickly rise with the development of cardiomyopathy and reached over 30-fold by 13 days of age over control mice (Fig 4A). This resulted in a significant increase of GDF15 protein in both the heart and the plasma in a similar kinetic pattern (Fig 4B–D and Appendix Fig S4A). Immunohistochemistry further showed that while completely absent in the control mouse hearts, GDF15 protein is abundant in the αKOγKO mouse hearts (Fig 4D). Coimmunostaining with cardiomyocyte marker troponin I allowing muscle fiber visualization revealed that GDF15 was located in the cytoplasm of cardiomyocytes and did not appear to be present in any other cell types of the heart (Fig 4E).

GDF15 is a *bona fide* heart-derived hormone that regulates liver GH signaling

These findings extend beyond the αKOγKO mouse model and have broad implications. Plasma GDF15 level was reported to be elevated in many forms of adult heart disease in both patients and animal models and was therefore recently proposed as an independent biomarker for heart diseases (Wollert & Kempf, 2012; Baggen *et al*, 2017; Wollert *et al*, 2017). However, the exact organ source and biological function of increased circulating GDF15 in heart disease remain little understood. To determine whether GDF15 is essential in mediating body growth inhibition in αKOγKO mice, we first tested this *in vitro* using GDF15 antibody to specifically deplete GDF15 in control and αKOγKO mouse plasma (Appendix Fig S4B). GDF15-depleted αKOγKO plasma largely lost its ability to inhibit GH signaling in primary hepatocytes (Appendix Fig S4C). This result suggests that GDF15 is the major GH-inhibiting factor in αKOγKO plasma. We next aimed to determine whether cardiac-derived GDF15 is critical in inhibiting liver GH signaling *in vivo*. We designed an AAV9-*Gdf15* shRNA vector to specifically knockdown *Gdf15* expression in the mouse heart (Fig 5A). Pericardial injection of AAV9 has been shown to achieve stable and relatively cardiac-specific expression of transgenes compared to other AAV serotypes (Bish *et al*, 2008). Since *Gdf15* is exclusively expressed in αKOγKO mouse cardiomyocytes (Fig 4E), we designed the AAV9 vector to ensure that *Gdf15* shRNA is solely expressed in αKOγKO mouse cardiomyocytes (Myh6-Cre^{+}) but not elsewhere (Myh6-Cre^{-}) (Fig 5A). The specificity of our strategy was experimentally confirmed as non-cardiac expression of *Gdf15* was not affected (Appendix Fig S4D). One week after pericardial injection of AAV9-shRNA, we found that cardiomyocyte-specific knockdown of *Gdf15* almost completely normalized cardiac *Gdf15* expression and plasma GDF15 concentration (Fig 5B and C). Importantly, the development of lethal cardiomyopathy in αKOγKO mice was little affected by cardiac *Gdf15* knockdown based on cardiac histology and cardiomyopathy marker *Bnp* expression (Fig 5D). These results provide definitive evidence that the elevated plasma GDF15 is exclusively produced by cardiomyocytes. In addition, normalization of circulating GDF15 in αKOγKO mice restored liver GH signaling (significantly increased STAT5 phosphorylation, Fig 5E) and doubled circulating IGF1 (Fig 5F) without affecting circulating GH levels (Fig 5G). Although the early lethality of αKOγKO mice (regardless of receiving control or *Gdf15* shRNA due to heart failure; Wang *et al*, 2015b) prevented us from keeping monitoring their body weight following this molecular reversal of liver GH inhibition, these results demonstrate that GDF15 is a *bona fide* heart-derived hormone that regulates liver GH signaling.

Plasma GDF15 is elevated in children with heart disease and FTT

Last, to substantiate the clinical significance of our findings beyond animal models, we asked whether GDF15 potentially underlies clinical FTT associated with pediatric heart disease, which often features

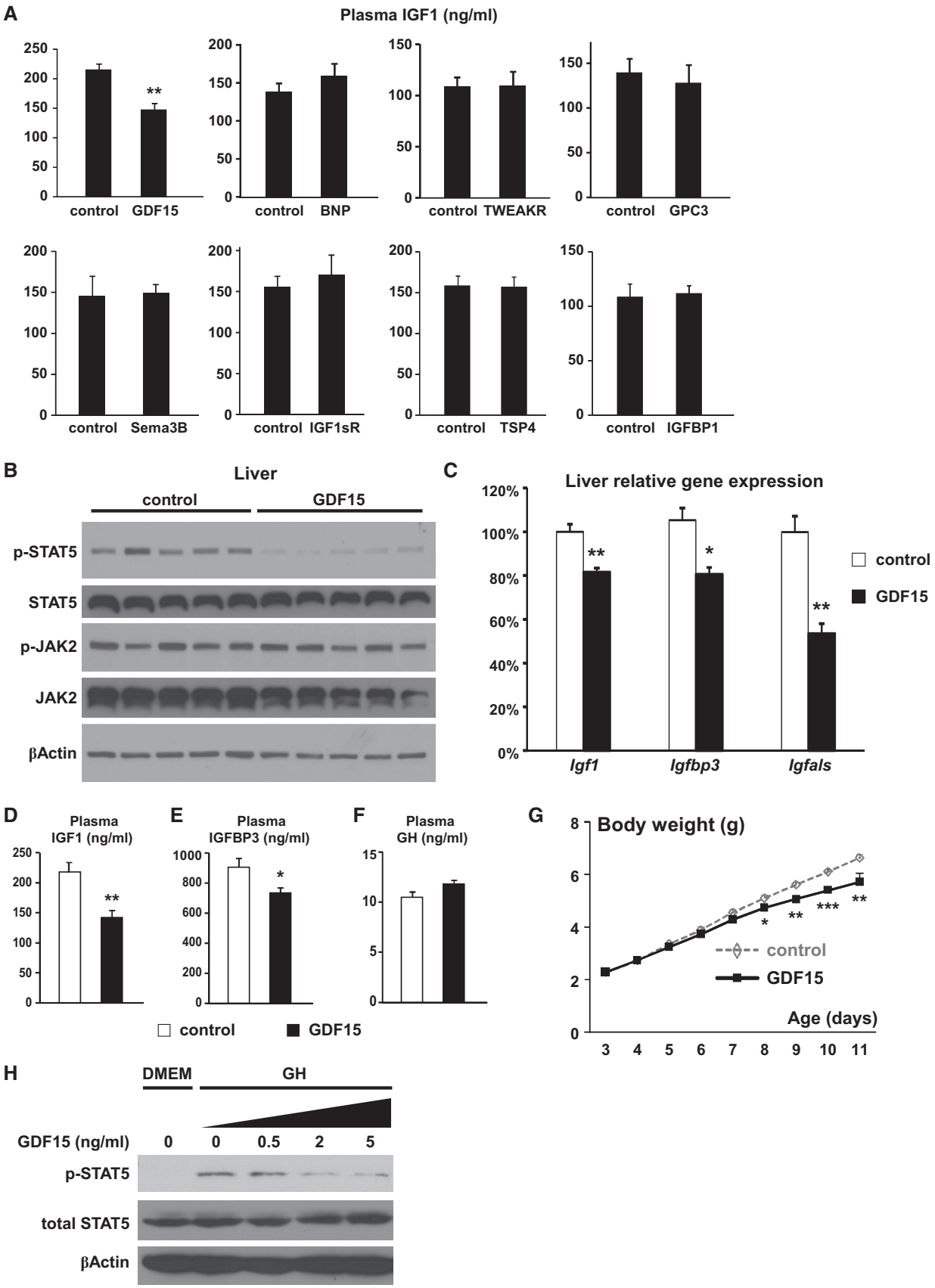

Figure 3.

Figure 3. GDF15 is a candidate heart-derived hormone that inhibits liver GH signaling and body growth.

A Plasma IGF1 concentrations (ng/ml) in 7-day-old weight- and gender-matched littermate WT mice injected with control or different proteins were measured by ELISA (n = 3–5 mice per group, daily i.p. injection from 5 days of age).

B–G Liver phosphorylated and total STAT5 and JAK2 as well as β-actin (loading control) determined by Western blot (B); liver expression of *Igf1*, *Igfbp3*, and *Igfals* quantified by qPCR (C); plasma IGF1 (D), IGFBP3 (E), and GH concentrations (F) measured by ELISA; and daily body weight (G) in weight- and gender-matched littermate WT mice injected with control or GDF15 (n = 5 per group, daily i.p. injection from 3 days of age).

H Overnight-fasted (in DMEM) WT mouse primary hepatocytes were first treated with different concentrations of GDF15 for 30 min and then with 20 ng/ml GH for 15 min. Cellular levels of phosphorylated STAT5, total STAT5, and β-actin (loading control) were determined by Western blot.

Data information: $*P < 0.05$, $**P < 0.01$, and $***P < 0.001$ between control and GDF15 by t-test. All values are mean + s.e.m.
Source data are available online for this figure.

lower circulating IGF1 and IGFBP3 levels (Barton *et al*, 1996; Dinleyici *et al*, 2007; Surmeli-Onay *et al*, 2011; Peng *et al*, 2013). We measured plasma GDF15 concentrations in children diagnosed with heart disease and with either normal body weight or FTT. Both groups of children with heart disease had significantly higher plasma GDF15 levels than gender- and age-matched healthy control children (Fig 6A), consistent with previous findings that plasma GDF15 was increased in adult heart disease (Wollert & Kempf, 2012; Baggen *et al*, 2017; Wollert *et al*, 2017). Importantly, plasma GDF15 level is further significantly increased (another 80% higher) in children with concomitant heart disease and FTT than those with heart disease but normal body weight (Fig 6A), supporting elevated GDF15 as an underlying mechanism linking pediatric heart disease and FTT.

Discussion

The rapid body growth and increased nutrients/energy demand during the pediatric period require accompanying increase of cardiac function. Here, we identified a novel endocrine mechanism by which the heart communicates with the rest of the body to coordinate body growth and cardiac function. The heart synthesizes and secretes GDF15 to inhibit body growth, thereby relieving potential extra cardiac burden as well as helping the body adapt to decreased cardiac output, a theme also seen in ANP and BNP (Fig 6B). Both GDF15 and ANP/BNP are synthesized as prohormones and processed to become active hormones. Cardiac and circulating levels of both GDF15 and ANP/BNP are highly elevated in many forms of heart disease. BNP is well established and widely used clinically for diagnosis of heart disease especially heart failure; GDF15 was also recently proposed as an independent plasma biomarker for heart diseases (Wollert & Kempf, 2012; Baggen *et al*, 2017; Wollert *et al*, 2017). Most importantly, both GDF15 and ANP/BNP are used as hormones by the heart to effect systemic changes that relieve cardiac burden: GDF15 inhibits body growth and ANP/BNP decrease blood pressure. These similarities suggest a unified endocrine mechanism that the heart exploits to coordinate cardiac function and the rest of the body (Fig 6B).

GDF15 was previously shown to mediate adult body weight loss in cachexia and obesity settings (Johnen *et al*, 2007; Tsai *et al*, 2013), through its action in the hypothalamus (reducing *Npy* and increasing *Pomc* expression) that regulates food intake. Of note body weight loss in such adult conditions predominantly impacts specific tissues (muscle and adipose tissue in cachexia; adipose tissue in obesity), with most other organs and height/body length largely unaffected. Our studies reveal a completely different and new role of GDF15 in the pediatric period. We did not observe any changes in hypothalamic *Npy* and *Pomc* expression in either cardiac αKOγKO mice or GDF15-injected young WT mice (Appendix Figs S1B and S3C), probably because the appetite-regulating neural circuits in the hypothalamus in these young mice (1–2 weeks old) are still developing and functionally immature compared to those in adult mice (Nilsson *et al*, 2005). We find that GDF15 inhibits pediatric body growth that affects all organs (proportionally smaller and lighter in weight), rather than selectively targeting only muscle or adipose tissue. Accordingly, GDF15 functions through a distinct mechanism of inhibiting liver GH signaling that affects whole-body growth and all organs in the pediatric period.

We observed a fourfold to fivefold increase of circulating GDF15 in αKOγKO mice (Fig 4C) and similar changes in children with heart disease (Fig 6A). Such change is consistent within the range reported in human biomarker studies (Wollert & Kempf, 2012; Baggen *et al*, 2017; Wollert *et al*, 2017). Of note the normal heart produces undetectable level of GDF15 (Fig 4B and D), therefore the basal level of circulating GDF15 (Fig 4C) most likely comes from non-cardiac sources. Our cardiac-specific *Gdf15* knockdown studies suggest that cardiac-derived GDF15 in the heart disease condition contributed to all the elevated circulating GDF15 above basal level (Fig 5). This additional circulating GDF15 from the heart clearly has a significant biological impact on liver GH signaling (Fig 5). One possible explanation is that such a fourfold to fivefold increase in GDF15 concentration is enough to make a significant difference in its signaling. Another possible explanation is that heart-derived GDF15 is biochemically distinct from the basal circulating GDF15 from non-cardiac sources and potentially possesses higher biological activities. Future studies will investigate the factors that modulate GDF15 activity, and determine the detailed molecular mechanism of GDF15 signaling.

We designed AAV9-sh*Gdf15* vectors to specifically knockdown cardiomyocyte *Gdf15* in αKOγKO mice (Fig 5). In this experiment, we injected AAV-shRNA to 2-day-old mice, the age right when initial molecular changes of cardiac dysfunction were observed in cardiac αKOγKO mice (Wang *et al*, 2015b). It was expected that injected AAV9-*Gdf15* shRNA would take some time (probably in days) to be well expressed and take effect to completely block cardiac GDF15 synthesis. By this time, it is highly likely that liver GH signaling and circulating IGF1 would have already significantly decreased. We therefore anticipated that reduced liver GH signaling in αKOγKO mice would be partially reversed in the days following AAV9-sh*Gdf15* injection. We did observe that once cardiac and circulating GDF15 levels were completely normalized 1 week after AAV9-sh*Gdf15* injection, downstream liver STAT5 phosphorylation was largely restored and circulating IGF1 level was partially

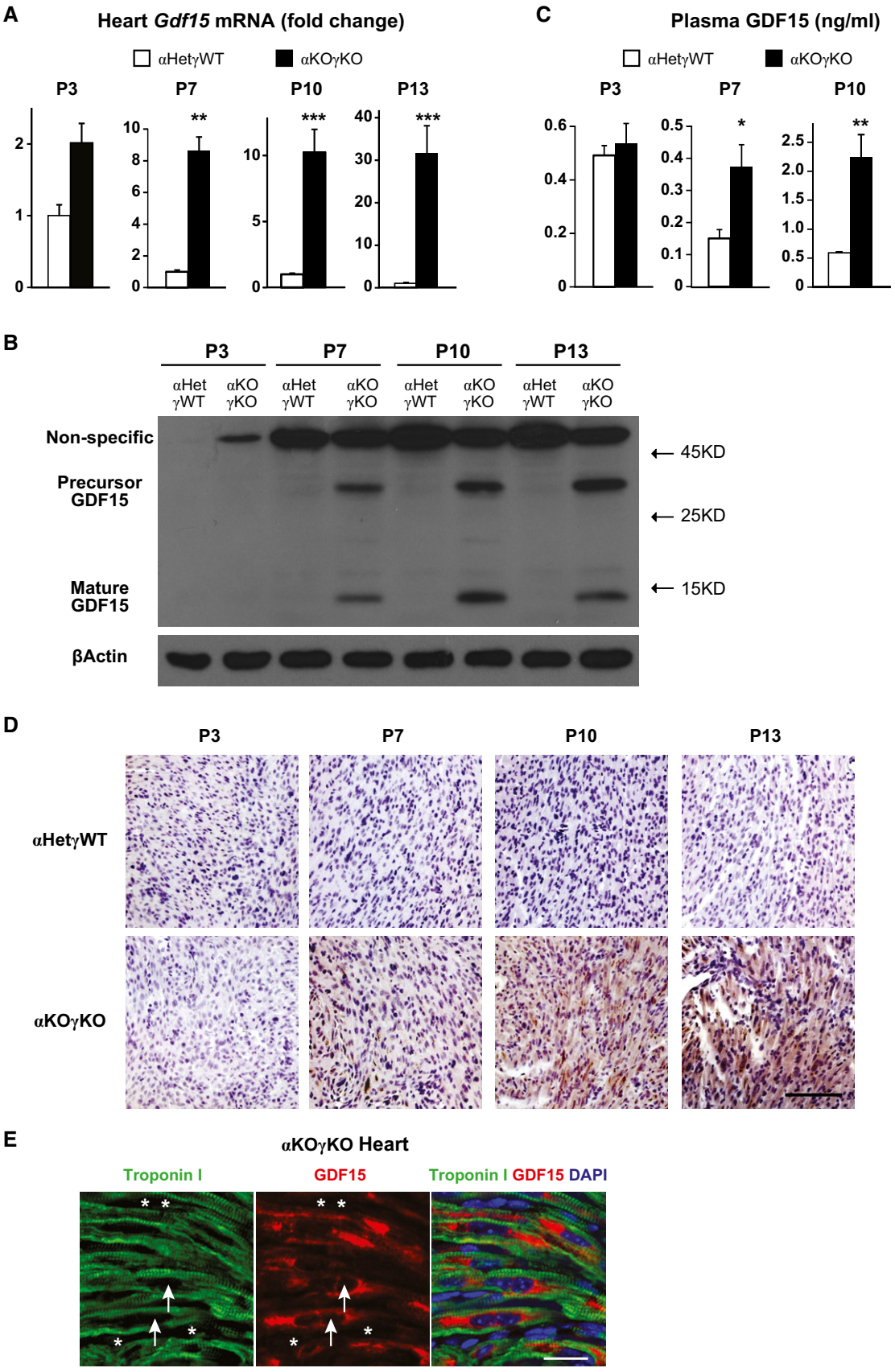

Figure 4.

Figure 4. GDF15 is increased in pediatric heart disease and produced in cardiomyocytes.

A Expression of *Gdf15* in 3- (n = 5–7 mice per group), 7- (n = 6 mice per group), 10- (n = 8–10 mice per group), and 13-day-old (n = 12–13 mice per group) littermate mouse hearts quantified by qPCR.

B GDF15 protein level in 3-, 7-, 10-, and 13-day-old littermate mouse hearts determined by Western blot. β-Actin serves as a loading control.

C Plasma GDF15 concentrations in 3- (n = 5–7 mice per group), 7- (n = 6 mice per group), and 10-day-old littermate mice (n = 8–10 mice per group) measured by ELISA.

D Representative pictures of 3-, 7-, 10-, and 13-day-old littermate αHetγWT and αKOγKO mouse heart sections stained with GDF15 antibody (brown) and counterstained with hematoxylin (purple). Scale bar: 100 μm.

E Representative pictures of 16-day-old αKOγKO mouse hearts stained with GDF15 (red) and cardiac troponin I (green) antibodies. Arrows point to the nucleus of cardiomyocytes, and asterisks mark the nucleus of non-cardiomyocytes. Scale bar: 20 μm.

Data information: $*P < 0.05$, $**P < 0.01$, and $***P < 0.001$ between αKOγKO and all other littermate control genotypes by t-test. All values are mean + s.e.m.

reversed. Although it appears that GDF15 is the major circulating factor in αKOγKO plasma that inhibits hepatocyte GH signaling *in vitro* (Appendix Fig S4B and C), it is possible that additional GDF15-independent mechanisms are involved. These include mechanisms through the nervous system that sense cardiac health and in turn regulate body growth, other heart-derived endocrine signals (including those unexamined candidates from our plasma proteomics and cardiac RNA-Seq studies), or a combination of nervous and endocrine mechanisms. Future studies in these areas will further broaden our understandings of the communication between the heart and rest of the body. Nevertheless, our current results clearly demonstrate that heart-derived GDF15 is essential for altered liver GH signaling in FTT associated with pediatric heart disease.

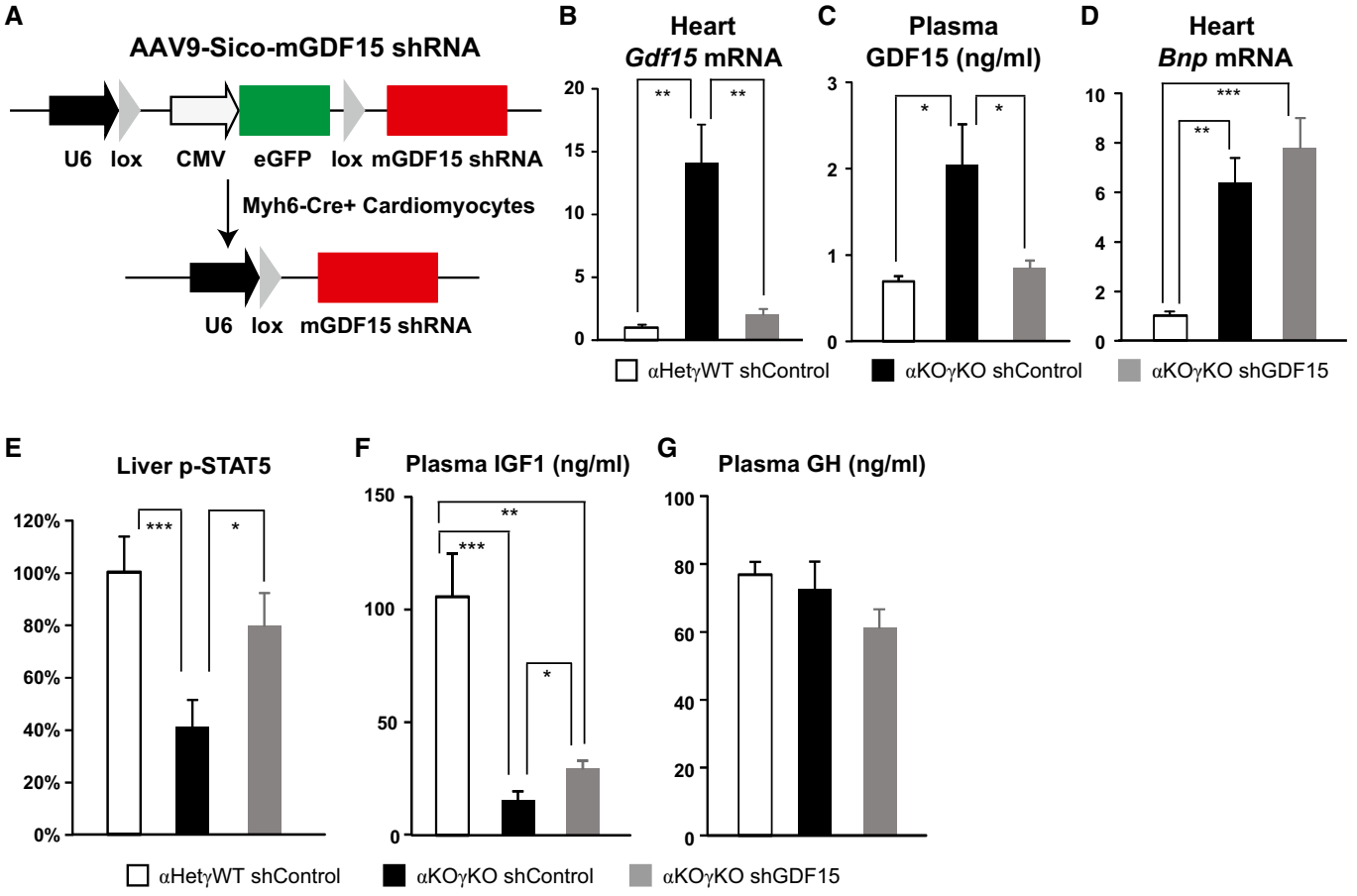

Figure 5. GDF15 is a *bona fide* heart-derived hormone that regulates liver GH signaling.

A Design of AAV9-mGDF15 shRNA construct to specifically knockdown GDF15 in Cre^+ cardiomyocytes.

B–G Cardiac *Gdf15* expression quantified by qPCR (B), plasma GDF15 concentrations measured by ELISA (C), cardiac *Bnp* expression quantified by qPCR (D), liver phosphorylated STAT5 level measured by ELISA (E), and plasma IGF1 (F) and GH concentrations (G) measured by ELISA in 9- to 10-day-old littermate control and αKOγKO mice (n = 8–12 mice per group) that received pericardial injection of AAV9-control or *Gdf15* shRNA at 2 days of age. $*P < 0.05$, $**P < 0.01$, and $***P < 0.001$ by t-test. Values are mean + s.e.m.

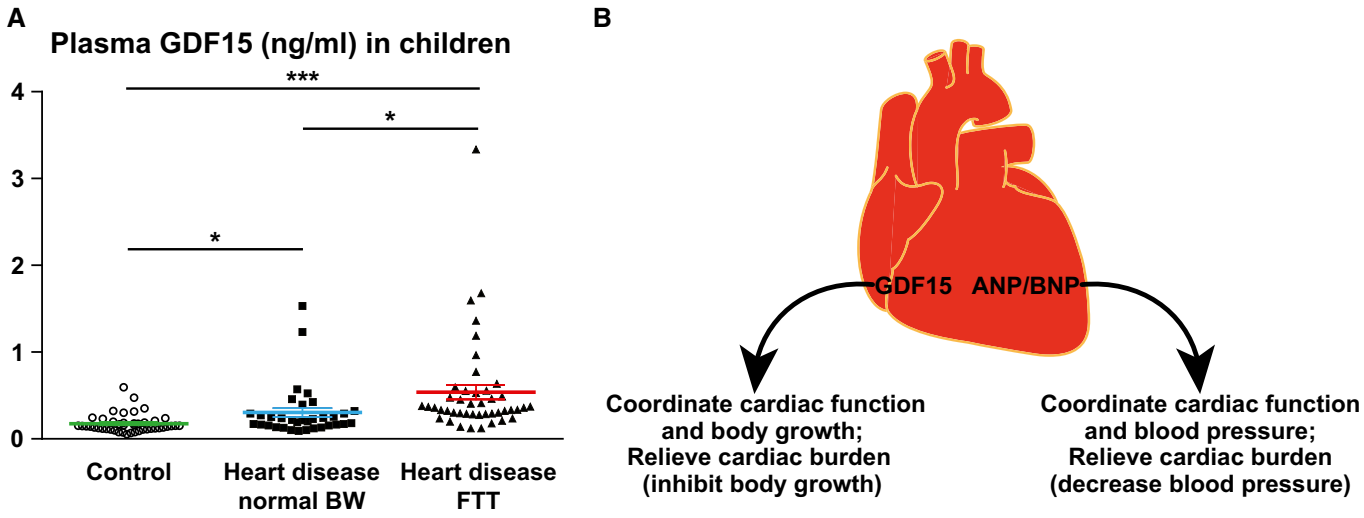

Figure 6. Plasma GDF15 is elevated in children with concomitant heart disease and FTT.

A Plasma GDF15 concentrations in 2- to 3-year-old children diagnosed with heart disease with either normal body weight (n = 35) or FTT (n = 45) and in age- and gender-matched healthy controls (n = 45) were measured by ELISA. *P < 0.05 and ***P < 0.001 by t-test. Values are mean ± s.e.m.

B Cartoon illustrating how GDF15 and ANP/BNP relieve cardiac burden and coordinate cardiac function with the rest of the body.

The vital function of the heart has been known for thousands of years. Besides ANP and BNP discovered over 30 years ago (de Bold, 1985; Frohlich, 1985; McGrath *et al*, 2005; Clerico *et al*, 2011; Ogawa & de Bold, 2014), only small numbers of heart-secreted factors are known (Shimano *et al*, 2012; Karsenty & Olson, 2016). However, they are not established as endocrine hormones because their known functions to date are largely limited to mere biomarkers of cardiac health or autocrine/paracrine factors that affect cardiomyocyte or cardiac fibroblast biology locally (Shimano *et al*, 2012; Karsenty & Olson, 2016). Potential heart-derived endocrine factors were suggested that impact liver and adipose tissue lipid metabolism in a few recent studies (Grueter *et al*, 2012; Baskin *et al*, 2014; Magida & Leinwand, 2014), but the exact identities of such factors remain to be determined (Karsenty & Olson, 2016). By identifying GDF15 as a new heart-derived hormone and revealing its biological function, our findings support the importance of the endocrine function of the heart and advance our understanding of the heart and its role in whole-organism homeostasis. Our studies also uncover an underlying mechanism of FTT associated with pediatric heart disease. Intriguingly, plasma GDF15 was recently reported to be increased in mitochondrial disease patients, which often features slowed body growth as well (Yatsuga *et al*, 2015; Fujita *et al*, 2016; Montero *et al*, 2016). Whether GDF15 is critical in this context remains to be determined.

Materials and Methods

Animal studies

All animal studies were approved by and performed under the guidelines of the Institutional Animal Care and Use Committee of the Children's Hospital of Philadelphia (CHOP). All mice were backcrossed at least six generations to and maintained in the C57BL6/J background. Mice were maintained in a temperature- and light-controlled environment with *ad libitum* access to water. Mice in holding cages (after weaning at around 28 days of age) received a standard chow diet (Lab Diet 5L0D, 58% calories from carbohydrate, 13.5% calories from fat, and 28.5% calories from proteins); nurturing moms and their pups before weaning received a breeder diet (Lab Diet 5058, 55% calories from carbohydrate, 22% calories from fat, and 23% calories from proteins). The breeding strategy to generate experimental cohorts (αHetγWT, αHetγKO, αKOγWT, and αKOγKO littermates at 1:1:1:1 ratio) was previously described (Wang *et al*, 2015b). For postnatal body growth analysis, the breeding pairs were monitored daily for birth of pups. The first day we observed new pups born was deemed as P0, and the pups were toe-clipped for identification and genotyping. We chose body weight over bone or body length to determine body growth because body weight can be more accurately measured using a digital scale with 0.01 gram precision. Mice were weighed daily between 10 am and 2 pm. Both male and female pups exhibited lethal cardiomyopathy and FTT phenotypes, and therefore, both genders were included in the study. We determined the minimum number of animals needed using power calculations based on the literature, our preliminary results and sample variation aiming to ensure 90% power. Only littermate mice were used and they were randomized to ensure that the same age, gender, and weight (mean and variation, where applicable) are represented in all groups. Investigators were blinded to the sample group allocation wherever possible. The number of mice used in each experiment and number of times experiments are replicated are described in figure legends or related Materials and Methods sections. Only mice living for at least 13 days were included in the body weight curve (Fig 1; because some αKOγKO die before this age). All tissues were collected and weighed between 12 and 4 pm to avoid the impact of circadian rhythm.

ELISA

Mouse blood was collected in lithium-heparin-coated microvette CB300LH (Sarstedt), and plasma was collected after spinning down at 3,000 *g* for 5 min at 4°C. Plasma protein levels were measured using ELISA kits: mouse GH (Millipore EZRMGH-45K), mouse IGF1 (Abcam ab108874), mouse IGFBP3 (R&D MGB300), mouse GDF15 (R&D MGD150), and human GDF15 (R&D DY957). Separately, mouse livers were homogenized with kit-provided lysis buffer containing protease and phosphatase inhibitors (Roche). Phosphorylated and total STAT5 and JAK2 levels were measured using the following ELISA kits and normalized to total protein amount: p-STAT5 (Tyr694, Cell Signaling #7113C), total STAT5 (Abcam ab205714), p-JAK2 (Tyr1007/1008, ThermoFisher Scientific KHO5621), and total JAK2 (Invitrogen KH05521).

Plasma proteomics

EDTA plasma was collected from 16-day-old littermate αHetγWT and αKOγKO mice (n = 3 mice per group) and stored at −80°C until analysis. Measurement of relative plasma protein levels using the SOMAscan platform was performed at SomaLogic Inc. (Gold *et al*, 2010).

Gene expression analysis

We isolated total RNA from mouse tissues or cells using RNAzol RT (Molecular Research Center) following the manufacturer's instructions. We synthesized cDNA from 1 μg total RNA using iScript cDNA synthesis kit (Bio-Rad) and quantified mRNA levels by real-time qPCR using SYBR Green (Bio-Rad). We ran samples in technical triplicates and calculated relative mRNA levels using a standard curve and normalized to 36b4 mRNA level in the same sample. The qPCR primer sequences are listed in Appendix Table S3.

RNA-Seq

Total RNA from 16-day-old littermate mouse (αHetγWT, αHetγKO, αKOγWT, and αKOγKO) hearts was extracted using RNAzol RT. We prepared two independent samples per genotype for RNA-Seq, with each sample comprised of equal amount of pooled RNA from three biological replicates (total of six littermate hearts per genotype used). Library was constructed using TrueSeq Library Prep kit (Illumina), and sequencing and bioinformatic analysis were performed by BGI@CHOP (PE100, 20 million reads). The raw and processed data are deposited in the GEO database (accession number GSE88761, https://www.ncbi.nlm.nih.gov/geo/query/acc.cgi?token=cpqnciqcrxchngl&acc=GSE88761).

Protein analysis

For whole-cell extract preparation, cells or 20 mg of tissues was homogenized and kept in 400 μl (20×) cold RIPA buffer containing protease/phosphatase inhibitors on ice for 10 min. The homogenates were spun down at 13,000 *g* for 10 min, and the supernatant was collected as whole-cell extract. For nuclear/cytosolic extract preparation, 20 mg of tissues was homogenized and kept in 400 μl cold buffer containing 10 mM HEPES (pH 7.4), 1.5 mM $MgCl_2$, 10 mM KCl, 0.5 mM DTT, and protease and phosphatase inhibitors on ice for 10 min. The homogenates were spun down at 13,000 *g* for 10 min, and the supernatant was collected as cytosolic extract. The pellets were resuspended in 300 μl cold buffer containing 10 mM HEPES (pH 7.4), 1.5 mM $MgCl_2$, 420 mM NaCl, 0.2 mM EDTA, 25% glycerol, 0.5 mM DTT, and protease/phosphatase inhibitors and shaken overnight at 4°C. They were then spun down at 13,000 *g* for 20 min, and the supernatant was collected as nuclear extract. Protein concentration was quantified by a BCA assay kit (ThermoFisher Scientific). Western blot was performed as previously described following standard procedures (Wang *et al*, 2015b). Primary antibodies used were p-STAT5 (Cell Signaling #9359, 1:1,000), STAT5 (Cell Signaling #9358, 1:1,000), p-JAK2 (Cell Signaling #3776, 1:1,000), JAK2 (Millipore 06-1310, 1 μg/ml), GDF15 (Abcam ab189358, 1 μg/ml), β-actin (Cell Signaling #4970, 1:1,000), and TFIIH (Santa Cruz sc-293, 1:2,000).

Plasma fractionation and GDF15 depletion by immunoprecipitation

Pooled plasma from 3 to 4 16-day-old αHetγWT or αKOγKO mice was used for each fractionation or GDF15 depletion experiment. Plasma was separated into high (> 3 KD) and low (< 3 KD) molecular weight fractions using Amicon Ultra 0.5-ml centrifugal 3 KD Filters (Millipore) following the manufacturer's instructions. For GDF15 depletion, plasma was incubated with 1 μg mouse GDF15 capture antibody (from ELISA kit R&D DY6385) and shaken at 4°C overnight. 250 μl dynabeads protein G (ThermoFisher Scientific 100.04D) was then added to the plasma and shaken at room temperature for 2 h. The mixture was separated using magnet, and the supernatant was collected as GDF15-depleted plasma. GDF15 concentration in plasma before and after GDF15 depletion was determined using ELISA (R&D DY6385).

Mouse primary hepatocyte isolation and GH signaling studies

Primary hepatocytes were isolated from young WT mice as previously described (Pei *et al*, 2006). Briefly, 3- to 4-week-old mouse was anesthetized and perfused at 37°C with 10 mM HEPES-buffered HBSS (1 ml/min for 5 min) and then with 0.1% type I collagenase (Worthington LS004194) in Williams E media (1 ml/min for 5 min), entering the hepatic portal vein and exiting the inferior vena cava. The perfused liver was removed and shaken to disperse cells into hepatocyte attachment media (DMEM/F12 supplemented with 0.2 mg/ml BSA, 1 mg/ml D-galactose, 0.03 mg/ml proline, 5 mM sodium pyruvate, 1× insulin-transferrin-selenium-A (ThermoFisher Scientific 51300044), 1× antibiotic-antimycotic (ThermoFisher Scientific 15240062), and 10% FBS). After mixing cells with Percoll (final concentration of Percoll is 45%) and centrifugation to collect all the viable cells, we resuspended cells in hepatocyte attachment media and plated them on collagen I-coated 24-well plates with a density of 0.2–0.3 million cells per well. 3 h later, cells were washed with DMEM to remove non-attached cells and fasted overnight in DMEM. The next morning, cells were treated with DMEM, DMEM plus 50% plasma, or 50% plasma fractions for 1 h. Alternatively, cells were first treated with different concentration of GDF15 (R&D 8146-GD/CF) for 30 min and then treated with 20 ng/ml GH (R&D 1067-GH-025/CF) for 15 min. For Western blot, cells were washed with

ice-cold PBS for three times and lysed with 60 μl lysis buffer (30 μl RIPA buffer and 30 μl 2× Laemmli sample buffer from Bio-Rad, plus protease and phosphatase inhibitors and 2.5% β-mercaptoethanol). For determining protein tyrosine phosphatase (PTP) activity, cells were washed three times with ice-cold PBS and lysed in a buffer containing 150 mM NaCl, 50 mM Tris pH 7.4, 1% NP-40, and protease inhibitors (Sorenson & Sheibani, 2002). 1 μl cell lysates (around 2 μg proteins) from each group were incubated at 37°C for 30 min with 0.2 mM PTP substrate RRLIEDAEpYAARG (Upstate 12-217) in a final volume of 50 μl of assay buffer (25 mM HEPES pH 7.2, 50 mM NaCl, 5 mM DTT, and 2.5 mM EDTA) (Kakazu *et al*, 2008). Amount of phosphate released was measured by malachite green phosphate assay kit (Cayman Chemical 10009325) following manufacturer's instructions. This was normalized to total protein, which was determined using Pierce BCA Protein Assay Kit (ThermoFisher Scientific 23225).

Protein injection

Recombinant proteins were purchased from commercial sources: GDF15 (R&D 8146-GD/CF), IGFBP1 (R&D 1588-B1), Sema3B (R&D 5440-S3/CF), GPC3 (R&D 2119-GP/CF), TWEAKR/TNFRSF12 (R&D 1610-TW), TSP4 (R&D 7860-TH), IGF1sR (IGF1R 1-936, R&D 6630-GR/CF), and BNP 1-32 (Tocris Bioscience 3522). They were reconstituted per vendor's recommendations and further diluted in PBS for *in vivo* i.p. injection. For *in vivo* experiments, we used gender- and body weight (BW)-matched WT mice all from the same litter to exclude the impact of mom's nurturing ability on BW among litters. We repeated all short- and long-term GDF15 injections at least four times and other protein injections at least two times and obtained the same results. For short-term injection, gender- and BW-matched 5-day-old WT mice all from the same litter (n = 3–5 per group) were i.p. injected between 11 am and 1 pm with control (same solvent diluted in PBS) or indicated protein every 24 h, three times total. Mouse plasma was collected 1.5 h after the last injection (7 days old). The injection doses were based on literature and product information from the vendors: 500 μg/kg BW for BNP and GPC3, 100 μg/kg BW for GDF15, TWEAKR, Sema3B, TSP4, IGFBP1, and IGF1sR. For long-term injection (illustrated in Appendix Fig S3A), gender- and BW-matched (BW of all littermate pups within 10% variation) 3-day-old WT mice all from the same litter (n = 4–5 per group) received daily i.p. injection between 11 am and 1 pm of control, 400 μg/kg BW GDF15 or 500 μg/kg BW BNP. Plasma and tissues were collected at the end of the experiment, 1.5 h after the final injection.

Histology

Histological studies were performed as previously described (Pei *et al*, 2011, 2015). Mice were euthanized and perfused with 3 ml PBS. Tissues were then dissected and fixed in 4% paraformaldehyde in PBS overnight. Tissues were embedded in paraffin or frozen blocks. For heart immunohistochemistry, 5–8 μm paraffin sections were used. After deparaffinization, sections were incubated in AR buffer (Vector Lab H-3300) for antigen retrieval (microwave for 5 min). Sections were then rinsed in PBST and blocked with 2% horse serum for 1 h and incubated with GDF15 (Abcam ab189358, 10 μg/ml) or troponin I (Abcam ab47003, 10 μg/ml) antibodies overnight at 4°C. The sections were then incubated with biotin-labeled secondary antibodies (5 μg/ml) and ABC reagent (Vectastain Elite ABC Reagent RTU, Vector Lab PK-7100), and stained using peroxidase substrate solution (Vector Lab). After counterstain with hematoxylin (Vector Lab H-3401) and dehydration, the sections were mounted and imaged using a Zeiss Axio microscope. For immunofluorescence, the sections were incubated with fluorescence-labeled secondary antibodies and mounted and imaged using a Zeiss LSM710 confocal microscope.

AAV injection

AAV9-Sico-mouse *Gdf15* shRNA (based on shAAV-260008) or scramble control shRNA was custom-built and manufactured by Vector Biolabs. Pericardial injection of 3×10^{11} genome copies AAV9 was performed in 2-day-old mice using a Hamilton syringe by adapting procedures previously described without using ultrasound guidance (Laakmann *et al*, 2013). αKOγKO mice were randomized to receive AAV9-*Gdf15* or control shRNA, and littermate control αHetγWT mice received AAV9-control shRNA. As quality control and based upon pre-established criteria, mice dead before 9 days of age or with unsuccessful cardiac *Gdf15* knockdown (presumably due to unsuccessful injection or ineffective AAV infection) were excluded from the study (2 of 10 αKOγKO mice that received AAV9-sh *Gdf15* and survived to 9–10 days of age were excluded from the study shown in Fig 5; similar success rate was observed in control groups).

Human plasma samples

Plasma samples were from the CHOP Center for Applied Genomics biobank. Plasma samples from three groups of children were used (Appendix Table S4). Group 1: age- and gender-matched healthy controls. Group 2: 2- to 3-year-old children diagnosed with congenital heart disease and/or pediatric cardiomyopathy, with normal body weight (within 40–70% range of the standard body weight chart of the individual's age; 50% is the median body weight) at the time of sample collection. Group 3: 2- to 3-year-old children diagnosed with congenital heart disease and/or pediatric cardiomyopathy, with FTT (within 0–8.5% range of the standard body weight chart of the individual's age; most were also diagnosed with FTT) at the time of sample collection. Informed consent was obtained from all subjects and the experiments conformed to the principles set out in the WMA Declaration of Helsinki and the Department of Health and Human Services Belmont Report.

Statistical analysis

Two-tailed distribution, two-sample unequal variance t-test was used to determine the statistical significance between results of two independent groups, using either Microsoft Excel (animal studies) or GraphPad Prism (human studies, allowing automatic identification and exclusion of no more than 1 outlier out of > 35 biological samples per group based on the built-in ROUT method), with $P < 0.05$ deemed as statistically significant. The P-values of all figures are provided in Appendix Table S5.

Expanded View for this article is available online.

The paper explained

Problem
Endocrine organs and the hormones they secrete regulate many essential functions in our body. The vital role of the heart has been known for thousands of years, but its function as an important endocrine organ remains little understood.

Results
Here, we identify a new heart-derived hormone called growth differentiation factor 15 (GDF15) that regulates body growth. GDF15 synthesis and secretion by cardiomyocytes are increased in pediatric heart disease. Circulating GDF15 in turn acts on the liver to inhibit growth hormone (GH) signaling and body growth. Blocking cardiomyocyte production of GDF15 normalizes circulating GDF15 level and restores liver GH signaling, establishing GDF15 as a *bona fide* heart-derived hormone. Plasma GDF15 is increased in children with concomitant heart disease and failure to thrive (FTT).

Impact
Our study advances the field of cardiac endocrinology by revealing GDF15 as a heart-derived hormone that coordinates cardiac function and body growth. These results also provide a potential mechanism for the well-established clinical observation that children with heart diseases often develop FTT.

Acknowledgements
We thank Drs. Douglas Wallace, Mitchell Lazar, Matthew Weitzman, Amita Sehgal, Michael Marks, Mark Kahn, Jonathan Epstein, Morris Birnbaum, and Elizabeth Goldmuntz for critical discussion of the project. We thank Dr. Benjamin Prosser for showing us pericardial injection techniques. The authors and this work were supported by the Office of the Assistant Secretary of Defense for Health Affairs through the Peer Reviewed Medical Research Program under Award No. W81XWH-16-1-0400, a grant from the W.W. Smith Charitable Trust (H1407), pilot awards from the Diabetes Research Center at the University of Pennsylvania from a grant sponsored by NIH DK 19525, and NIH DK111495 (L.P.), DK099379 (B.J.W.), HG008684, and MH096891 (H.H.). X.Z. is supported by the China Scholarship Council.

Author contributions
LP conceived and directed the project. TW, JL, and LP performed most of the experiments including independently repeated experiments. CM, KL, and XZ provided technical assistance. BJW is a pathologist who evaluated, read, and scored the histology studies. HH provided human plasma samples and contributed to the analysis and interpretation of the results. TW and LP wrote, and all authors reviewed and/or edited the manuscript.

Conflict of interest
The authors declare that they have no conflict of interest.

References

Baek SJ, Kim KS, Nixon JB, Wilson LC, Eling TE (2001) Cyclooxygenase inhibitors regulate the expression of a TGF-beta superfamily member that has proapoptotic and antitumorigenic activities. *Mol Pharmacol* 59: 901 – 908

Baggen VJ, van den Bosch AE, Eindhoven JA, Schut AW, Cuypers JA, Witsenburg M, de Waart M, van Schaik RH, Zijlstra F, Boersma E *et al* (2017) Prognostic value of N-terminal Pro-B-type natriuretic peptide, Troponin-T, and growth-differentiation factor 15 in adult congenital heart disease. *Circulation* 135: 264 – 279

Baik M, Yu JH, Hennighausen L (2011) Growth hormone-STAT5 regulation of growth, hepatocellular carcinoma, and liver metabolism. *Ann N Y Acad Sci* 1229: 29 – 37

Barton JS, Hindmarsh PC, Preece MA (1996) Serum insulin-like growth factor 1 in congenital heart disease. *Arch Dis Child* 75: 162 – 163

Baskin KK, Grueter CE, Kusminski CM, Holland WL, Bookout AL, Satapati S, Kong YM, Burgess SC, Malloy CR, Scherer PE *et al* (2014) MED13-dependent signaling from the heart confers leanness by enhancing metabolism in adipose tissue and liver. *EMBO Mol Med* 6: 1610 – 1621

Bauskin AR, Zhang HP, Fairlie WD, He XY, Russell PK, Moore AG, Brown DA, Stanley KK, Breit SN (2000) The propeptide of macrophage inhibitory cytokine (MIC-1), a TGF-beta superfamily member, acts as a quality control determinant for correctly folded MIC-1. *EMBO J* 19: 2212 – 2220

Bish LT, Morine K, Sleeper MM, Sanmiguel J, Wu D, Gao G, Wilson JM, Sweeney HL (2008) Adeno-associated virus (AAV) serotype 9 provides global cardiac gene transfer superior to AAV1, AAV6, AAV7, and AAV8 in the mouse and rat. *Hum Gene Ther* 19: 1359 – 1368

de Bold AJ (1985) Atrial natriuretic factor: a hormone produced by the heart. *Science* 230: 767 – 770

Bootcov MR, Bauskin AR, Valenzuela SM, Moore AG, Bansal M, He XY, Zhang HP, Donnellan M, Mahler S, Pryor K *et al* (1997) MIC-1, a novel macrophage inhibitory cytokine, is a divergent member of the TGF-beta superfamily. *Proc Natl Acad Sci USA* 94: 11514 – 11519

Bottner M, Laaff M, Schechinger B, Rappold G, Unsicker K, Suter-Crazzolara C (1999) Characterization of the rat, mouse, and human genes of growth/differentiation factor-15/macrophage inhibiting cytokine-1 (GDF-15/MIC-1). *Gene* 237: 105 – 111

Chen Y, Wen R, Yang S, Schuman J, Zhang EE, Yi T, Feng GS, Wang D (2003) Identification of Shp-2 as a Stat5A phosphatase. *J Biol Chem* 278: 16520 – 16527

Chen Y, Zhang Y, Yin Y, Gao G, Li S, Jiang Y, Gu X, Luo J (2005) SPD–a web-based secreted protein database. *Nucleic Acids Res* 33: D169 – D173

Clerico A, Giannoni A, Vittorini S, Passino C (2011) Thirty years of the heart as an endocrine organ: physiological role and clinical utility of cardiac natriuretic hormones. *Am J Physiol Heart Circ Physiol* 301: H12 – H20

Cole SZ, Lanham JS (2011) Failure to thrive: an update. *Am Fam Physician* 83: 829 – 834

Cui Y, Hosui A, Sun R, Shen K, Gavrilova O, Chen W, Cam MC, Gao B, Robinson GW, Hennighausen L (2007) Loss of signal transducer and activator of transcription 5 leads to hepatosteatosis and impaired liver regeneration. *Hepatology* 46: 504 – 513

Czech MP (1989) Signal transmission by the insulin-like growth factors. *Cell* 59: 235 – 238

Deng Y, Scherer PE (2010) Adipokines as novel biomarkers and regulators of the metabolic syndrome. *Ann N Y Acad Sci* 1212: E1 – E19

Dinleyici EC, Kilic Z, Buyukkaragoz B, Ucar B, Alatas O, Aydogdu SD, Dogruel N (2007) Serum IGF-1, IGFBP-3 and growth hormone levels in children with congenital heart disease: relationship with nutritional status, cyanosis and left ventricular functions. *Neuro Endocrinol Lett* 28: 279 – 283

Fairlie WD, Moore AG, Bauskin AR, Russell PK, Zhang HP, Breit SN (1999) MIC-1 is a novel TGF-beta superfamily cytokine associated with macrophage activation. *J Leukoc Biol* 65: 2 – 5

Forchielli ML, McColl R, Walker WA, Lo C (1994) Children with congenital heart disease: a nutrition challenge. *Nutr Rev* 52: 348 – 353

Frohlich ED (1985) The heart. An endocrine organ (revisited). *Arch Intern Med* 145: 809 – 811

Fujita Y, Taniguchi Y, Shinkai S, Tanaka M, Ito M (2016) Secreted growth differentiation factor 15 as a potential biomarker for mitochondrial dysfunctions in aging and age-related disorders. *Geriatr Gerontol Int* 16 (Suppl 1): 17 – 29

Giguere V (2008) Transcriptional control of energy homeostasis by the estrogen-related receptors. *Endocr Rev* 29: 677 – 696

Gold L, Ayers D, Bertino J, Bock C, Bock A, Brody EN, Carter J, Dalby AB, Eaton BE, Fitzwater T *et al* (2010) Aptamer-based multiplexed proteomic technology for biomarker discovery. *PLoS One* 5: e15004

Gribble FM, Reimann F (2016) Enteroendocrine cells: chemosensors in the intestinal epithelium. *Annu Rev Physiol* 78: 277 – 299

Grueter CE, van Rooij E, Johnson BA, DeLeon SM, Sutherland LB, Qi X, Gautron L, Elmquist JK, Bassel-Duby R, Olson EN (2012) A cardiac microRNA governs systemic energy homeostasis by regulation of MED13. *Cell* 149: 671 – 683

Huss JM, Kelly DP (2005) Mitochondrial energy metabolism in heart failure: a question of balance. *J Clin Invest* 115: 547 – 555

Johnen H, Lin S, Kuffner T, Brown DA, Tsai VW, Bauskin AR, Wu L, Pankhurst G, Jiang L, Junankar S *et al* (2007) Tumor-induced anorexia and weight loss are mediated by the TGF-beta superfamily cytokine MIC-1. *Nat Med* 13: 1333 – 1340

Kakazu A, Sharma G, Bazan HE (2008) Association of protein tyrosine phosphatases (PTPs)-1B with c-Met receptor and modulation of corneal epithelial wound healing. *Invest Ophthalmol Vis Sci* 49: 2927 – 2935

Karsenty G, Olson EN (2016) Bone and muscle endocrine functions: unexpected paradigms of inter-organ communication. *Cell* 164: 1248 – 1256

Kempf T, Eden M, Strelau J, Naguib M, Willenbockel C, Tongers J, Heineke J, Kotlarz D, Xu J, Molkentin JD *et al* (2006) The transforming growth factor-beta superfamily member growth-differentiation factor-15 protects the heart from ischemia/reperfusion injury. *Circ Res* 98: 351 – 360

Laakmann S, Fortmuller L, Piccini I, Grote-Wessels S, Schmitz W, Breves G, Kirchhof P, Fabritz L (2013) Minimally invasive closed-chest ultrasound-guided substance delivery into the pericardial space in mice. *Naunyn Schmiedebergs Arch Pharmacol* 386: 227 – 238

Liu S, Alexander RK, Lee CH (2014) Lipid metabolites as metabolic messengers in inter-organ communication. *Trends Endocrinol Metab* 25: 356 – 363

Magida JA, Leinwand LA (2014) Metabolic crosstalk between the heart and liver impacts familial hypertrophic cardiomyopathy. *EMBO Mol Med* 6: 482 – 495

McGrath MF, de Bold ML, de Bold AJ (2005) The endocrine function of the heart. *Trends Endocrinol Metab* 16: 469 – 477

Menon G, Poskitt EM (1985) Why does congenital heart disease cause failure to thrive? *Arch Dis Child* 60: 1134 – 1139

Milman S, Huffman DM, Barzilai N (2016) The somatotropic axis in human aging: framework for the current state of knowledge and future research. *Cell Metab* 23: 980 – 989

Montero R, Yubero D, Villarroya J, Henares D, Jou C, Rodriguez MA, Ramos F, Nascimento A, Ortez CI, Campistol J *et al* (2016) GDF-15 Is elevated in children with mitochondrial diseases and is induced by mitochondrial dysfunction. *PLoS One* 11: e0148709

Nilsson I, Johansen JE, Schalling M, Hokfelt T, Fetissov SO (2005) Maturation of the hypothalamic arcuate agouti-related protein system during postnatal development in the mouse. *Brain Res Dev Brain Res* 155: 147 – 154

Nydegger A, Bines JE (2006) Energy metabolism in infants with congenital heart disease. *Nutrition* 22: 697 – 704

Ogawa T, de Bold AJ (2014) The heart as an endocrine organ. *Endocr Connect* 3: R31 – R44

Paralkar VM, Vail AL, Grasser WA, Brown TA, Xu H, Vukicevic S, Ke HZ, Qi H, Owen TA, Thompson DD (1998) Cloning and characterization of a novel member of the transforming growth factor-beta/bone morphogenetic protein family. *J Biol Chem* 273: 13760 – 13767

Pei L, Waki H, Vaitheesvaran B, Wilpitz DC, Kurland IJ, Tontonoz P (2006) NR4A orphan nuclear receptors are transcriptional regulators of hepatic glucose metabolism. *Nat Med* 12: 1048 – 1055

Pei L, Leblanc M, Barish G, Atkins A, Nofsinger R, Whyte J, Gold D, He M, Kawamura K, Li HR *et al* (2011) Thyroid hormone receptor repression is linked to type I pneumocyte-associated respiratory distress syndrome. *Nat Med* 17: 1466 – 1472

Pei L, Mu Y, Leblanc M, Alaynick W, Barish GD, Pankratz M, Tseng TW, Kaufman S, Liddle C, Yu RT *et al* (2015) Dependence of hippocampal function on ERRgamma-regulated mitochondrial metabolism. *Cell Metab* 21: 628 – 636

Peng J, Fu J, Deng SZ, Wang RG, Liu L, Sun DM, Xia K (2013) Changes in serum insulin-like growth factor-1 and insulin-like growth factor-binding protein-3, and their significance in children with left-to-right shunt congenital heart disease associated with heart failure. *Zhongguo Dang Dai Er Ke Za Zhi* 15: 277 – 280

Pilecka I, Whatmore A, Hooft van Huijsduijnen R, Destenaves B, Clayton P (2007) Growth hormone signalling: sprouting links between pathways, human genetics and therapeutic options. *Trends Endocrinol Metab* 18: 12 – 18

Poskitt EM (1993) Failure to thrive in congenital heart disease. *Arch Dis Child* 68: 158 – 160

Potthoff MJ, Kliewer SA, Mangelsdorf DJ (2012) Endocrine fibroblast growth factors 15/19 and 21: from feast to famine. *Genes Dev* 26: 312 – 324

Rigacci S, Talini D, Berti A (2003) LMW-PTP associates and dephosphorylates STAT5 interacting with its C-terminal domain. *Biochem Biophys Res Commun* 312: 360 – 366

Rotwein P (2012) Mapping the growth hormone–Stat5b–IGF-I transcriptional circuit. *Trends Endocrinol Metab* 23: 186 – 193

Savage MO, Hwa V, David A, Rosenfeld RG, Metherell LA (2011) Genetic defects in the growth hormone-IGF-I axis causing growth hormone insensitivity and impaired linear growth. *Front Endocrinol (Lausanne)* 2: 95

Shimano M, Ouchi N, Walsh K (2012) Cardiokines: recent progress in elucidating the cardiac secretome. *Circulation* 126: e327 – e332

Sorenson CM, Sheibani N (2002) Altered regulation of SHP-2 and PTP 1B tyrosine phosphatases in cystic kidneys from bcl-2 -/- mice. *Am J Physiol Renal Physiol* 282: F442 – F450

Stefan N, Haring HU (2013) The role of hepatokines in metabolism. *Nat Rev Endocrinol* 9: 144 – 152

Surmeli-Onay O, Cindik N, Kinik ST, Ozkan S, Bayraktar N, Tokel K (2011) The effect of corrective surgery on serum IGF-1, IGFBP-3 levels and growth in children with congenital heart disease. *J Pediatr Endocrinol Metab* 24: 483 – 487

Tsai VW, Macia L, Johnen H, Kuffner T, Manadhar R, Jorgensen SB, Lee-Ng KK, Zhang HP, Wu L, Marquis CP *et al* (2013) TGF-b superfamily cytokine MIC-1/GDF15 is a physiological appetite and body weight regulator. *PLoS One* 8: e55174

Unsicker K, Spittau B, Krieglstein K (2013) The multiple facets of the TGF-beta family cytokine growth/differentiation factor-15/macrophage inhibitory cytokine-1. *Cytokine Growth Factor Rev* 24: 373 – 384

Villena JA, Kralli A (2008) ERRalpha: a metabolic function for the oldest orphan. *Trends Endocrinol Metab* 19: 269 – 276

Wang GX, Zhao XY, Lin JD (2015a) The brown fat secretome: metabolic functions beyond thermogenesis. *Trends Endocrinol Metab* 26: 231 – 237

Wang T, McDonald C, Petrenko NB, Leblanc M, Giguere V, Evans RM, Patel VV, Pei L (2015b) Estrogen-related receptor alpha (ERRalpha) and ERRgamma are essential coordinators of cardiac metabolism and function. *Mol Cell Biol* 35: 1281 – 1298

Wollert KC, Kempf T (2012) Growth differentiation factor 15 in heart failure: an update. *Curr Heart Fail Rep* 9: 337 – 345

Wollert KC, Kempf T, Wallentin L (2017) Growth differentiation factor 15 as a biomarker in cardiovascular disease. *Clin Chem* 63: 140 – 151

Xu J, Kimball TR, Lorenz JN, Brown DA, Bauskin AR, Klevitsky R, Hewett TE, Breit SN, Molkentin JD (2006) GDF15/MIC-1 functions as a protective and antihypertrophic factor released from the myocardium in association with SMAD protein activation. *Circ Res* 98: 342 – 350

Yancy CW, Jessup M, Bozkurt B, Butler J, Casey DE Jr, Drazner MH, Fonarow GC, Geraci SA, Horwich T, Januzzi JL *et al* (2013) 2013 ACCF/AHA guideline for the management of heart failure: a report of the American College of Cardiology Foundation/American Heart Association Task Force on practice guidelines. *Circulation* 128: e240 – e327

Yatsuga S, Fujita Y, Ishii A, Fukumoto Y, Arahata H, Kakuma T, Kojima T, Ito M, Tanaka M, Saiki R *et al* (2015) Growth differentiation factor 15 as a useful biomarker for mitochondrial disorders. *Ann Neurol* 78: 814 – 823

Yokoyama-Kobayashi M, Saeki M, Sekine S, Kato S (1997) Human cDNA encoding a novel TGF-beta superfamily protein highly expressed in placenta. *J Biochem* 122: 622 – 626

Zhang Y, Proenca R, Maffei M, Barone M, Leopold L, Friedman JM (1994) Positional cloning of the mouse obese gene and its human homologue. *Nature* 372: 425 – 432

APPENDIX

GDF15 is a heart-derived hormone that regulates body growth

Ting Wang[1,2,#,‡], Jian Liu[1,2,#], Caitlin McDonald[1,2], Katherine Lupino[1,2], Xiandun Zhai[1,2,5], Benjamin J. Wilkins[2], Hakon Hakonarson[3], Liming Pei[1,2,4*]

This appendix includes 4 figures and 5 tables.

Table of Contents **Page**

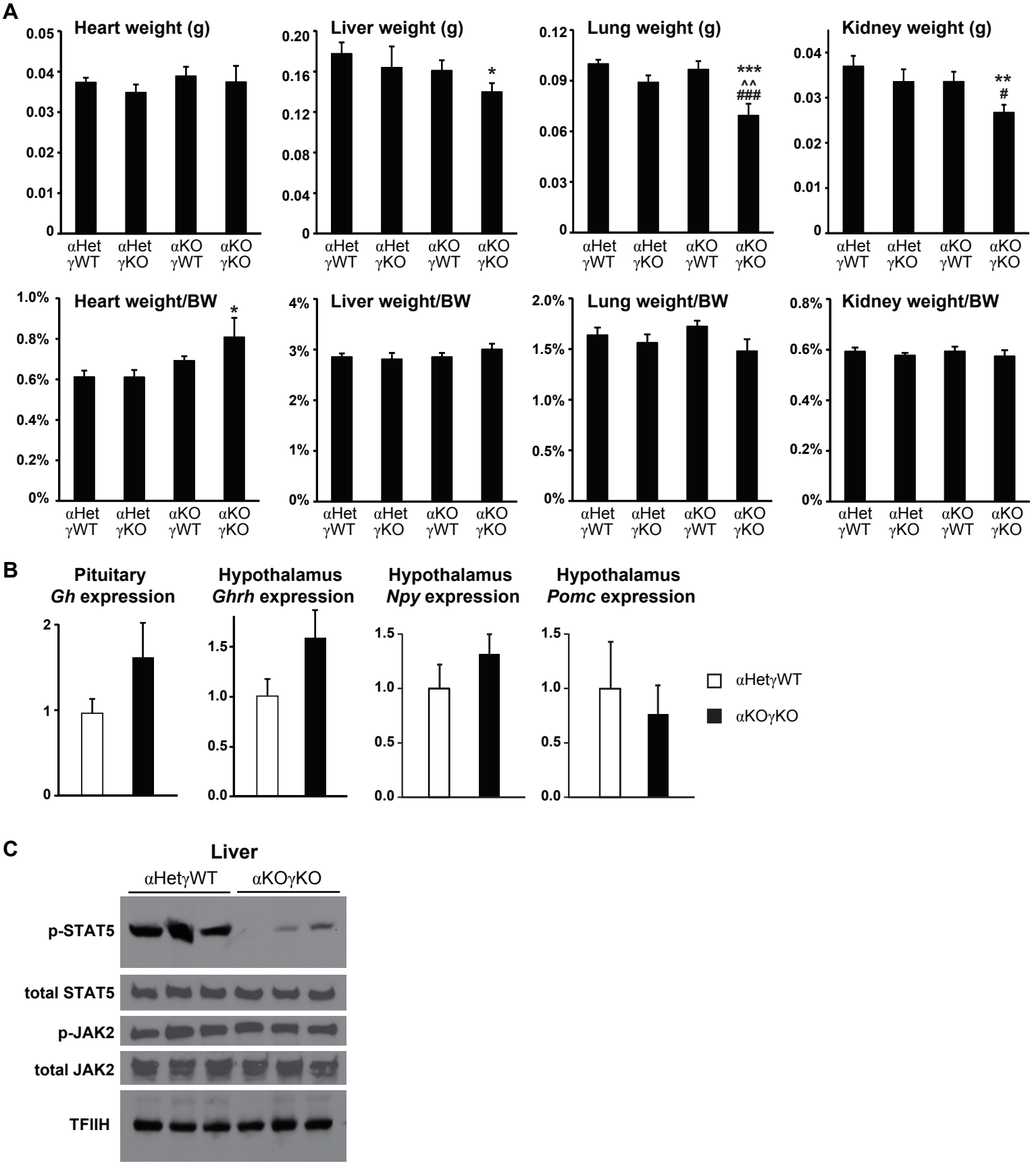

Appendix Figure S1. FTT and impaired liver GH signaling in αKOγKO mice.

A Absolute (top) and relative weight (bottom, normalized to body weight of individual mouse) of different organs in 10-day-old littermate mice (n=6-9 mice per grop). *p<0.05, **p<0.01 and ***p<0.001 between αKOγKO and αHetγWT; ^^p<0.01 between αKOγKO and αHetγKO; #p<0.05 and ###p<0.001 between αKOγKO and αKOγWT by t-test.

B Expression of pituitary *Gh* and hypothalamus *Ghrh*, *Npy* and *Pomc* in 10-day-old littermate mice was determined by qPCR (n=9 mice per group). All values are presented as mean + s.e.m.

C Phosphorylated and total STAT5 and JAK2 levels in 16-day-old littermate mouse livers (n=3 mice per group) were determined by Western blot. TFIIH serves as loading control.

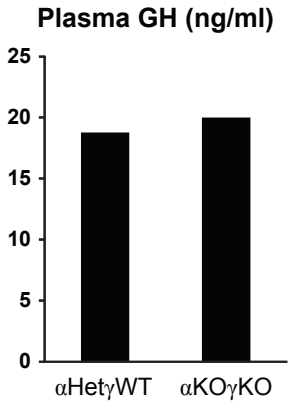

Appendix Figure S2. GH concentration in pooled plasma used to treat WT mouse primary hepatocytes.

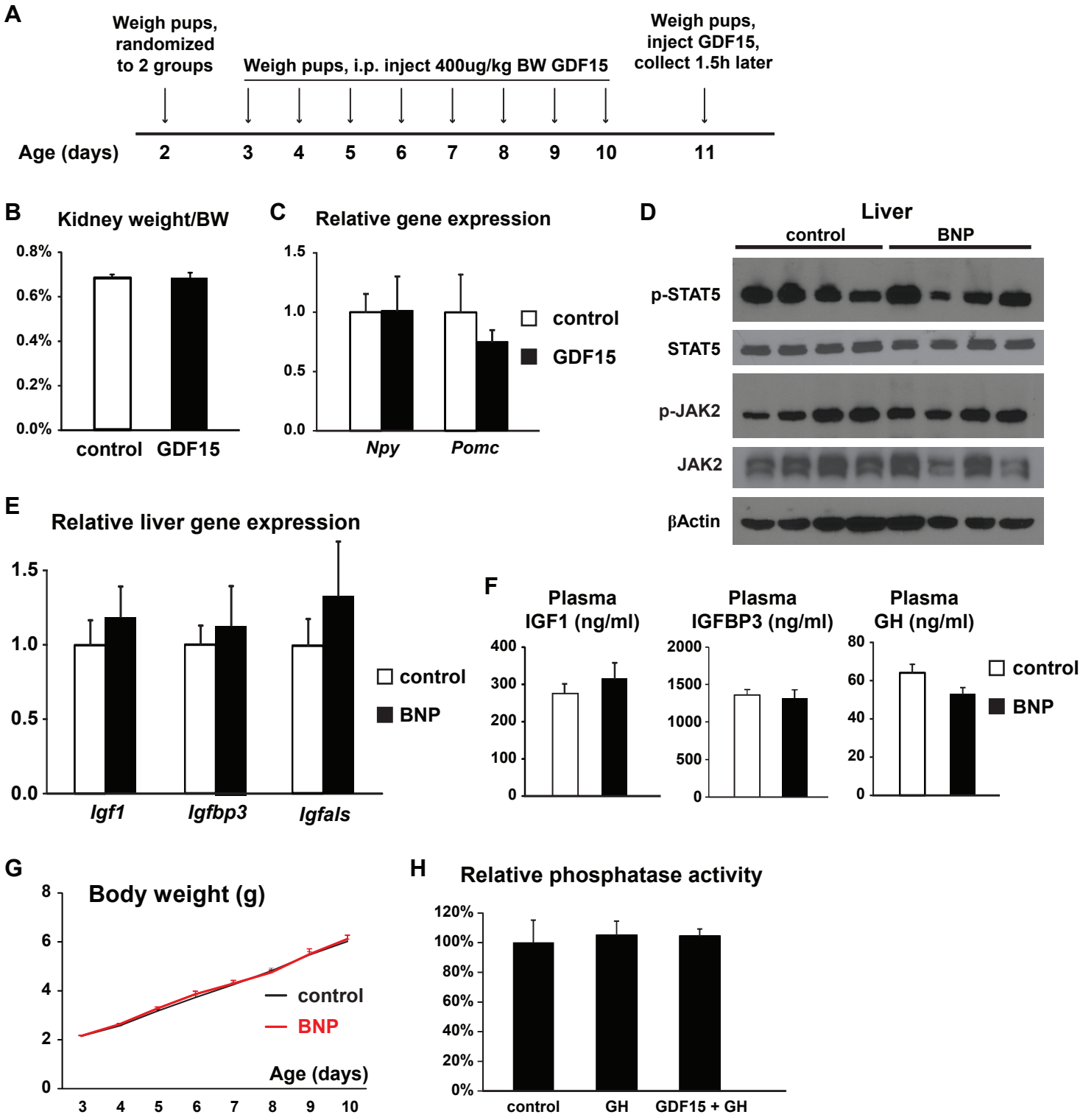

Appendix Figure S3. Impact of GDF15 and BNP on liver GH signaling and body growth.

A Scheme of long term GDF15 treatment in young WT mice. A similar scheme is used for long term BNP treatment in young WT mice.

B Relative kidney weight (normalized to body weight of individual mouse) of weight and gender-matched littermate WT mice injected with control or GDF15 (n=5).

C Expression of hypothalamic *Npy* and *Pomc* in weight and gender-matched littermate WT mice injected with control or GDF15 (n=5).

D-G Liver phosphorylated and total STAT5 and JAK2 levels (D), liver expression of STAT5 target genes *Igf1*, *Igfbp3* and *Igfals* (E), plasma IGF1, IGFBP3 and GH concentrations (F), and body weight (G) in weight and gender-matched littermate WT mice injected with control or BNP (n=4 mice per group, 500 µg/kg BW daily i.p. injection from 3 days of age).

H Overnight-fasted (in DMEM) WT mouse primary hepatocytes (n=2) were first treated with 2 ng/ml GDF15 for 30 minutes, and then with 20 ng/ml GH for 15 minutes. Protein tyrosine phosphotase activities were measured and normalized to total cellular protein amount.

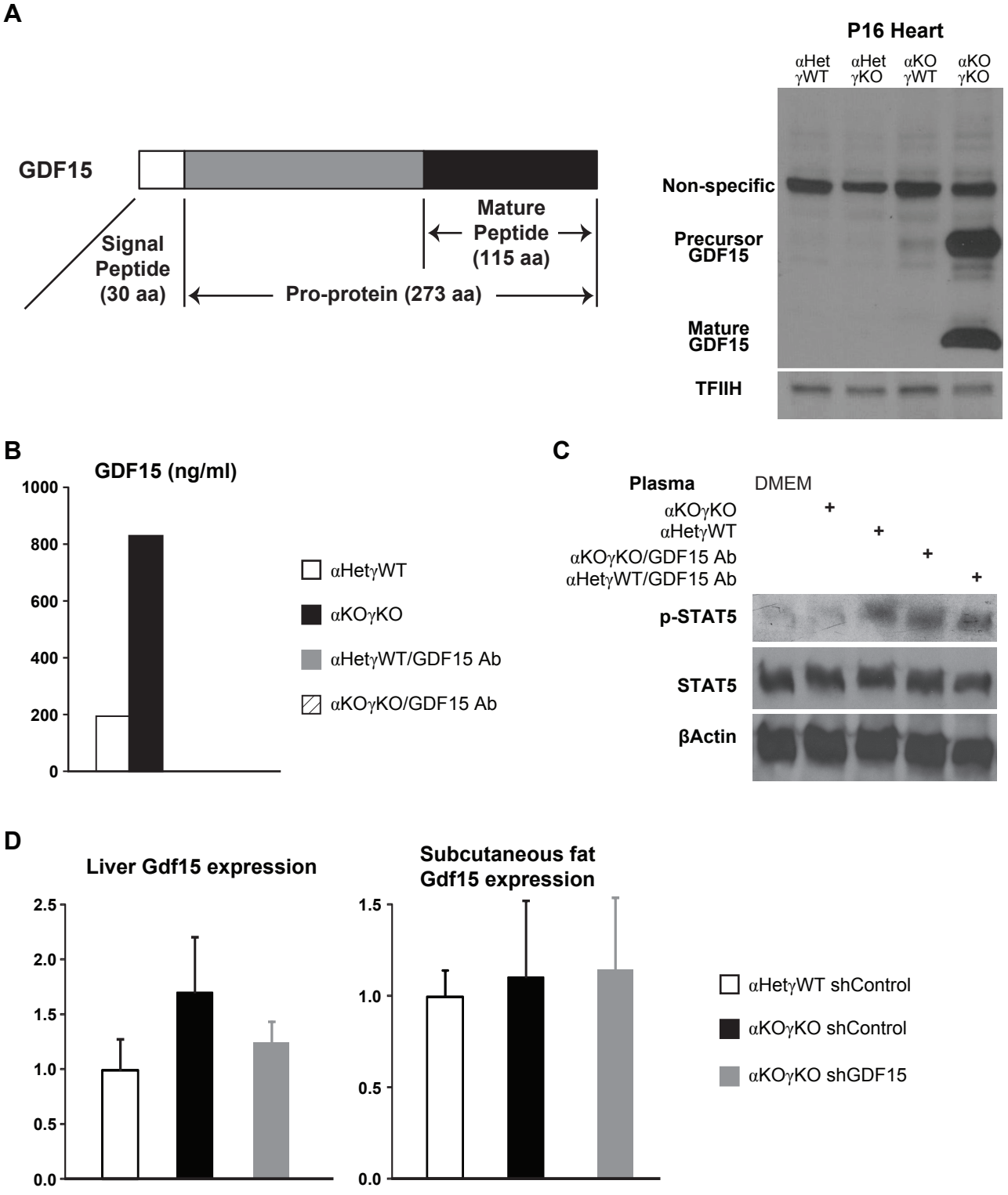

Appendix Figure S4. GDF15 is a major circulating factor in αKOγKO plasma that inhibits hepatocyte GH signaling.

A Left: primary structure of mouse GDF15 protein (based on NP_035949.2). Right: GDF15 protein level in 16-day-old littermate mouse hearts determined by Western blot. TFIIH serves as loading control.

B Plasma GDF15 levels before and after GDF15 antibody incubation were measured by ELISA.

C WT mouse primary hepatocytes were treated for 1 hour with DMEM (control) or mouse plasma pre-incubated with GDF15 antibody. Phosphorylated and total STAT5 were determined by Western blot with βActin as loading control.

D Liver and subcutaneous fat *Gdf15* expression in 9-10 days old littermate control and αKOγKO mice (n=8-12 mice per group) that received pericardial injection of AAV9-control or *Gdf15* shRNA at 2 days of age. Values are mean + s.e.m.

Appendix Table S1. Relative plasma protein levels in 16-day-old αHetγWT and αKOγKO mice (n=3 mice per group) measured by SOMAscan. The proteins are ordered based on fold change (last column). The proteins labeled in blue fonts (end of table) were tested in Fig 3A.

		αHetγWT			αKOγKO			αHetγWT	αKOγKO		Fold (αKOγKO
TargetFullName	EntrezGene	#1	#2	#3	#1	#2	#3	Average	Average	t-test	/αHetγWT)
Insulin-like growth factor I	IGF1	20367.7	16447.2	18374.6	1991.2	1033.9	995.5	18396.5	1340.2	0.002	0.073
Complement C1q subcomponent	C1QA C1QB C1QC	472.0	419.5	474.2	378.7	50.5	49.1	455.2	159.4	0.111	0.350
Insulin-like growth factor-binding protein 5	IGFBP5	107058.8	80090.1	95908.1	60254.3	17965.5	24462.8	94352.3	34227.5	0.025	0.363
Protein kinase B alpha/beta/gamma	AKT1 AKT2 AKT3	9017.7	8718.6	7651.4	7046.2	1055.7	1370.3	8462.6	3157.4	0.107	0.373
Platelet-derived growth factor subunit B	PDGFB	1003.7	1744.4	567.5	397.0	737.0	233.6	1105.2	455.9	0.190	0.412
Creatine kinase M-type:Creatine kinase B-type heterodimer	CKB CKM	6972.1	4723.2	4859.0	1220.9	2600.0	3269.9	5518.1	2363.6	0.030	0.428
Metalloproteinase inhibitor 3	TIMP3	18439.3	24492.2	13119.1	6810.9	13080.1	4347.4	18683.5	8079.5	0.068	0.432
Adenylate kinase isoenzyme 1	AK1	3773.9	9047.6	2458.6	1962.0	1982.3	2786.0	5093.4	2243.4	0.292	0.440
Fractalkine	CX3CL1	431.9	398.3	415.8	385.4	79.1	87.8	415.3	184.1	0.147	0.443
Kallikrein-12	KLK12	1696.5	1502.7	1726.9	1372.7	438.7	405.0	1642.0	738.8	0.098	0.450
DNA repair protein RAD51 homolog 1	RAD51	843.1	744.8	817.2	700.1	193.9	191.0	801.7	361.7	0.118	0.451
Semaphorin-3E	SEMA3E	188.7	159.8	224.2	92.2	80.6	89.2	190.9	87.3	0.027	0.457
Serine/threonine-protein kinase PAK 3	PAK3	611.0	543.6	584.4	525.6	136.8	140.7	579.7	267.7	0.134	0.462
Protein kinase C beta type (splice variant beta-II)	PRKCB	185.4	432.4	204.0	169.6	135.5	85.6	273.9	130.2	0.206	0.475
Angiopoietin-1	ANGPT1	2019.6	2355.6	1394.5	912.0	1140.4	706.2	1923.2	919.5	0.053	0.478
Cathepsin D	CTSD	1228.6	1238.4	1256.4	1164.6	342.5	322.6	1241.1	609.9	0.151	0.491
Interleukin-37	IL37	493.3	391.8	412.1	425.4	110.2	114.2	432.4	216.6	0.167	0.501
Vascular cell adhesion protein 1	VCAM1	2918.5	2556.6	2665.1	2788.4	768.6	655.5	2713.4	1404.2	0.197	0.517
Casein kinase II 2-alpha:2-beta heterotetramer	CSNK2A1 CSNK2B	2185.0	5778.1	5298.0	1695.8	3429.1	1807.0	4420.4	2310.6	0.194	0.523
Fibroblast growth factor 1	FGF1	1719.8	3544.5	1345.0	813.0	818.3	1865.9	2203.1	1165.7	0.268	0.529
Tyrosine-protein kinase ZAP-70	ZAP70	1725.8	1626.3	1740.7	1697.4	499.9	509.9	1697.6	902.4	0.183	0.532
Allograft inflammatory factor 1	AIF1	938.4	1290.3	1326.1	826.2	619.8	475.5	1184.9	640.5	0.029	0.541
Probable G-protein coupled receptor 114	GPR114	217.5	215.2	215.8	192.3	79.1	84.9	216.2	118.8	0.118	0.549
Lymphotoxin alpha2:beta1	LTA LTB	710.0	725.2	823.8	562.0	359.6	325.1	753.0	415.6	0.028	0.552

Tumor necrosis factor receptor superfamily member 11B	TNFRSF11B	4213.5	4039.8	4607.0	3561.5	1887.3	1775.5	4286.8	2408.1	0.073	0.562
Apolipoprotein E	APOE	481.6	596.7	549.8	449.8	257.5	209.0	542.7	305.4	0.066	0.563
High mobility group protein B1	HMGB1	2420.9	4841.1	2904.2	2270.1	1760.2	1707.3	3388.7	1912.5	0.178	0.564
Glutamate carboxypeptidase 2	FOLH1	1091.8	1003.9	1086.2	1022.7	387.6	404.8	1060.6	605.0	0.159	0.570
Cyclin-dependent kinase 5:Cyclin-dependent kinase 5 activator 1 complex	CDK5 CDK5R1	624.6	562.8	603.9	595.0	211.7	223.2	597.1	343.3	0.179	0.575
Corticotropin	POMC	539.9	471.6	779.6	467.8	256.0	309.9	597.0	344.6	0.098	0.577
Pulmonary surfactant-associated protein D	SFTPD	52307.4	82092.6	61360.4	28529.0	43598.7	42521.2	65253.5	38216.3	0.072	0.586
Aspartate aminotransferase, cytoplasmic	GOT1	9515.1	6838.2	7210.2	4459.6	4648.8	4736.2	7854.5	4614.9	0.059	0.588
Junctional adhesion molecule B	JAM2	1056.2	1269.6	1306.5	793.6	703.7	644.0	1210.8	713.8	0.010	0.590
Mast/stem cell growth factor receptor Kit	KIT	265.1	292.3	283.2	243.0	129.8	125.3	280.2	166.0	0.092	0.593
Interleukin-16	IL16	2110.4	2468.2	1978.9	2215.4	781.5	933.8	2185.8	1310.2	0.186	0.599
GTP-binding nuclear protein Ran	RAN	185.9	672.8	434.4	300.5	260.6	214.5	431.0	258.5	0.344	0.600
Fatty acid-binding protein, heart	FABP3	5997.2	11190.9	3333.2	4433.5	3350.1	4614.3	6840.4	4132.6	0.361	0.604
Complement component C8	C8A C8B C8G	1163.3	1083.6	1135.2	1079.3	497.8	480.6	1127.4	685.9	0.152	0.608
Advanced glycosylation end product-specific receptor, soluble	AGER	116.6	92.6	227.2	96.4	82.8	86.7	145.5	88.6	0.303	0.609
Death-associated protein kinase 2	DAPK2	2090.1	3956.5	4529.6	1854.2	3069.6	1535.8	3525.4	2153.2	0.203	0.611
Chordin-like protein 1	CHRDL1	1591.4	1473.0	1503.1	1671.7	482.8	637.2	1522.5	930.6	0.253	0.611
Cofilin-1	CFL1	1693.2	1763.7	1829.1	1525.9	894.8	853.9	1762.0	1091.5	0.087	0.619
Vascular endothelial growth factor receptor 3	FLT4	9553.3	8203.5	8573.0	5188.6	5876.8	5294.3	8776.6	5453.2	0.005	0.621
Low molecular weight phosphotyrosine protein phosphatase	ACP1	588.8	985.2	1036.3	502.0	673.1	447.2	870.1	540.8	0.131	0.621
Interleukin-13 receptor subunit alpha-1	IL13RA1	490.7	429.8	417.8	279.8	259.9	292.2	446.1	277.3	0.009	0.622
Gro-beta/gamma	CXCL3 CXCL2	4833.9	5662.7	4810.7	3113.2	4382.4	2029.6	5102.4	3175.1	0.089	0.622
Complement C3b, inactivated	C3	4759.4	3942.3	4107.1	1640.6	3279.3	3120.9	4269.6	2680.3	0.074	0.628
Follicle stimulating hormone	CGA FSHB	100.7	69.5	98.7	71.2	56.4	42.3	89.6	56.6	0.067	0.632
Carbonic anhydrase-related protein 10	CA10	248.9	217.6	238.3	241.5	100.1	105.3	234.9	149.0	0.201	0.634
Ubiquitin-conjugating enzyme E2 N	UBE2N	11433.4	18023.0	20659.9	9203.8	13578.8	9297.2	16705.4	10693.3	0.147	0.640
Importin subunit beta-1	KPNB1	10500.6	21177.2	18454.6	9694.0	16446.2	6174.7	16710.8	10771.6	0.248	0.645
Coagulation Factor V	F5	36228.4	32792.6	30620.4	19819.5	17323.1	27130.7	33213.8	21424.4	0.037	0.645

Tumor necrosis factor receptor superfamily member 3	LTBR	2008.3	1930.8	2195.6	1726.5	1164.7	1088.5	2044.9	1326.6	0.055	0.649
Stress-induced-phosphoprotein 1	STIP1	11072.7	22296.9	21811.6	9894.9	16575.8	9379.6	18393.7	11950.1	0.224	0.650
Tartrate-resistant acid phosphatase type 5	ACP5	3975.4	3474.6	3963.9	2631.5	2077.7	2794.7	3804.6	2501.3	0.010	0.657
Copine-1	CPNE1	167.1	313.9	286.6	169.1	200.7	135.4	255.9	168.4	0.182	0.658
Biglycan	BGN	4608.8	3740.4	3769.2	3510.8	2428.7	2066.7	4039.5	2668.7	0.067	0.661
Vacuolar protein sorting-associated protein VTA1 homolog	VTA1	1999.7	3679.6	3586.7	1864.0	2665.2	1658.1	3088.7	2062.4	0.195	0.668
Ectodysplasin-A, secreted form	EDA	774.1	704.2	806.6	759.6	382.7	387.5	761.6	509.9	0.176	0.670
Hemoglobin	HBA1 HBB	77662.6	76719.8	85462.7	76318.8	85684.1	134.4	79948.4	54045.8	0.440	0.676
Insulin-like growth factor-binding protein 4	IGFBP4	208.7	213.3	217.7	148.6	145.9	141.1	213.2	145.2	0.000	0.681
Secreted frizzled-related protein 3	FRZB	1397.3	1409.4	1442.7	1370.3	754.0	770.2	1416.5	964.8	0.155	0.681
Killer cell immunoglobulin-like receptor 2DL4	KIR2DL4	382.4	754.5	637.8	335.5	558.3	319.4	591.6	404.4	0.243	0.684
Ephrin type-A receptor 1	EPHA1	1062.9	780.8	780.3	665.9	616.8	512.6	874.7	598.4	0.081	0.684
Desmoglein-1	DSG1	999.3	986.9	1024.7	962.4	544.9	556.2	1003.6	687.8	0.147	0.685
Tropomyosin beta chain	TPM2	1228.4	1004.2	1160.8	1208.5	532.7	591.2	1131.1	777.5	0.239	0.687
Heterogeneous nuclear ribonucleoprotein A/B	HNRNPAB	11107.5	16724.1	14947.5	9448.2	10251.8	9761.4	14259.7	9820.5	0.113	0.689
Connective tissue growth factor	CTGF	724.5	687.2	639.2	438.0	438.8	538.0	683.6	471.6	0.008	0.690
Apoptosis regulator Bcl-2	BCL2	327.0	379.4	374.3	279.5	245.4	221.3	360.2	248.7	0.009	0.690
Transforming growth factor beta-1	TGFB1	816.0	809.0	829.6	708.0	476.3	511.4	818.2	565.2	0.072	0.691
C-C motif chemokine 28	CCL28	301.3	304.2	338.5	286.7	178.4	190.0	314.7	218.4	0.094	0.694
GDNF family receptor alpha-2	GFRA2	4763.1	4227.6	4219.1	3202.9	3335.5	2676.2	4403.3	3071.5	0.008	0.698
Receptor-type tyrosine-protein kinase FLT3	FLT3	876.8	1355.0	1404.8	777.0	1018.7	753.5	1212.2	849.7	0.152	0.701
Phosphatidylinositol 4,5-bisphosphate 3-kinase catalytic subunit gamma isoform	PIK3CG	516.5	525.6	497.8	507.7	295.0	276.8	513.3	359.8	0.173	0.701
Proliferation-associated protein 2G4	PA2G4	6892.6	14550.7	14139.9	7361.2	11707.7	5895.8	11861.1	8321.6	0.316	0.702
Inosine-5'-monophosphate dehydrogenase 1	IMPDH1	4061.4	7371.6	7048.4	3335.5	5908.2	3723.2	6160.5	4322.3	0.242	0.702
Cyclin-dependent kinase 8:Cyclin-C complex	CDK8 CCNC	571.5	564.4	573.1	557.9	322.2	319.4	569.7	399.8	0.165	0.702
Reticulon-4 receptor	RTN4R	2131.8	1738.9	1991.1	1486.8	1145.8	1499.2	1953.9	1377.3	0.024	0.705
Thyroid peroxidase	TPO	860.4	851.8	973.3	753.2	558.5	597.2	895.2	636.3	0.028	0.711
Junctional adhesion molecule C	JAM3	703.4	1118.3	1063.2	560.4	848.8	642.5	961.6	683.9	0.160	0.711

Peptidyl-prolyl cis-trans isomerase D	PPID	2997.9	4964.9	5261.4	2568.0	4466.5	2379.0	4408.1	3137.8	0.262	0.712
NAD-dependent protein deacetylase sirtuin-2	SIRT2	12524.9	21262.8	23076.5	11701.0	17447.1	11488.9	18954.7	13545.7	0.242	0.715
Protein kinase C alpha type	PRKCA	2126.4	4335.7	2317.3	2455.7	2882.6	941.2	2926.5	2093.2	0.418	0.715
Cyclin-dependent kinase 2:Cyclin-A2 complex	CDK2 CCNA2	575.8	803.9	711.1	425.5	598.9	471.5	696.9	498.6	0.082	0.715
40S ribosomal protein S7	RPS7	3169.6	9696.9	5757.9	3896.2	7255.8	2175.5	6208.1	4442.5	0.507	0.716
Inorganic pyrophosphatase	PPA1	11346.6	9789.0	10668.8	7743.4	8035.2	7040.7	10601.5	7606.4	0.008	0.717
beta-adrenergic receptor kinase 1	ADRBK1	847.6	1339.3	955.0	779.9	819.7	661.6	1047.3	753.7	0.180	0.720
Low affinity immunoglobulin epsilon Fc receptor	FCER2	442.6	457.0	459.3	410.3	294.9	273.5	453.0	326.2	0.094	0.720
Heparin cofactor 2	SERPIND1	95764.5	74814.3	87775.9	58372.6	60809.2	67000.0	86118.2	62060.6	0.043	0.721
Drebrin-like protein	DBNL	637.2	1249.4	874.9	639.1	802.0	550.8	920.5	664.0	0.286	0.721
L-Selectin	SELL	337.1	591.9	461.4	305.4	399.7	298.8	463.5	334.6	0.216	0.722
Inhibin beta A chain	INHBA	5163.8	3713.7	3976.2	3748.0	2505.3	3084.7	4284.6	3112.7	0.113	0.726
Ribosomal protein S6 kinase alpha-5	RPS6KA5	37.5	60.5	50.0	29.8	44.7	33.3	49.3	35.9	0.180	0.728
SUMO-conjugating enzyme UBC9	UBE2I	3358.5	4891.9	4686.4	2798.2	3714.6	2957.2	4312.3	3156.7	0.123	0.732
Troponin I, cardiac muscle	TNNI3	5299.9	14526.6	2844.7	5743.2	2784.1	8071.2	7557.1	5532.8	0.641	0.732
Growth/differentiation factor 5	GDF5	359.0	397.8	387.1	285.7	287.7	265.7	381.3	279.7	0.004	0.734
Amphiregulin	AREG	456.2	745.1	707.8	382.6	590.4	427.8	636.4	466.9	0.208	0.734
Cytokine receptor common subunit gamma	IL2RG	548.5	915.9	814.4	452.5	703.3	518.6	759.6	558.1	0.213	0.735
Rab GDP dissociation inhibitor beta	GDI2	40349.5	41216.1	44228.0	29558.4	36189.8	26715.0	41931.2	30821.1	0.043	0.735
Pyridoxal phosphate phosphatase	PDXP	586.2	986.4	936.5	458.7	795.9	590.8	836.4	615.1	0.242	0.735
Tumor necrosis factor receptor superfamily member 13B	TNFRSF13B	243.6	251.0	251.1	220.0	158.7	171.2	248.6	183.3	0.071	0.737
Serine/threonine-protein kinase receptor R3	ACVRL1	337.7	373.9	376.3	294.1	263.8	244.9	362.6	267.6	0.008	0.738
Arginase-1	ARG1	352.7	363.8	352.4	335.6	222.6	230.9	356.3	263.0	0.123	0.738
Cadherin-12	CDH12	200.3	286.2	254.4	166.3	201.8	179.3	247.0	182.5	0.109	0.739
Fibroblast growth factor 16	FGF16	397.7	600.8	544.0	317.1	474.6	351.0	514.2	380.9	0.163	0.741
Catalase	CAT	7708.6	14513.2	17354.0	7615.3	15381.2	6394.7	13191.9	9797.1	0.445	0.743
Complement factor H-related protein 5	CFHR5	221.1	347.2	275.8	197.8	240.1	189.4	281.4	209.1	0.176	0.743
Coagulation Factor X	F10	250.6	237.4	213.8	186.2	153.7	182.4	233.9	174.1	0.016	0.744
Protein jagged-1	JAG1	2485.9	2039.0	2122.1	1785.3	1480.9	1706.4	2215.7	1657.5	0.034	0.748
Complement factor D	CFD	558.4	513.0	559.4	563.7	330.9	326.6	543.6	407.1	0.220	0.749

Superoxide dismutase [Cu-Zn]	SOD1	245.5	365.9	332.2	213.6	272.3	222.2	314.5	236.0	0.147	0.750
Dickkopf-like protein 1	DKKL1	1383.1	2116.0	2060.5	1209.5	1757.5	1207.6	1853.2	1391.5	0.201	0.751
Programmed cell death 1 ligand 2	PDCD1LG2	228.8	361.4	312.0	187.3	290.0	200.8	300.7	226.0	0.214	0.752
Creatine kinase M-type	CKM	2309.6	2173.7	1560.7	1412.2	1471.9	1660.3	2014.7	1514.8	0.153	0.752
Platelet-derived growth factor subunit A	PDGFA	344.6	435.6	367.1	271.3	299.5	292.1	382.4	287.6	0.063	0.752
Interferon gamma	IFNG	237.9	371.3	327.3	204.2	276.6	225.6	312.2	235.5	0.182	0.754
Acid sphingomyelinase-like phosphodiesterase 3a	SMPDL3A	10291.2	14302.3	12579.3	7648.7	10517.8	9899.7	12390.9	9355.4	0.110	0.755
Casein kinase II 2-alpha':2-beta heterotetramer	CSNK2A2 CSNK2B	91.6	191.6	138.5	76.2	156.7	85.8	140.6	106.2	0.423	0.756
Casein kinase II subunit alpha	CSNK2A1	128.1	173.1	171.2	113.4	132.8	112.4	157.5	119.5	0.107	0.759
Glycogen synthase kinase-3 alpha/beta	GSK3A GSK3B	3503.0	5326.7	5697.3	3795.2	3892.7	3344.7	4842.3	3677.5	0.224	0.759
ATP synthase subunit beta, mitochondrial	ATP5B	621.2	627.3	768.5	582.4	521.3	432.1	672.3	511.9	0.070	0.761
Endoplasmic reticulum aminopeptidase 1	ERAP1	185.1	250.5	272.9	193.4	174.3	173.9	236.2	180.5	0.163	0.764
Prostaglandin G/H synthase 2	PTGS2	250.0	425.2	281.0	234.9	251.1	245.2	318.7	243.7	0.299	0.765
Prefoldin subunit 5	PFDN5	522.6	689.1	648.6	556.7	496.4	373.1	620.1	475.4	0.122	0.767
CD27 antigen	CD27	31173.8	25967.0	28832.9	16978.2	20783.7	28151.6	28657.9	21971.2	0.167	0.767
Delta-like protein 1	DLL1	2848.3	2392.4	2445.0	2076.7	1753.7	2067.8	2561.9	1966.1	0.033	0.767
Interleukin-23 receptor	IL23R	226.7	333.2	320.3	195.8	270.2	210.0	293.4	225.3	0.178	0.768
Interleukin-22	IL22	204.7	268.7	263.0	167.0	212.3	186.4	245.5	188.6	0.091	0.768
Platelet-activating factor acetylhydrolase IB subunit beta	PAFAH1B2	833.5	1122.4	1288.2	712.0	978.1	805.7	1081.4	831.9	0.197	0.769
Dickkopf-related protein 4	DKK4	2035.0	1896.3	2104.7	1638.9	1339.8	1666.3	2012.0	1548.3	0.028	0.770
Ubiquitin-conjugating enzyme E2 L3	UBE2L3	391.4	601.5	580.0	319.3	494.5	397.2	524.3	403.7	0.228	0.770
Desmoglein-2	DSG2	478.5	401.3	1882.6	375.0	353.2	1400.8	920.8	709.7	0.741	0.771
Protein 4.1	EPB41	2432.6	6177.9	4298.9	3550.9	4353.7	2073.4	4303.1	3326.0	0.493	0.773
Tyrosine-protein kinase Yes	YES1	567.2	728.2	767.7	522.9	605.1	466.8	687.7	531.6	0.111	0.773
Tyrosine-protein phosphatase non-receptor type 1	PTPN1	2180.8	2167.1	2198.7	2056.4	1493.3	1516.0	2182.2	1688.6	0.115	0.774
Calcineurin subunit B type 1	PPP3R1	4698.0	6486.1	6715.4	3661.5	5815.8	4403.4	5966.5	4626.9	0.210	0.775
DNA topoisomerase 1	TOP1	224.0	294.7	293.8	204.1	238.2	189.2	270.8	210.5	0.107	0.777
Tyrosine-protein kinase CSK	CSK	2982.9	4870.6	3561.9	2928.6	3792.1	2155.2	3805.1	2958.6	0.313	0.778
Endothelin-converting enzyme 1	ECE1	442.0	616.4	584.4	368.7	499.1	410.7	547.6	426.2	0.147	0.778
UMP-CMP kinase	CMPK1	2206.4	2783.7	3416.0	1734.6	2521.9	2286.8	2802.0	2181.1	0.223	0.778

Immunoglobulin G	IGHG1 IGHG2 IGHG3 IGHG4 IGK IGL	420.5	678.4	608.0	354.8	550.8	423.3	569.0	443.0	0.265	0.779
Nascent polypeptide-associated complex subunit alpha	NACA	4825.7	7647.9	8541.6	4691.5	7220.7	4477.4	7005.1	5463.2	0.343	0.780
Interleukin-1 receptor-like 2	IL1RL2	226.8	241.9	241.5	194.0	182.8	178.9	236.7	185.2	0.002	0.782
Kremen protein 2	KREMEN2	684.7	695.4	718.6	661.5	492.3	488.4	699.6	547.4	0.112	0.782
Apolipoprotein E (isoform E2)	APOE	300.1	425.7	350.8	257.2	305.7	281.2	358.9	281.4	0.156	0.784
cGMP-dependent 3',5'-cyclic phosphodiesterase	PDE2A	5359.4	7378.0	7542.4	4441.2	6685.2	4812.1	6759.9	5312.8	0.217	0.786
Histone deacetylase 8	HDAC8	723.4	740.7	773.6	736.3	511.9	513.2	745.9	587.1	0.163	0.787
1-phosphatidylinositol 4,5-bisphosphate phosphodiesterase gamma-1	PLCG1	319.0	245.9	306.5	253.9	214.9	217.5	290.5	228.8	0.093	0.788
NSFL1 cofactor p47	NSFL1C	353.0	508.6	420.5	348.4	418.9	244.6	427.4	337.3	0.255	0.789
Peroxiredoxin-6	PRDX6	1556.5	1516.6	1772.9	1249.8	1696.8	881.3	1615.3	1276.0	0.284	0.790
Interleukin-17F	IL17F	72.5	71.9	77.2	70.4	49.7	55.1	73.9	58.4	0.122	0.791
Luteinizing hormone	CGA LHB	215.4	338.5	300.2	191.9	268.4	215.9	284.7	225.4	0.251	0.792
Kallikrein-6	KLK6	1902.4	1662.5	1670.0	1455.8	1475.9	1213.2	1745.0	1381.6	0.035	0.792
40S ribosomal protein SA	RPSA	1533.8	1306.6	1415.6	1068.4	1194.0	1114.8	1418.7	1125.7	0.028	0.794
Troponin I, fast skeletal muscle	TNNI2	2539.6	2074.2	2472.6	2687.7	1262.7	1672.8	2362.1	1874.4	0.371	0.794
C-C motif chemokine 1	CCL1	1281.9	1089.4	1233.6	1236.1	795.5	832.1	1201.6	954.6	0.215	0.794
Tyrosine-protein kinase JAK2	JAK2	714.0	602.6	595.2	479.1	468.7	572.3	637.3	506.7	0.063	0.795
Matrix metalloproteinase-17	MMP17	255.5	263.4	244.5	204.6	209.3	193.6	254.5	202.5	0.002	0.796
NKG2D ligand 3	ULBP3	102.3	144.1	139.2	86.9	121.6	98.5	128.5	102.3	0.196	0.796
Coagulation factor IX	F9	126541.9	91636.1	115667.0	88241.0	79804.8	97772.4	111281.7	88606.1	0.146	0.796
Low-density lipoprotein receptor-related protein 8	LRP8	301.6	305.7	325.8	253.4	240.5	249.6	311.0	247.8	0.005	0.797
C-C motif chemokine 5	CCL5	261.9	353.2	328.6	217.0	285.0	250.2	314.6	250.7	0.137	0.797
Methionine aminopeptidase 2	METAP2	7391.9	18779.2	12962.2	10975.6	12010.2	8262.9	13044.4	10416.2	0.515	0.799
Dermatopontin	DPT	4339.3	3483.4	3549.4	3489.2	2395.9	3204.2	3790.7	3029.8	0.152	0.799
Oncostatin-M	OSM	777.6	712.1	1017.2	732.6	573.0	699.1	835.6	668.2	0.207	0.800
Adiponectin	ADIPOQ	59.7	76.0	64.5	45.9	59.6	54.6	66.7	53.4	0.103	0.800
Laminin	LAMA1 LAMB1 LAMC1	84.1	107.9	100.1	67.5	90.3	76.6	97.4	78.1	0.117	0.802
Fibroblast growth factor 8 isoform A	FGF8	69.4	101.3	94.4	63.3	83.1	66.4	88.4	70.9	0.216	0.803
Dickkopf-related protein 1	DKK1	1604.2	1540.2	1766.3	1316.1	1149.7	1482.1	1636.9	1316.0	0.059	0.804

Histone-lysine N-methyltransferase EHMT2	EHMT2	1773.6	1715.4	1913.3	1116.8	1401.3	1827.5	1800.8	1448.5	0.225	0.804
Creatine kinase B-type	CKB	1297.5	829.3	1248.5	939.7	790.3	987.8	1125.1	905.9	0.276	0.805
Mitogen-activated protein kinase 1	MAPK1	560.8	771.4	660.5	513.4	567.6	525.6	664.2	535.5	0.161	0.806
Vascular endothelial growth factor receptor 2	KDR	790.8	1179.5	1168.9	715.7	1066.8	750.3	1046.4	844.3	0.301	0.807
AH receptor-interacting protein	AIP	352.1	474.4	459.5	317.6	377.0	343.0	428.7	345.9	0.152	0.807
Transforming growth factor-beta-induced protein ig-h3	TGFBI	38395.9	30011.2	38790.0	32550.9	20924.4	33073.6	35732.4	28849.6	0.239	0.807
Vitamin K-dependent protein C	PROC	149.3	205.4	180.9	140.3	154.6	137.7	178.5	144.2	0.160	0.808
Calcium/calmodulin-dependent protein kinase kinase 1	CAMKK1	212.3	326.1	291.0	192.0	266.5	212.1	276.5	223.5	0.270	0.809
Calcium/calmodulin-dependent protein kinase type II subunit beta	CAMK2B	505.9	732.5	445.1	471.2	447.5	444.0	561.2	454.2	0.346	0.809
Membrane frizzled-related protein	MFRP	101823.6	93145.0	79481.5	75435.7	78689.1	68222.9	91483.4	74115.9	0.099	0.810
Fibroblast growth factor receptor 2	FGFR2	268.7	77.4	356.6	191.1	74.9	303.4	234.2	189.8	0.696	0.810
3-hydroxy-3-methylglutaryl-coenzyme A reductase	HMGCR	148.5	162.9	149.0	141.5	111.9	119.7	153.5	124.4	0.061	0.810
Neurexophilin-1	NXPH1	1291.4	1424.1	1119.1	1108.6	1107.9	895.9	1278.2	1037.5	0.104	0.812
Alcohol dehydrogenase [NADP(+)]	AKR1A1	38392.8	28180.0	30431.5	25927.6	29308.4	23594.2	32334.8	26276.7	0.181	0.813
Inhibitor of growth protein 1	ING1	842.2	1126.9	1118.7	677.5	930.4	902.4	1029.3	836.8	0.195	0.813
Extracellular matrix protein 1	ECM1	226.1	223.4	231.4	235.9	162.2	155.9	227.0	184.7	0.241	0.814
Tumor necrosis factor ligand superfamily member 11	TNFSF11	197.4	222.7	239.0	179.8	191.2	165.5	219.7	178.8	0.056	0.814
Cyclin-dependent kinase inhibitor 1B	CDKN1B	290.4	414.4	393.1	294.9	308.8	290.2	366.0	298.0	0.216	0.814
C-X-C motif chemokine 5	CXCL5	274.6	291.3	319.2	246.6	240.4	233.8	295.0	240.3	0.043	0.814
SLIT and NTRK-like protein 5	SLITRK5	2088.8	1373.8	1574.7	1539.6	1114.2	1449.8	1679.1	1367.9	0.293	0.815
Ubiquitin	RPS27A	57186.6	70672.6	86911.8	58837.3	65149.3	51144.9	71590.3	58377.2	0.263	0.815
Seizure 6-like protein 2	SEZ6L2	350.4	501.1	471.7	287.5	423.4	368.8	441.1	359.9	0.254	0.816
Kinesin-like protein KIF23	KIF23	151.6	234.3	204.8	148.8	184.4	148.9	196.9	160.7	0.274	0.816
Malate dehydrogenase, cytoplasmic	MDH1	138773.9	136748.8	100111.6	92786.3	106056.0	107943.8	125211.4	102262.0	0.201	0.817
Beta-endorphin	POMC	148.0	140.0	182.4	145.1	113.1	126.0	156.8	128.1	0.154	0.817
Neuronal cell adhesion molecule	NRCAM	1036.5	821.9	944.6	760.7	688.1	841.0	934.3	763.3	0.096	0.817
Calcium/calmodulin-dependent protein kinase type II subunit delta	CAMK2D	1495.9	1889.6	1267.0	1309.2	1266.6	1225.3	1550.8	1267.0	0.258	0.817
Protein disulfide-isomerase A3	PDIA3	705.4	987.9	995.7	612.8	890.4	693.9	896.3	732.4	0.265	0.817

Opioid-binding protein/cell adhesion molecule	OPCML	1859.8	1685.5	1712.2	1586.6	1535.2	1175.9	1752.5	1432.6	0.117	0.817
SHC-transforming protein 1	SHC1	2972.5	3943.6	4153.6	2950.5	3589.6	2519.4	3689.9	3019.8	0.236	0.818
Interleukin-2 receptor subunit alpha	IL2RA	1223.1	362.7	379.3	953.5	319.3	337.1	655.0	536.6	0.755	0.819
Decorin	DCN	186.3	259.6	234.6	167.3	214.3	176.0	226.8	185.9	0.199	0.819
Bone morphogenetic protein 1	BMP1	9811.2	7872.6	8696.7	6776.5	6628.3	8212.3	8793.5	7205.7	0.104	0.819
Peptidyl-prolyl cis-trans isomerase E	PPIE	244.3	343.7	326.7	241.0	272.4	237.3	304.9	250.2	0.210	0.821
Kallikrein-14	KLK14	2327.6	3316.6	3199.5	1992.8	3026.5	2242.6	2947.9	2420.6	0.298	0.821
Calcium/calmodulin-dependent protein kinase type 1D	CAMK1D	661.3	624.0	677.5	623.5	484.7	503.7	654.3	537.3	0.101	0.821
Hyaluronan and proteoglycan link protein 1	HAPLN1	24298.0	18879.8	21487.2	17632.5	16137.4	19334.8	21555.0	17701.6	0.117	0.821
Complement component C6	C6	492.5	549.8	523.6	385.2	449.8	453.2	522.0	429.4	0.032	0.823
Eukaryotic translation initiation factor 5A-1	EIF5A	11847.4	24206.0	21496.3	15059.0	20667.2	11695.4	19183.2	15807.2	0.506	0.824
Ephrin type-B receptor 6	EPHB6	12137.9	8943.9	11473.0	9973.8	7448.5	9416.0	10851.6	8946.1	0.203	0.824
Macrophage scavenger receptor types I and II	MSR1	319.1	368.2	390.0	242.6	311.0	336.3	359.1	296.6	0.154	0.826
DnaJ homolog subfamily B member 1	DNAJB1	116.1	230.2	210.2	138.7	200.9	120.4	185.5	153.3	0.499	0.827
Mannose-binding protein C	MBL2	217.1	302.4	285.6	179.1	248.1	238.8	268.4	222.0	0.245	0.827
Retinol-binding protein 4	RBP4	344.1	535.1	413.9	362.1	402.5	308.8	431.0	357.8	0.326	0.830
Serine/threonine-protein kinase 17B	STK17B	1511.6	1950.7	2170.9	1316.6	1799.1	1562.5	1877.7	1559.4	0.260	0.830
Growth-regulated alpha protein	CXCL1	394.4	427.5	453.3	341.1	366.5	351.5	425.1	353.0	0.036	0.831
Retinoic acid receptor responder protein 2	RARRES2	84182.5	68765.5	76084.7	66721.4	51617.8	72024.0	76344.2	63454.4	0.170	0.831
Heterogeneous nuclear ribonucleoproteins A2/B1	HNRNPA2B1	36132.1	40899.8	39119.4	29582.4	32715.0	34408.9	38717.1	32235.4	0.031	0.833
Glycylpeptide N-tetradecanoyltransferase 1	NMT1	671.2	960.9	1033.2	637.7	850.8	730.7	888.4	739.7	0.322	0.833
Complement decay-accelerating factor	CD55	118.7	165.2	140.8	114.6	125.3	113.9	141.6	117.9	0.215	0.833
Elongation factor 1-beta	EEF1B2	435.0	629.9	566.2	370.1	574.1	415.1	543.7	453.1	0.344	0.833
Interleukin-5	IL5	3644.4	4404.3	5073.7	2830.7	4000.6	4108.8	4374.1	3646.7	0.279	0.834
Erythropoietin receptor	EPOR	92187.3	91829.6	75512.8	74672.7	74288.9	67617.5	86509.9	72193.0	0.106	0.835
Serine/threonine-protein kinase 16	STK16	496.7	492.1	487.9	462.4	378.0	393.5	492.2	411.3	0.088	0.836
Prolactin	PRL	1020.9	1306.6	1205.9	845.8	1087.0	1024.4	1177.8	985.7	0.159	0.837

Tumor necrosis factor receptor superfamily member 25	TNFRSF25	125.8	92.6	321.5	99.0	77.4	275.6	180.0	150.7	0.774	0.837
C-C motif chemokine 23	CCL23	89.1	84.3	84.1	81.8	65.6	68.5	85.8	72.0	0.097	0.838
C-type lectin domain family 7 member A	CLEC7A	546.0	612.9	683.1	439.3	537.2	568.1	614.0	514.9	0.148	0.839
Carboxypeptidase E	CPE	2267.7	1935.4	2612.5	2111.1	1550.1	2055.5	2271.9	1905.6	0.239	0.839
Dual specificity tyrosine-phosphorylation-regulated kinase 3	DYRK3	572.8	705.6	818.7	490.1	673.7	597.2	699.0	587.0	0.281	0.840
Ras GTPase-activating protein 1	RASA1	581.4	506.8	531.2	587.4	373.3	399.8	539.8	453.5	0.329	0.840
Limbic system-associated membrane protein	LSAMP	12129.8	9974.3	9862.7	11140.8	7820.8	7894.8	10655.6	8952.1	0.275	0.840
Fibroblast growth factor 7	FGF7	280.0	343.1	315.4	241.4	293.7	253.4	312.8	262.8	0.109	0.840
Angiotensin-converting enzyme 2	ACE2	109.2	134.0	138.0	89.6	114.1	116.9	127.1	106.9	0.182	0.841
Collectin-12	COLEC12	703.6	840.7	848.9	571.7	715.6	727.0	797.7	671.4	0.140	0.842
C-C motif chemokine 3-like 1	CCL3L1	649.5	639.8	685.1	589.8	535.2	538.1	658.1	554.4	0.011	0.842
Proteasome subunit alpha type-6	PSMA6	177.0	253.3	244.4	171.1	219.0	178.6	224.9	189.6	0.293	0.843
Hepatitis A virus cellular receptor 2	HAVCR2	180.4	224.0	205.0	153.0	184.2	176.7	203.1	171.3	0.119	0.843
Peroxiredoxin-5, mitochondrial	PRDX5	786.8	676.1	490.1	630.2	521.9	495.3	651.0	549.1	0.369	0.844
Angiopoietin-related protein 4	ANGPTL4	6688.6	7080.8	8585.3	5102.4	6392.0	7393.2	7451.6	6295.9	0.260	0.845
Testican-2	SPOCK2	1636.7	1083.0	1740.2	1641.2	1072.5	1056.7	1486.6	1256.8	0.458	0.845
Ephrin type-B receptor 2	EPHB2	7272.5	5390.0	6872.1	5963.3	4923.2	5635.7	6511.5	5507.4	0.218	0.846
Basal Cell Adhesion Molecule	BCAM	173.5	148.5	154.4	151.9	120.5	130.7	158.8	134.4	0.113	0.846
Fatty acid-binding protein, epidermal	FABP5	1439.2	690.2	443.7	566.6	943.9	667.0	857.7	725.8	0.712	0.846
Inosine-5'-monophosphate dehydrogenase 2	IMPDH2	3015.2	3985.4	4013.9	2611.9	3706.3	3006.2	3671.5	3108.1	0.286	0.847
Azurocidin	AZU1	95.1	125.7	116.4	85.2	107.6	92.7	112.4	95.2	0.205	0.847
CD97 antigen	CD97	890.5	807.5	865.9	851.4	657.0	664.0	854.6	724.1	0.166	0.847
Basigin	BSG	11615.1	14121.7	14936.0	9436.6	13387.9	11638.7	13557.6	11487.7	0.246	0.847
Tyrosine-protein kinase BTK	BTK	1978.7	3970.4	2406.6	2400.3	3185.5	1509.3	2785.2	2365.0	0.618	0.849
Cadherin-3	CDH3	6937.5	6253.1	6804.9	5415.9	5083.8	6479.4	6665.2	5659.7	0.124	0.849
Mitogen-activated protein kinase kinase kinase 7:TGF-beta-activated kinase 1 and MAP3K7-binding protein 1 fusion	MAP3K7 TAB1	1341.7	1601.1	1900.7	1098.5	1533.6	1481.3	1614.5	1371.1	0.316	0.849
Serine protease 27	PRSS27	1750.5	2145.1	2491.7	1505.8	2028.0	1893.9	2129.1	1809.2	0.300	0.850
Leucine-rich repeat transmembrane protein FLRT1	FLRT1	203.0	239.5	220.4	178.0	203.1	182.3	221.0	187.8	0.070	0.850

Stabilin-2	STAB2	407.3	421.9	463.2	375.8	380.3	343.1	430.8	366.4	0.040	0.851
Alpha-2-HS-glycoprotein	AHSG	391.2	395.0	405.2	303.7	370.0	341.4	397.1	338.4	0.086	0.852
Hsp90 co-chaperone Cdc37	CDC37	123.3	148.1	141.9	103.5	121.9	126.9	137.8	117.4	0.120	0.852
Fc receptor-like protein 3	FCRL3	776.3	160.0	167.2	595.3	167.8	178.2	367.8	313.8	0.839	0.853
Bone morphogenetic protein receptor type-1A	BMPR1A	209.8	151.8	210.4	181.3	122.4	184.7	190.7	162.8	0.377	0.854
Bcl-2-like protein 1	BCL2L1	201.3	184.0	191.6	201.5	145.6	145.7	192.3	164.3	0.268	0.854
Estrogen receptor	ESR1	123.8	131.0	139.1	98.7	117.5	120.4	131.3	112.2	0.089	0.855
Interleukin-3 receptor subunit alpha	IL3RA	131.7	171.6	255.9	115.6	155.0	207.3	186.4	159.3	0.584	0.855
Midkine	MDK	314.1	324.9	320.0	298.0	266.0	256.8	319.7	273.6	0.059	0.856
Microtubule-associated protein tau	MAPT	319.0	320.2	309.8	270.8	274.0	267.8	316.3	270.9	0.001	0.856
Low affinity immunoglobulin gamma Fc region receptor II-a/b	FCGR2A FCGR2B	143.1	106.0	93.3	135.2	75.6	82.4	114.1	97.7	0.534	0.856
Anterior gradient protein 2 homolog	AGR2	347.5	455.3	402.8	333.2	352.2	347.3	401.9	344.2	0.202	0.857
Protein kinase C gamma type	PRKCG	64.4	80.1	51.9	63.0	51.2	54.1	65.5	56.1	0.377	0.857
Tumor necrosis factor receptor superfamily member 11A	TNFRSF11A	372.9	451.9	548.1	312.5	448.8	416.1	457.6	392.5	0.377	0.858
Carbonic anhydrase 1	CA1	156.8	192.2	174.3	148.1	156.5	144.7	174.4	149.8	0.126	0.859
Fibroblast growth factor 18	FGF18	142.4	139.7	129.9	113.5	114.0	126.4	137.3	118.0	0.027	0.859
Insulin-like growth factor-binding protein 7	IGFBP7	235.9	251.4	253.2	225.4	219.1	191.8	246.8	212.1	0.058	0.859
RGM domain family member B	RGMB	267.2	290.2	274.8	227.0	238.0	250.5	277.4	238.5	0.015	0.860
Follistatin	FST	123.5	154.5	143.3	113.6	130.8	118.5	140.4	121.0	0.154	0.861
Inducible T-cell costimulator	ICOS	512.9	458.4	548.5	389.2	399.1	521.8	506.6	436.7	0.249	0.862
Cytochrome P450 3A4	CYP3A4	15774.5	23119.6	15342.1	16158.2	19689.6	10913.3	18078.7	15587.0	0.526	0.862
Cytotoxic and regulatory T-cell molecule	CRTAM	97.4	118.2	112.4	86.8	103.6	92.6	109.3	94.3	0.135	0.863
Beta-Ala-His dipeptidase	CNDP1	367.1	493.2	420.6	356.7	399.6	349.4	427.0	368.6	0.247	0.863
Complement C1s subcomponent	C1S	885.0	1092.2	986.3	774.7	937.3	851.3	987.8	854.4	0.158	0.865
GDNF family receptor alpha-3	GFRA3	508.4	522.7	559.9	429.5	483.0	463.7	530.3	458.7	0.031	0.865
Desert hedgehog protein N-product	DHH	209.1	290.8	263.4	190.0	251.7	218.6	254.4	220.1	0.320	0.865
Matrilin-2	MATN2	42975.5	30609.5	39199.4	34514.3	24903.0	38251.1	37594.8	32556.1	0.404	0.866
Insulin-like growth factor-binding protein 3	IGFBP3	254.0	237.4	274.9	263.5	192.1	208.1	255.4	221.2	0.254	0.866
Fibroblast growth factor receptor 4	FGFR4	450.0	503.1	549.2	369.9	476.9	455.1	500.8	434.0	0.200	0.867
Mammaglobin-B	SCGB2A1	24255.4	21409.1	22231.7	17843.9	19890.1	21118.0	22632.1	19617.3	0.078	0.867

Tumor necrosis factor receptor superfamily member 10A	TNFRSF10A	243.7	307.3	262.7	227.3	245.5	232.8	271.2	235.2	0.189	0.867
Cathepsin S	CTSS	111.3	81.7	76.0	107.9	62.3	63.2	89.7	77.8	0.561	0.868
Dynactin subunit 2	DCTN2	83.0	103.5	115.0	89.5	96.5	75.6	100.5	87.2	0.310	0.868
Adapter molecule crk	CRK	5835.0	6809.0	5909.7	5851.5	5722.7	4528.6	6184.6	5367.6	0.200	0.868
Insulin-degrading enzyme	IDE	1990.2	1836.5	2375.9	2102.1	1623.7	1658.5	2067.5	1794.8	0.287	0.868
Brevican core protein	BCAN	73.5	100.7	103.6	66.0	83.1	92.1	92.6	80.4	0.379	0.868
Fibroblast growth factor 6	FGF6	166.0	218.2	204.6	148.6	197.1	165.8	196.3	170.5	0.290	0.869
Cell adhesion molecule 3	CADM3	266.5	346.3	323.9	243.4	293.7	276.9	312.2	271.3	0.231	0.869
Dual specificity mitogen-activated protein kinase kinase 1	MAP2K1	980.9	956.9	777.8	790.3	845.1	725.6	905.2	787.0	0.201	0.869
Breast cancer anti-estrogen resistance protein 3	BCAR3	883.6	1056.3	1206.7	743.6	1023.4	969.6	1048.9	912.2	0.342	0.870
Thyroxine-Binding Globulin	SERPINA7	175.8	156.7	153.8	164.7	135.1	123.6	162.1	141.1	0.228	0.871
Apolipoprotein D	APOD	2038.5	2661.0	2627.7	1827.3	2504.3	2051.5	2442.4	2127.7	0.330	0.871
Bone morphogenetic protein 6	BMP6	1136.3	1194.5	1315.4	872.2	1122.0	1183.3	1215.4	1059.2	0.243	0.871
Protein kinase C iota type	PRKCI	409.6	455.3	432.5	352.7	410.2	368.5	432.5	377.1	0.067	0.872
Calcium/calmodulin-dependent protein kinase type 1	CAMK1	3091.0	3547.5	3598.1	3328.1	3688.9	1917.0	3412.2	2978.0	0.511	0.873
OX-2 membrane glycoprotein	CD200	218.0	250.9	253.5	191.1	214.9	225.3	240.8	210.4	0.119	0.874
Noggin	NOG	371.4	462.1	486.0	369.3	423.4	361.4	439.8	384.7	0.258	0.875
Persulfide dioxygenase ETHE1, mitochondrial	ETHE1	312.2	305.9	327.0	260.1	258.6	308.8	315.0	275.8	0.128	0.876
Ubiquitin carboxyl-terminal hydrolase isozyme L1	UCHL1	1645.5	1933.6	1958.2	1488.9	2014.6	1345.5	1845.8	1616.3	0.388	0.876
Ubiquitin-fold modifier-conjugating enzyme 1	UFC1	3156.1	3564.1	3559.1	3234.7	3196.5	2576.0	3426.4	3002.4	0.182	0.876
Keratin, type I cytoskeletal 18	KRT18	155.5	188.6	173.0	138.2	162.3	152.7	172.4	151.1	0.153	0.876
Tissue-type plasminogen activator	PLAT	144.8	148.9	141.6	136.5	118.4	126.7	145.1	127.2	0.060	0.877
Dynein light chain roadblock-type 1	DYNLRB1	1069.9	1352.0	963.8	1022.1	922.3	1024.1	1128.6	989.5	0.353	0.877
Protein kinase C theta type	PRKCQ	471.9	527.3	501.3	404.1	456.3	456.4	500.2	438.9	0.061	0.878
Endoplasmic reticulum resident protein 29	ERP29	1194.1	1152.5	1175.3	997.2	986.7	1107.0	1174.0	1030.3	0.054	0.878
Cytoskeleton-associated protein 2	CKAP2	22249.9	21198.9	26509.9	19398.8	21150.1	20858.5	23319.6	20469.1	0.215	0.878
Interleukin-1 Receptor accessory protein	IL1RAP	121422.4	87197.5	108643.5	97847.4	82157.6	98523.0	105754.5	92842.7	0.336	0.878
Focal adhesion kinase 1	PTK2	45.8	47.9	45.9	41.3	40.6	40.7	46.5	40.9	0.009	0.878
Ephrin type-B receptor 4	EPHB4	18304.4	17957.6	19083.9	16509.2	16556.7	15540.2	18448.6	16202.0	0.009	0.878
Calreticulin	CALR	982.4	1136.7	1184.9	830.3	1088.9	983.1	1101.3	967.4	0.241	0.878

Vascular endothelial growth factor C	VEGFC	472.3	446.9	489.9	446.5	370.0	423.8	469.7	413.4	0.115	0.880
Galectin-4	LGALS4	137.3	149.5	141.4	125.0	128.7	123.6	142.7	125.8	0.028	0.881
Interleukin-22 receptor subunit alpha-1	IL22RA1	139.6	171.8	143.3	144.9	131.9	123.9	151.6	133.6	0.219	0.881
Thrombospondin-1	THBS1	150.3	192.2	179.8	145.7	170.9	143.7	174.1	153.4	0.253	0.881
Anti-Muellerian hormone type-2 receptor	AMHR2	10373.4	5753.9	49761.0	8509.1	5242.7	44337.4	21962.8	19363.1	0.897	0.882
3-phosphoinositide-dependent protein kinase 1	PDPK1	145.8	215.1	191.0	170.0	167.2	149.4	184.0	162.2	0.399	0.882
Complement C5b-C6 complex	C5 C6	42.7	44.0	45.4	48.4	34.0	34.1	44.0	38.8	0.391	0.882
Aurora kinase B	AURKB	362.6	361.5	399.8	335.5	334.5	321.3	374.6	330.4	0.059	0.882
Estradiol 17-beta-dehydrogenase 1	HSD17B1	496.8	591.9	620.7	464.9	548.5	495.9	569.8	503.1	0.221	0.883
Coagulation Factor XI	F11	113.8	119.2	116.2	116.4	96.6	95.6	116.4	102.9	0.179	0.884
AMP Kinase (alpha2beta2gamma1)	PRKAA2 PRKAB2 PRKAG1	535.6	791.4	795.2	550.0	784.8	541.3	707.4	625.4	0.523	0.884
Bone sialoprotein 2	IBSP	237.9	165.1	158.1	205.0	149.2	142.7	187.0	165.6	0.546	0.886
Ribosome maturation protein SBDS	SBDS	664.8	1013.8	930.6	658.5	939.3	713.1	869.7	770.3	0.506	0.886
Programmed cell death 1 ligand 1	CD274	190.5	188.6	197.6	175.6	153.0	182.2	192.2	170.3	0.121	0.886
Ficolin-2	FCN2	317.4	351.7	365.8	295.9	329.3	291.8	345.0	305.7	0.105	0.886
Neurotrophin-3	NTF3	70.7	71.6	74.2	56.4	62.9	72.6	72.2	64.0	0.220	0.886
Retinoblastoma-associated protein	RB1	482.0	531.8	522.4	450.4	454.2	457.7	512.1	454.1	0.060	0.887
cGMP-inhibited 3',5'-cyclic phosphodiesterase A	PDE3A	867.8	1016.5	1262.5	676.3	1100.3	1015.8	1048.9	930.8	0.533	0.887
Methionine aminopeptidase 1	METAP1	408.1	923.3	549.6	609.1	685.2	375.9	627.0	556.7	0.720	0.888
Disintegrin and metalloproteinase domain-containing protein 9	ADAM9	264.5	84.0	83.2	216.7	80.7	86.1	143.9	127.8	0.842	0.888
Caspase-3	CASP3	378.4	398.6	418.8	298.4	363.3	400.6	398.6	354.1	0.272	0.888
GRB2-related adapter protein 2	GRAP2	493.3	549.1	608.7	397.8	526.7	542.6	550.4	489.0	0.345	0.889
Heterogeneous nuclear ribonucleoprotein Q	SYNCRIP	527.6	598.2	605.3	531.7	532.7	474.1	577.0	512.8	0.115	0.889
Serine/threonine-protein kinase MRCK beta	CDC42BPB	243.9	318.7	291.4	248.0	269.9	241.8	284.7	253.2	0.285	0.890
Stromal cell-derived factor 1	CXCL12	2834.0	2889.2	2737.2	3264.4	1901.4	2360.4	2820.1	2508.7	0.519	0.890
Afamin	AFM	345.7	331.0	333.9	359.1	272.2	267.9	336.9	299.7	0.337	0.890
Proto-oncogene tyrosine-protein kinase Src	SRC	352.1	552.9	407.2	465.3	418.3	284.1	437.4	389.2	0.584	0.890
Apolipoprotein E (isoform E3)	APOE	157.2	180.4	177.4	150.0	164.7	143.7	171.7	152.8	0.122	0.890
Repulsive guidance molecule A	RGMA	7164.9	5953.6	6162.4	6143.7	5131.1	5887.6	6427.0	5720.8	0.219	0.890

Histone H1.2	HIST1H1C	119.6	241.2	187.2	172.0	173.3	142.5	182.7	162.6	0.632	0.890
T-lymphocyte activation antigen CD80	CD80	242.0	219.5	219.9	240.1	174.5	192.3	227.1	202.3	0.334	0.891
Pituitary adenylate cyclase-activating polypeptide 27	ADCYAP1	608.9	760.5	717.0	555.8	676.5	626.4	695.5	619.6	0.258	0.891
Angiopoietin-1 receptor, soluble	TEK	159.2	182.1	178.1	144.2	162.7	156.0	173.1	154.3	0.106	0.891
Calcium/calmodulin-dependent protein kinase type II subunit alpha	CAMK2A	219.8	272.7	209.5	210.2	207.0	208.7	234.0	208.6	0.324	0.892
Plexin-C1	PLXNC1	73.5	71.9	74.5	75.0	61.0	60.1	73.3	65.4	0.240	0.892
Interleukin-34	IL34	208.3	185.7	192.1	211.1	159.9	151.9	195.4	174.3	0.377	0.892
S-phase kinase-associated protein 1	SKP1	1378.8	1480.7	1489.6	1210.2	1348.7	1321.3	1449.7	1293.4	0.049	0.892
Carbonic anhydrase 4	CA4	607.8	568.1	612.5	616.2	492.2	487.6	596.1	532.0	0.264	0.892
Neutrophil-activating peptide 2	PPBP	190.8	189.1	186.7	184.0	162.9	158.8	188.9	168.6	0.118	0.893
Protein kinase C zeta type	PRKCZ	455.9	522.7	436.0	390.4	456.9	415.9	471.5	421.1	0.203	0.893
Cadherin-15	CDH15	1305.8	1651.2	1809.0	1249.1	1573.6	1436.7	1588.7	1419.8	0.400	0.894
Collagen alpha-1(VIII) chain	COL8A1	101.5	73.5	574.3	102.8	70.3	496.7	249.8	223.3	0.907	0.894
Netrin-4	NTN4	287.3	306.1	288.0	244.2	247.5	296.3	293.8	262.7	0.198	0.894
Cytokine receptor-like factor 2	CRLF2	274.0	308.2	308.0	242.0	289.3	265.3	296.7	265.5	0.156	0.895
AMP Kinase (alpha1beta1gamma1)	PRKAA1 PRKAB1 PRKAG1	244.5	125.7	124.3	217.8	110.0	114.8	164.8	147.5	0.761	0.895
Ubiquitin+1, truncated mutation for UbB	RPS27A	35657.6	41209.5	46889.9	36815.1	40104.4	33944.4	41252.3	36954.6	0.327	0.896
Interleukin-3	IL3	551.0	709.9	596.0	534.3	557.9	575.7	619.0	556.0	0.313	0.898
Bactericidal permeability-increasing protein	BPI	438.6	495.3	470.5	370.3	446.3	445.5	468.1	420.7	0.201	0.899
CD48 antigen	CD48	99.0	121.6	105.1	97.0	95.8	100.3	108.6	97.7	0.246	0.900
MAP kinase-activated protein kinase 3	MAPKAPK3	270.7	398.4	260.3	280.1	285.3	271.3	309.8	278.9	0.559	0.900
Kynureninase	KYNU	127.5	137.4	136.4	130.4	120.7	110.2	133.8	120.4	0.136	0.900
GTPase KRas	KRAS	115.5	130.8	129.2	103.2	117.1	118.0	125.2	112.8	0.143	0.901
High affinity nerve growth factor receptor	NTRK1	849.9	882.6	904.4	675.8	820.6	879.7	879.0	792.0	0.285	0.901
Mitogen-activated protein kinase 3	MAPK3	6305.4	6474.1	6385.3	5577.8	5800.3	5896.6	6388.3	5758.2	0.010	0.901
Non-receptor tyrosine-protein kinase TYK2	TYK2	6378.3	6864.7	7865.9	5256.6	6977.2	6795.7	7036.3	6343.2	0.380	0.901
Protein jagged-2	JAG2	116.2	126.1	131.0	111.2	112.3	113.4	124.4	112.3	0.105	0.902
Apolipoprotein B	APOB	115.9	99.0	111.0	105.6	88.7	99.9	108.6	98.1	0.209	0.903

Cathepsin H	CTSH	264.6	318.6	315.7	240.3	290.2	281.3	299.6	270.6	0.282	0.903
Matrix metalloproteinase-16	MMP16	439.7	513.0	554.1	392.5	488.9	479.6	502.3	453.7	0.345	0.903
Alpha-soluble NSF attachment protein	NAPA	194.0	230.3	218.0	183.0	219.1	178.3	214.1	193.5	0.287	0.904
Tyrosine-protein kinase Tec	TEC	138.3	213.3	166.0	159.2	163.1	145.9	172.5	156.1	0.534	0.905
Membrane metallo-endopeptidase-like 1	MMEL1	337.7	398.8	391.8	314.3	348.8	357.8	376.1	340.3	0.210	0.905
Platelet endothelial cell adhesion molecule	PECAM1	178.3	178.9	181.2	163.3	160.2	164.1	179.5	162.5	0.001	0.906
Leukotriene A-4 hydrolase	LTA4H	363.8	410.1	512.3	330.5	452.5	382.3	428.7	388.4	0.516	0.906
Cytosolic non-specific dipeptidase	CNDP2	445.1	459.5	419.8	509.8	358.9	331.5	441.5	400.1	0.535	0.906
Translationally-controlled tumor protein	TPT1	80441.7	99502.7	114890.1	80980.3	101610.9	85292.9	98278.2	89294.7	0.495	0.909
Hemojuvelin	HFE2	30621.8	22818.2	26097.2	26287.7	21875.6	24112.9	26512.4	24092.1	0.417	0.909
Eukaryotic initiation factor 4A-III	EIF4A3	125.6	189.8	154.8	142.5	150.2	134.6	156.7	142.4	0.525	0.909
Interleukin-27 receptor subunit alpha	IL27RA	149.5	154.6	147.6	149.0	129.7	131.8	150.6	136.8	0.143	0.909
Interleukin-17 receptor C	IL17RC	313.5	272.6	298.8	273.3	265.7	265.2	295.0	268.1	0.148	0.909
alpha-2-macroglobulin receptor-associated protein	LRPAP1	107.7	173.6	123.3	130.7	132.8	104.5	134.9	122.7	0.618	0.910
Mediator of RNA polymerase II transcription subunit 1	MED1	105.8	132.3	132.8	106.4	118.4	112.6	123.6	112.5	0.339	0.910
Kininogen-1	KNG1	83.2	115.6	104.6	83.4	106.6	86.0	101.1	92.0	0.492	0.910
Bone morphogenetic protein 10	BMP10	2197.5	2084.1	2190.8	1654.3	1896.5	2346.2	2157.5	1965.7	0.445	0.911
Mesothelin	MSLN	108.8	140.5	125.2	99.0	128.8	113.7	124.8	113.8	0.431	0.912
Abelson tyrosine-protein kinase 2	ABL2	906.3	1040.5	1213.2	747.3	1079.1	1058.3	1053.3	961.6	0.547	0.913
Urokinase plasminogen activator surface receptor	PLAUR	320.6	349.1	329.1	285.0	318.1	308.8	332.9	304.0	0.091	0.913
Ubiquitin-fold modifier 1	UFM1	750.8	753.3	648.4	681.4	726.9	558.2	717.5	655.5	0.374	0.914
Interleukin-12 receptor subunit beta-2	IL12RB2	212.5	204.1	215.4	192.9	184.6	200.0	210.7	192.5	0.035	0.914
High affinity cAMP-specific 3',5'-cyclic phosphodiesterase 7A	PDE7A	122.0	130.6	125.9	109.3	123.7	113.0	126.2	115.3	0.112	0.914
Peptidyl-prolyl cis-trans isomerase A	PPIA	126520.4	107245.1	128873.2	104496.5	111528.1	115514.5	120879.6	110513.0	0.269	0.914
Activated Protein C	PROC	251.1	275.5	278.4	220.5	252.6	263.1	268.3	245.4	0.222	0.915
Peptidyl-prolyl cis-trans isomerase F, mitochondrial	PPIF	1294.8	1523.2	1583.4	1157.0	1430.1	1443.5	1467.1	1343.5	0.390	0.916
Tyrosine-protein kinase transmembrane receptor ROR1	ROR1	154.4	174.3	159.3	141.9	144.2	160.9	162.7	149.0	0.182	0.916
Protein FAM107A	FAM107A	110.0	110.1	113.4	99.0	102.8	103.9	111.2	101.9	0.009	0.917

Tenascin	TNC	182.1	178.8	171.5	182.1	151.4	154.6	177.5	162.7	0.265	0.917
Growth/differentiation factor 11	GDF11	6562.6	5242.9	5663.6	5594.7	5460.5	4962.3	5823.0	5339.2	0.348	0.917
Contactin-4	CNTN4	648.4	697.6	714.9	614.9	639.0	637.0	687.0	630.3	0.090	0.918
Nucleoside diphosphate kinase A	NME1	1437.9	1809.5	1624.9	1332.3	1651.9	1487.0	1624.1	1490.4	0.399	0.918
Tumor necrosis factor receptor superfamily member 14	TNFRSF14	54.2	59.9	59.3	55.0	51.9	52.4	57.8	53.1	0.104	0.919
Calpain I	CAPN1 CAPNS1	16995.1	19549.2	22640.4	19077.2	17461.2	17840.6	19728.2	18126.3	0.433	0.919
Matrilysin	MMP7	158.2	175.5	165.9	154.7	154.0	150.4	166.5	153.0	0.106	0.919
Cathepsin G	CTSG	390.0	393.4	406.1	322.9	375.8	395.6	396.5	364.8	0.279	0.920
Complement component C7	C7	100.7	113.6	107.5	103.2	99.2	93.9	107.3	98.8	0.145	0.921
C-C motif chemokine 17	CCL17	140.5	133.2	136.5	139.1	115.3	123.3	136.7	125.9	0.258	0.921
Cadherin-5	CDH5	29001.6	22781.8	25729.9	25052.8	21768.5	24574.6	25837.8	23798.6	0.393	0.921
Toll-like receptor 4:Lymphocyte antigen 96 complex	TLR4 LY96	137.2	204.7	147.1	156.7	158.8	135.1	163.0	150.2	0.614	0.921
Peptidyl-prolyl cis-trans isomerase B	PPIB	1507.7	1563.7	1624.4	1202.6	1464.9	1661.6	1565.3	1443.0	0.458	0.922
Interleukin-17 receptor D	IL17RD	82.8	83.6	80.9	76.4	76.4	75.2	82.4	76.0	0.006	0.922
40S ribosomal protein S3	RPS3	92.8	123.8	110.2	104.7	111.2	85.4	108.9	100.4	0.514	0.922
Neurogenic locus notch homolog protein 2	NOTCH2	182.4	169.3	175.3	165.5	150.5	169.9	175.7	162.0	0.133	0.922
Lamin-B1	LMNB1	126.9	158.0	155.2	122.4	147.0	136.4	146.7	135.3	0.408	0.922
C-C motif chemokine 27	CCL27	141.4	161.2	149.7	134.5	147.6	135.0	150.8	139.0	0.183	0.922
Delta-like protein 4	DLL4	74.7	81.9	76.3	70.5	67.6	76.9	77.6	71.7	0.168	0.923
Methyl-CpG-binding domain protein 4	MBD4	117.5	112.7	498.1	104.3	98.2	469.9	242.8	224.1	0.921	0.923
CD226 antigen	CD226	494.6	488.8	545.3	404.0	483.3	524.8	509.6	470.7	0.401	0.924
Growth arrest-specific protein 1	GAS1	241.3	254.0	270.3	226.6	241.0	240.2	255.2	235.9	0.135	0.925
Glia-derived nexin	SERPINE2	405.9	436.5	396.4	382.1	412.8	350.9	412.9	381.9	0.234	0.925
Histone acetyltransferase KAT6A	KAT6A	206.2	229.4	212.4	226.5	198.9	175.0	216.0	200.1	0.409	0.927
Macrophage colony-stimulating factor 1	CSF1	225.5	267.4	244.1	212.3	242.4	228.3	245.7	227.7	0.300	0.927
Leptin	LEP	245.4	293.1	301.8	241.1	269.8	267.9	280.1	259.6	0.376	0.927
L-lactate dehydrogenase B chain	LDHB	28401.4	32882.8	25126.9	24329.0	27697.4	28082.2	28803.7	26702.9	0.469	0.927
Complement component 1 Q subcomponent-binding protein, mitochondrial	C1QBP	14389.1	12627.4	13869.5	11930.5	12476.8	13557.4	13628.7	12654.9	0.242	0.929
Eotaxin	CCL11	122.3	105.7	110.5	110.3	101.4	103.3	112.8	105.0	0.255	0.931
Cathepsin E	CTSE	76.8	81.3	72.4	73.4	71.8	69.4	76.8	71.5	0.164	0.931
Semaphorin-3A	SEMA3A	135.1	149.5	176.2	128.4	135.8	165.0	153.6	143.1	0.556	0.931

Sialic acid-binding Ig-like lectin 14	SIGLEC14	281.2	274.4	251.6	225.6	227.8	298.5	269.1	250.6	0.531	0.931
Granulocyte colony-stimulating factor receptor	CSF3R	533.9	488.9	514.5	437.4	481.7	513.1	512.4	477.4	0.257	0.932
Group 10 secretory phospholipase A2	PLA2G10	140.4	134.3	132.6	139.9	122.3	117.3	135.8	126.5	0.308	0.932
CD40 ligand	CD40LG	115.4	123.0	122.2	108.4	108.2	119.5	120.2	112.0	0.152	0.932
Parathyroid hormone	PTH	112.8	120.5	118.7	101.0	108.0	119.1	117.3	109.4	0.268	0.932
C-C motif chemokine 3	CCL3	221.2	183.9	184.0	181.7	180.0	187.5	196.4	183.1	0.397	0.932
Interleukin-4	IL4	98.7	101.2	100.6	94.0	87.3	98.9	100.2	93.4	0.177	0.932
SLAM family member 7	SLAMF7	172.1	186.2	208.0	161.8	171.5	194.9	188.8	176.1	0.426	0.933
Phosphatidylinositol 4,5-bisphosphate 3-kinase catalytic subunit alpha isoform:Phosphatidylinositol 3-kinase regulatory subunit alpha complex	PIK3CA PIK3R1	855.7	754.3	724.1	835.5	684.5	657.4	778.0	725.8	0.491	0.933
Transcription factor IIIB 90 kDa subunit	BRF1	444.9	517.1	602.3	429.6	554.0	476.0	521.4	486.5	0.583	0.933
GDNF family receptor alpha-1	GFRA1	259.3	262.3	248.5	254.1	214.3	250.8	256.7	239.7	0.314	0.934
Interleukin-18 receptor accessory protein	IL18RAP	133.1	78.8	82.1	125.7	71.9	77.1	98.0	91.6	0.806	0.934
C-C motif chemokine 2	CCL2	57.2	68.4	66.4	57.3	60.5	61.6	64.0	59.8	0.350	0.934
Tumor necrosis factor receptor superfamily member 8	TNFRSF8	259.2	262.1	285.2	254.9	266.7	232.4	268.8	251.3	0.252	0.935
Carbonic anhydrase 13	CA13	104.9	117.8	114.2	101.8	115.4	97.9	112.3	105.0	0.335	0.935
N-acetyl-D-glucosamine kinase	NAGK	65.5	95.4	79.2	67.9	87.1	69.6	80.0	74.9	0.654	0.935
Fibroblast growth factor 9	FGF9	145.7	144.9	148.0	124.9	133.3	152.1	146.2	136.8	0.361	0.935
Protein SET	SET	2764.6	2745.0	2392.8	2108.1	2262.0	3023.8	2634.1	2464.6	0.624	0.936
Alpha-1-antichymotrypsin	SERPINA3	63.6	91.6	81.3	63.4	93.6	64.3	78.8	73.8	0.714	0.936
Interleukin-18 receptor 1	IL18R1	260.1	227.4	240.6	262.9	205.5	213.5	242.7	227.3	0.503	0.937
SLAM family member 5	CD84	2494.1	2403.0	2804.6	1935.9	2448.5	2829.9	2567.2	2404.8	0.612	0.937
cAMP-regulated phosphoprotein 19	ARPP19	77.4	84.0	79.3	76.1	74.1	75.5	80.2	75.2	0.116	0.938
AT-rich interactive domain-containing protein 3A	ARID3A	222.6	267.7	253.6	204.3	256.3	237.1	248.0	232.6	0.489	0.938
Cystatin-SA	CST2	166.7	114.2	129.8	127.0	118.4	140.1	136.9	128.5	0.656	0.939
OCIA domain-containing protein 1	OCIAD1	598.1	693.3	803.4	570.1	734.8	664.0	698.3	656.3	0.612	0.940
Proto-oncogene tyrosine-protein kinase receptor Ret	RET	239.7	227.6	232.8	234.8	211.4	212.0	233.4	219.4	0.204	0.940
Secreted frizzled-related protein 1	SFRP1	343.1	325.3	307.7	271.6	331.3	314.8	325.4	305.9	0.409	0.940
Galectin-8	LGALS8	55.3	51.9	50.9	50.0	48.2	50.6	52.7	49.6	0.131	0.941

Neutral ceramidase	ASAH2	253.8	259.5	302.1	246.4	275.6	245.8	271.8	255.9	0.439	0.942
Fibroblast growth factor 20	FGF20	129.8	119.2	122.1	118.9	114.0	116.6	123.7	116.5	0.137	0.942
D-dimer	FGA FGB FGG	74008.4	68586.8	73886.4	60454.1	60684.8	82941.2	72160.5	68026.7	0.639	0.943
CD109 antigen	CD109	189.9	196.0	201.7	177.7	185.5	191.0	195.9	184.7	0.098	0.943
NKG2D ligand 1	ULBP1	102.4	119.6	110.6	104.4	104.1	105.2	110.9	104.6	0.332	0.943
Heat shock protein HSP 90-alpha/beta	HSP90AA1 HSP90AB1	119230.0	103518.9	108126.5	97644.2	110442.3	104157.5	110291.8	104081.3	0.358	0.944
Arylsulfatase A	ARSA	140.1	146.8	146.7	127.9	145.4	135.9	144.5	136.4	0.245	0.944
Tumor necrosis factor receptor superfamily member 1A	TNFRSF1A	161.6	191.4	169.1	147.2	162.0	183.6	174.0	164.3	0.521	0.944
Cystatin-F	CST7	208.0	208.1	201.8	183.2	197.0	203.4	206.0	194.5	0.187	0.944
Haptoglobin	HP	64.2	77.5	73.6	74.7	66.9	61.9	71.8	67.8	0.509	0.945
Platelet-derived growth factor receptor beta	PDGFRB	246.4	235.8	247.1	231.7	229.7	228.0	243.1	229.8	0.058	0.945
Fibronectin Fragment 3	FN1	183.2	192.2	186.2	157.2	178.4	195.8	187.2	177.1	0.465	0.946
Tumor necrosis factor receptor superfamily member 13C	TNFRSF13C	411.0	444.8	538.0	400.8	473.5	445.0	464.6	439.8	0.606	0.947
Dentin matrix acidic phosphoprotein 1	DMP1	292.8	279.1	276.3	248.5	271.7	282.9	282.7	267.7	0.278	0.947
Leucine carboxyl methyltransferase 1	LCMT1	1275.1	1107.0	1257.7	1119.1	1204.2	1124.4	1213.3	1149.2	0.365	0.947
Interleukin-12	IL12A IL12B	381.9	382.7	358.5	373.8	350.3	339.8	374.4	354.6	0.202	0.947
Tumor necrosis factor receptor superfamily member 6B	TNFRSF6B	70.8	86.0	69.8	78.7	66.6	69.4	75.5	71.6	0.572	0.947
Thymic stromal lymphopoietin	TSLP	99.8	102.0	110.5	99.6	98.3	98.0	104.1	98.6	0.234	0.947
Small glutamine-rich tetratricopeptide repeat-containing protein alpha	SGTA	717.6	840.6	763.7	743.1	748.9	710.3	774.0	734.1	0.385	0.948
B-cell receptor CD22	CD22	538.9	528.5	562.6	514.6	518.4	513.2	543.3	515.4	0.106	0.949
Nuclear receptor subfamily 1 group D member 1	NR1D1	83.8	90.4	92.3	84.1	83.1	85.6	88.8	84.3	0.213	0.949
MAP kinase-activated protein kinase 5	MAPKAPK5	250.6	223.5	215.0	224.3	207.8	221.8	229.7	218.0	0.400	0.949
Junctional adhesion molecule-like	AMICA1	128.0	126.3	125.0	129.3	110.8	120.0	126.4	120.0	0.353	0.949
Ectonucleoside triphosphate diphosphohydrolase 5	ENTPD5	263.7	291.2	294.4	252.7	288.5	265.3	283.1	268.8	0.376	0.950
Angiogenin	ANG	128.6	139.6	123.0	101.3	87.2	183.0	130.4	123.8	0.847	0.950
Epidermal growth factor receptor substrate 15-like 1	EPS15L1	105.4	109.1	103.9	100.3	104.1	98.2	106.1	100.9	0.086	0.950
Hepatocyte growth factor	HGF	186.3	210.3	206.5	174.0	192.3	207.2	201.0	191.2	0.465	0.951
Interferon alpha-2	IFNA2	29.6	37.6	28.0	29.9	28.7	32.0	31.7	30.2	0.664	0.952

Tumor necrosis factor ligand superfamily member 8	TNFSF8	225.4	240.7	229.6	226.4	215.8	220.8	231.9	221.0	0.128	0.953
Pescadillo homolog	PES1	156.7	166.3	168.8	141.2	157.3	170.4	163.9	156.3	0.473	0.953
Bone morphogenetic protein receptor type-2	BMPR2	188.3	171.1	167.4	185.8	157.7	158.8	175.6	167.4	0.511	0.953
Serine/threonine-protein kinase TBK1	TBK1	123.6	137.5	139.9	123.9	132.7	126.1	133.7	127.6	0.365	0.954
Phospholipase A2, membrane associated	PLA2G2A	234.7	215.3	231.4	231.1	198.5	221.4	227.1	217.0	0.432	0.955
SH2 domain-containing protein 1A	SH2D1A	719.7	682.3	764.4	513.4	661.5	896.0	722.1	690.3	0.804	0.956
Ficolin-1	FCN1	103.0	114.8	95.1	101.3	99.9	98.0	104.3	99.7	0.510	0.956
Fibroblast growth factor 10	FGF10	64.8	63.1	62.1	61.1	57.9	62.7	63.3	60.6	0.181	0.956
Discoidin domain-containing receptor 2	DDR2	2395.9	2378.4	2874.7	1914.5	2576.4	2825.9	2549.7	2438.9	0.748	0.957
Plasma serine protease inhibitor	SERPINA5	249.4	257.8	258.7	251.1	249.7	232.3	255.3	244.4	0.206	0.957
Parathyroid hormone-related protein	PTHLH	265.5	253.7	298.7	277.0	219.2	286.9	272.6	261.0	0.671	0.957
Interleukin-1 beta	IL1B	3067.4	2767.0	3002.7	2391.2	2668.2	3404.6	2945.7	2821.3	0.727	0.958
Peroxiredoxin-1	PRDX1	5537.5	7163.0	6211.7	5219.5	8831.1	4065.6	6304.1	6038.7	0.874	0.958
Intercellular adhesion molecule 1	ICAM1	1929.2	1655.4	1753.5	1654.3	1673.4	1786.0	1779.4	1704.6	0.467	0.958
Chitotriosidase-1	CHIT1	224.9	304.5	236.3	251.7	257.5	224.4	255.2	244.5	0.720	0.958
Sphingosine kinase 1	SPHK1	395.2	302.9	475.3	326.9	396.0	401.4	391.1	374.8	0.787	0.958
R-spondin-2	RSPO2	126.2	139.2	141.5	120.6	137.2	132.2	135.6	130.0	0.457	0.958
Protein amnionless	AMN	161.7	170.3	162.3	141.6	163.1	169.1	164.8	157.9	0.506	0.959
Alanine aminotransferase 1	GPT	11572.4	10939.9	11752.9	10616.1	11557.0	10680.4	11421.7	10951.2	0.298	0.959
Tissue factor pathway inhibitor	TFPI	293.9	324.0	305.9	252.6	293.8	339.4	307.9	295.3	0.672	0.959
C-X-C motif chemokine 16	CXCL16	491.8	532.6	518.6	501.0	490.3	488.7	514.3	493.3	0.215	0.959
Transforming growth factor beta-3	TGFB3	124.8	119.1	113.9	112.6	114.2	116.4	119.3	114.4	0.258	0.959
Disintegrin and metalloproteinase domain-containing protein 12	ADAM12	177.9	170.3	196.0	152.3	167.3	202.4	181.4	174.0	0.688	0.959
Neutrophil elastase	ELANE	121.7	121.8	131.6	113.6	115.7	130.5	125.0	119.9	0.469	0.959
Coagulation Factor VII	F7	166.3	175.2	177.7	173.2	167.3	157.6	173.1	166.0	0.290	0.959
Matrix metalloproteinase-9	MMP9	240.5	273.2	247.5	221.0	241.3	268.0	253.7	243.4	0.577	0.959
Cell surface glycoprotein CD200 receptor 1	CD200R1	99.1	96.8	106.4	98.0	90.3	101.9	100.8	96.7	0.419	0.960
Tumor necrosis factor receptor superfamily member 1B	TNFRSF1B	545.5	624.6	577.9	566.7	553.5	558.2	582.7	559.5	0.419	0.960
Tryptase beta-2	TPSB2	268.9	232.0	270.9	244.3	251.6	245.4	257.3	247.1	0.507	0.960
Tumor necrosis factor ligand superfamily member 15	TNFSF15	211.1	193.6	211.7	197.2	185.1	210.2	205.5	197.5	0.445	0.961

Gelsolin	GSN	101760.9	76633.3	94124.8	87520.2	85778.6	88667.8	90839.7	87322.2	0.684	0.961
NKG2-D type II integral membrane protein	KLRK1	134.1	359.5	138.6	139.1	328.6	140.4	210.7	202.7	0.938	0.962
Hepcidin	HAMP	115.4	112.6	116.2	110.6	110.2	110.6	114.7	110.5	0.058	0.963
Dickkopf-related protein 3	DKK3	178.2	191.4	169.3	170.8	166.1	182.2	179.6	173.0	0.459	0.963
Fibroblast growth factor 5	FGF5	107.1	114.9	102.5	103.5	103.8	105.6	108.2	104.3	0.398	0.964
N-acetylglucosamine-6-sulfatase	GNS	143.0	173.1	134.1	142.9	151.2	140.1	150.1	144.7	0.701	0.964
Kallikrein-4	KLK4	77.3	76.4	82.2	73.3	75.8	78.5	78.6	75.9	0.306	0.965
Cardiotrophin-1	CTF1	208.0	173.3	183.2	200.1	168.1	176.7	188.2	181.6	0.667	0.965
Kin of IRRE-like protein 3	KIRREL3	75.5	66.1	67.1	72.3	65.5	63.7	69.6	67.2	0.578	0.966
Interleukin-15 receptor subunit alpha	IL15RA	212.2	223.4	203.1	198.2	210.5	208.0	212.9	205.6	0.362	0.966
cAMP-specific 3',5'-cyclic phosphodiesterase 4D	PDE4D	405.4	498.1	460.7	400.6	489.5	428.6	454.7	439.6	0.707	0.967
Kallikrein-8	KLK8	187.0	181.5	192.0	180.8	185.3	175.8	186.8	180.6	0.205	0.967
Coagulation factor IXab	F9	35.8	39.4	34.9	33.4	36.5	36.6	36.7	35.5	0.529	0.967
Granulysin	GNLY	28.6	34.9	30.3	32.9	27.3	30.8	31.3	30.3	0.727	0.970
Cystatin-S	CST4	27.6	30.4	29.9	29.6	26.4	29.3	29.3	28.4	0.553	0.970
C-X-C motif chemokine 10	CXCL10	119.9	117.5	111.5	105.5	116.7	116.4	116.3	112.9	0.489	0.970
Interleukin-7 receptor subunit alpha	IL7R	90.8	94.4	92.7	91.2	88.4	90.2	92.6	89.9	0.115	0.971
Cyclin-dependent kinase 1:G2/mitotic-specific cyclin-B1 complex	CDC2 CCNB1	216.5	183.7	183.3	210.5	182.3	174.6	194.5	189.1	0.747	0.972
Phospholipase A2	PLA2G1B	237.5	196.8	195.6	206.9	224.2	181.8	210.0	204.3	0.774	0.973
Glucocorticoid receptor	NR3C1	43.9	55.1	49.1	45.3	51.9	47.2	49.4	48.1	0.764	0.975
Tropomyosin alpha-1 chain	TPM1	166.0	188.8	169.8	172.7	176.6	162.3	174.9	170.5	0.632	0.975
Neurogenic locus notch homolog protein 1	NOTCH1	5684.8	4849.0	5062.1	5017.4	4782.9	5411.7	5198.6	5070.7	0.703	0.975
Kallistatin	SERPINA4	130.6	117.0	126.5	134.2	111.5	119.5	124.7	121.7	0.726	0.976
C-type lectin domain family 4 member M	CLEC4M	58989.1	48111.2	52736.5	46132.0	50569.4	59383.7	53278.9	52028.4	0.816	0.977
Ectonucleoside triphosphate diphosphohydrolase 1	ENTPD1	808.9	725.9	761.2	785.3	725.1	731.8	765.3	747.4	0.592	0.977
Fibroblast growth factor 2	FGF2	202.6	217.4	202.2	188.9	176.0	242.8	207.4	202.6	0.838	0.977
Dipeptidyl peptidase 2	DPP7	2772.1	2629.3	2514.9	2401.6	2488.6	2844.0	2638.8	2578.1	0.720	0.977
Coagulation factor Xa	F10	118651.8	96666.1	112394.9	104199.1	101920.7	114209.4	109237.6	106776.4	0.765	0.977
Interferon lambda-1	IFNL1	94.8	105.0	106.5	86.2	106.4	106.9	102.1	99.8	0.788	0.978
Protein lin-7 homolog B	LIN7B	174.7	171.9	179.8	189.0	167.2	159.1	175.5	171.8	0.723	0.979
Corticosteroid-binding globulin	SERPINA6	93.4	113.1	108.4	99.7	103.4	105.4	105.0	102.8	0.758	0.980

C-C motif chemokine 13	CCL13	124.7	118.6	122.6	121.5	113.5	123.5	122.0	119.5	0.533	0.980
Artemin	ARTN	166.5	163.3	157.9	154.4	158.2	165.5	162.6	159.4	0.483	0.980
Serum amyloid A-1 protein	SAA1	129.9	120.3	132.1	118.1	132.3	124.5	127.4	125.0	0.676	0.981
Tumor necrosis factor receptor superfamily member 18	TNFRSF18	187.0	188.9	197.9	190.3	188.4	184.3	191.3	187.7	0.413	0.981
TGF-beta receptor type-2	TGFBR2	138.4	144.2	152.4	140.9	144.8	141.6	145.0	142.4	0.598	0.982
dCTP pyrophosphatase 1	DCTPP1	1536.8	1430.9	1338.3	1812.9	1361.5	1055.6	1435.3	1410.0	0.920	0.982
Histidine triad nucleotide-binding protein 1	HINT1	96.1	93.8	93.5	90.9	92.5	95.0	94.5	92.8	0.321	0.982
Phosphatidylinositol 3,4,5-trisphosphate 3-phosphatase and dual-specificity protein phosphatase PTEN	PTEN	218.6	201.6	225.0	198.3	201.1	234.6	215.1	211.3	0.800	0.983
Leptin receptor	LEPR	73.5	83.1	80.0	82.8	77.6	72.1	78.9	77.5	0.761	0.983
Lymphocyte activation gene 3 protein	LAG3	27.2	33.0	26.7	30.2	30.9	24.3	29.0	28.5	0.872	0.983
Tumor necrosis factor receptor superfamily member 17	TNFRSF17	88.3	90.4	88.8	78.8	88.4	95.7	89.2	87.6	0.785	0.983
Natural cytotoxicity triggering receptor 3	NCR3	71.8	69.3	69.2	63.2	71.4	72.1	70.1	68.9	0.721	0.983
Transmembrane glycoprotein NMB	GPNMB	20.3	25.2	20.5	21.4	19.8	23.7	22.0	21.6	0.862	0.983
Tyrosine-protein kinase Lck	LCK	154.1	128.8	127.8	147.2	127.0	129.8	136.9	134.7	0.845	0.984
Urokinase-type plasminogen activator	PLAU	183.4	201.9	194.3	186.8	201.5	182.1	193.2	190.1	0.719	0.984
WNT1-inducible-signaling pathway protein 1	WISP1	12711.2	11512.8	11422.2	10439.7	12001.1	12642.5	11882.1	11694.4	0.823	0.984
Interleukin-11	IL11	153.0	157.9	155.5	134.7	153.0	171.4	155.5	153.0	0.840	0.984
Killer cell immunoglobulin-like receptor 3DS1	KIR3DS1	86.5	91.5	91.1	92.7	84.3	88.1	89.7	88.4	0.674	0.985
Hepatoma-derived growth factor-related protein 2	HDGFRP2	166.4	166.4	172.1	165.4	163.1	168.9	168.3	165.8	0.382	0.985
Carbohydrate sulfotransferase 2	CHST2	85.2	106.6	99.7	91.1	109.6	86.5	97.2	95.7	0.887	0.985
Ephrin type-A receptor 5	EPHA5	73.0	85.6	79.2	80.0	80.3	74.1	79.3	78.1	0.802	0.986
Apolipoprotein A-I	APOA1	79.8	78.8	80.0	84.4	77.0	73.9	79.5	78.4	0.758	0.986
Cadherin-6	CDH6	161750.4	125021.9	147063.9	134636.4	136032.5	157437.1	144612.1	142702.0	0.891	0.987
Roundabout homolog 3	ROBO3	47.3	51.1	54.9	48.0	53.0	50.3	51.1	50.4	0.814	0.987
Syntaxin-1A	STX1A	79.8	78.1	73.7	79.9	76.0	72.7	77.2	76.2	0.736	0.987
Complement factor I	CFI	17857.6	15310.7	17171.8	15356.9	16357.6	17980.4	16780.0	16565.0	0.852	0.987
T-lymphocyte activation antigen CD86	CD86	52.6	52.4	59.9	51.7	49.2	61.9	55.0	54.3	0.888	0.987

Cytoplasmic protein NCK1	NCK1	181.4	164.8	176.7	179.1	171.5	165.8	174.3	172.1	0.748	0.988
Tyrosine-protein kinase receptor TYRO3	TYRO3	182.0	155.2	160.5	184.1	147.8	159.8	165.9	163.9	0.890	0.988
Endoglin	ENG	48.3	28.2	31.9	42.0	31.2	34.0	36.1	35.7	0.958	0.989
Angiostatin	PLG	43.8	55.3	46.6	50.5	50.7	42.9	48.6	48.0	0.908	0.989
Tumor necrosis factor receptor superfamily member 19L	RELT	37.1	39.0	38.5	38.5	38.0	36.9	38.2	37.8	0.618	0.990
Tyrosine-protein kinase ABL1	ABL1	92.5	87.6	97.4	83.5	99.4	91.7	92.5	91.5	0.868	0.990
Epithelial discoidin domain-containing receptor 1	DDR1	91.1	88.7	88.3	87.1	85.7	92.5	89.4	88.4	0.709	0.990
Integrin alpha-IIb: beta-3 complex	ITGA2B ITGB3	99.3	110.5	106.2	98.6	113.0	101.2	105.3	104.3	0.857	0.990
MAP kinase-activated protein kinase 2	MAPKAPK2	263.3	255.1	256.4	246.7	263.3	257.0	258.3	255.7	0.667	0.990
Prolactin receptor	PRLR	718.5	696.6	737.6	674.3	738.0	719.5	717.6	710.6	0.773	0.990
Interleukin-10 receptor subunit beta	IL10RB	238.4	218.0	228.1	236.0	221.2	220.9	228.2	226.0	0.796	0.991
alpha-L-iduronidase	IDUA	132.0	139.9	140.4	133.4	142.0	133.3	137.4	136.2	0.777	0.991
Interleukin-8	CXCL8	218.4	207.7	220.3	215.6	208.4	216.8	215.5	213.6	0.715	0.991
Ck-beta-8-1	CCL23	73.8	77.6	73.7	74.0	72.1	77.1	75.0	74.4	0.761	0.992
Mitogen-activated protein kinase 11	MAPK11	139.3	115.9	149.2	125.4	121.4	154.3	134.8	133.7	0.942	0.992
Wnt inhibitory factor 1	WIF1	6422.9	5326.9	6945.3	6885.3	4691.4	6979.4	6231.7	6185.4	0.961	0.993
Ferritin	FTH1 FTL	113.8	93.9	122.9	110.2	97.1	121.0	110.2	109.4	0.948	0.993
Matrix metalloproteinase-14	MMP14	203.8	183.8	193.9	193.2	190.8	193.5	193.8	192.5	0.840	0.993
Tyrosine-protein kinase Fyn	FYN	456.2	461.3	428.1	505.9	412.2	418.4	448.5	445.5	0.932	0.993
Tumor necrosis factor ligand superfamily member 12	TNFSF12	124.0	130.8	122.0	120.8	119.0	134.6	125.6	124.8	0.895	0.994
beta-nerve growth factor	NGF	83.2	89.1	101.0	77.9	95.2	98.6	91.1	90.6	0.952	0.994
Tumor necrosis factor ligand superfamily member 14	TNFSF14	61.7	67.5	64.5	71.7	60.2	60.7	64.6	64.2	0.935	0.994
Eukaryotic translation initiation factor 5	EIF5	420.2	696.2	1039.1	635.6	929.1	578.9	718.5	714.5	0.986	0.994
Baculoviral IAP repeat-containing protein 5	BIRC5	187.9	183.4	191.9	189.2	181.8	189.4	187.7	186.8	0.803	0.995
Kallikrein-11	KLK11	166.0	165.6	171.4	156.7	168.8	175.0	167.7	166.8	0.895	0.995
Layilin	LAYN	291.6	280.5	280.1	287.9	280.8	279.4	284.1	282.7	0.783	0.995
Interleukin-13	IL13	285.3	272.3	276.0	289.3	264.6	275.7	277.9	276.5	0.880	0.995
Ephrin-A5	EFNA5	3047.0	2433.4	2583.0	3203.5	2172.8	2650.2	2687.8	2675.5	0.974	0.995
Natural cytotoxicity triggering receptor 1	NCR1	530.5	513.6	535.2	535.9	535.1	501.2	526.4	524.1	0.868	0.996

Platelet factor 4	PF4	98.5	111.2	112.9	105.9	112.3	103.0	107.5	107.1	0.935	0.996
Interleukin-1 receptor type 1	IL1R1	32.8	31.7	32.2	33.3	30.9	32.1	32.2	32.1	0.873	0.996
Fibroblast growth factor receptor 3	FGFR3	199.9	206.1	205.9	194.0	205.3	210.1	204.0	203.1	0.884	0.996
C-C motif chemokine 21	CCL21	39.7	43.8	41.4	40.2	42.6	41.6	41.6	41.5	0.911	0.996
Killer cell lectin-like receptor subfamily F member 1	KLRF1	92.7	97.4	90.2	103.9	89.8	85.6	93.4	93.1	0.959	0.996
Netrin receptor UNC5C	UNC5C	62.3	65.6	71.0	67.7	59.4	71.1	66.3	66.1	0.960	0.996
Lysosomal protective protein	CTSA	168.4	153.4	161.4	172.6	149.7	159.3	161.1	160.5	0.950	0.997
Proprotein convertase subtilisin/kexin type 9	PCSK9	20.5	21.4	20.9	20.1	20.4	22.1	20.9	20.9	0.928	0.997
Toll-like receptor 2	TLR2	280.2	233.4	249.9	241.4	278.2	241.6	254.5	253.7	0.969	0.997
Collagenase 3	MMP13	101.8	104.3	96.4	94.7	102.7	104.2	100.8	100.5	0.940	0.997
Myeloblastin	PRTN3	43.0	43.5	43.6	45.8	40.8	43.2	43.4	43.3	0.951	0.998
C-C motif chemokine 24	CCL24	143.2	129.8	137.9	144.7	131.6	133.8	137.0	136.7	0.964	0.998
Tyrosine-protein phosphatase non-receptor type 11	PTPN11	3217.4	3463.0	3100.4	3845.7	3466.1	2451.1	3260.3	3254.3	0.990	0.998
Interleukin-25	IL25	67.2	56.3	54.2	63.9	55.4	58.1	59.2	59.1	0.984	0.998
Serum amyloid P-component	APCS	280.5	271.7	290.8	263.3	293.7	285.6	281.0	280.9	0.991	1.000
CMRF35-like molecule 6	CD300C	81.7	88.6	84.5	90.0	82.6	82.1	84.9	84.9	0.992	1.000
Platelet-activating factor acetylhydrolase	PLA2G7	292.5	264.1	256.7	292.0	267.9	253.1	271.1	271.0	0.995	1.000
Protein E7_HPV18	Human-virus	445.0	421.1	454.7	449.6	430.1	441.0	440.3	440.2	0.998	1.000

		αHetγWT			**αKOγKO**			**αHetγWT**	**αKOγKO**		**Fold (αKOγKO**
TargetFullName	**EntrezGene**	**#1**	**#2**	**#3**	**#1**	**#2**	**#3**	**Average**	**Average**	**t-test**	**/αHetγWT)**
C-C motif chemokine 15	CCL15	76.7	82.2	75.9	82.1	74.7	78	78.3	78.3	1.000	1.000
Stromelysin-2	MMP10	104.6	118.9	106.7	110.4	125.3	94.7	110.1	110.1	0.995	1.001
Fms-related tyrosine kinase 3 ligand	FLT3LG	222.4	229.6	223.3	231.8	219	225.6	225.1	225.5	0.937	1.002
Immunoglobulin E	IGHE IGK@ IGL@	51.8	52	50.2	50.3	51.6	52.4	51.3	51.4	0.911	1.002
Lysosome membrane protein 2	SCARB2	65	65.6	63.6	68.1	62.4	64.1	64.7	64.9	0.946	1.002
BMP-binding endothelial regulator protein	BMPER	62.7	73	65	69.1	67	65.1	66.9	67.1	0.964	1.002
Cytoplasmic tyrosine-protein kinase BMX	BMX	139.8	146.2	143.8	133.7	149.8	147.4	143.3	143.6	0.950	1.003
Sonic hedgehog protein	SHH	436.4	373	405.7	410.9	425.1	382.3	405.0	406.1	0.964	1.003
Oxidized low-density lipoprotein receptor 1	OLR1	49.7	49.5	48	49.2	48.7	49.7	49.1	49.2	0.841	1.003

Coiled-coil domain-containing protein 80	CCDC80	19353.4	15250.6	16658.3	17584	16189.8	17661.3	17087.4	17145.0	0.968	1.003
Fibronectin	FN1	209279.7	161572.2	199594.7	180997.9	183991.5	207468.6	190148.9	190819.3	0.971	1.004
Ephrin type-A receptor 2	EPHA2	96.3	93.9	96.8	92.6	96.1	99.4	95.7	96.0	0.877	1.004
Acidic leucine-rich nuclear phosphoprotein 32 family member B	ANP32B	95.9	131.9	163.3	137.6	127.2	127.9	130.4	130.9	0.981	1.004
Interleukin-27	IL27 EBI3	226.8	214.3	218.3	233.6	219.8	208.7	219.8	220.7	0.918	1.004
Tumor necrosis factor ligand superfamily member 4	TNFSF4	83.8	78.8	76.9	79.5	75.5	85.5	79.8	80.2	0.930	1.004
Neural cell adhesion molecule L1-like protein	CHL1	71.4	110.5	75	98.7	88.3	71	85.6	86.0	0.982	1.004
C-X-C motif chemokine 11	CXCL11	27	25.5	35.2	29.1	25.2	33.8	29.2	29.4	0.974	1.005
Intercellular adhesion molecule 3	ICAM3	211	219.6	203.9	217.1	209.4	210.9	211.5	212.5	0.862	1.005
Inter-alpha-trypsin inhibitor heavy chain H4	ITIH4	44.7	42.4	41.2	46.8	40.3	41.8	42.8	43.0	0.934	1.005
Ectonucleoside triphosphate diphosphohydrolase 3	ENTPD3	529.7	526.7	532.9	524.6	542.2	530.3	529.8	532.4	0.674	1.005
Histone acetyltransferase type B catalytic subunit	HAT1	70	75.3	78.4	70.5	78.3	76.1	74.6	75.0	0.911	1.005
Serine/threonine-protein kinase PAK 7	PAK7	280.1	241.3	252.3	282.4	250.2	245.3	257.9	259.3	0.936	1.005
Chymase	CMA1	149.4	165.2	156.3	159.7	161.1	152.8	157.0	157.9	0.874	1.006
Vasoactive Intestinal Peptide	VIP	123.4	146.6	144.2	124.1	145.4	147.1	138.1	138.9	0.943	1.006
Kallikrein-7	KLK7	18257.3	13696.6	15614.9	17562.4	13343.8	16953.5	15856.3	15953.2	0.961	1.006
3-hydroxyacyl-CoA dehydrogenase type-2	HSD17B10	176.1	167.3	172.5	163.8	171.7	183.8	172.0	173.1	0.871	1.007
Matrix extracellular phosphoglycoprotein	MEPE	33.4	33.7	34.6	32.3	34.5	35.6	33.9	34.1	0.839	1.007
Transketolase	TKT	28126.5	30359.1	25759	26604.3	33358.2	24906.4	28081.5	28289.6	0.947	1.007
Aggrecan core protein	ACAN	118.2	107.3	111.5	115.4	117.3	107.3	112.3	113.3	0.832	1.009
Transforming growth factor beta receptor type 3	TGFBR3	619	623.5	729.2	666.9	621.3	702.4	657.2	663.5	0.892	1.010
C-X-C motif chemokine 13	CXCL13	61.4	59.1	58.8	62.7	55.7	62.7	59.8	60.4	0.827	1.010
Teratocarcinoma-derived growth factor 1	TDGF1	119.8	120.2	119.3	114.9	123.9	124.4	119.8	121.1	0.715	1.011
Intercellular adhesion molecule 5	ICAM5	666.5	620.8	1139.6	599.7	591.7	1263.7	809.0	818.4	0.975	1.012
Trefoil factor 3	TFF3	126.2	126.5	123.2	114.6	116.7	149.2	125.3	126.8	0.904	1.012
Chromobox protein homolog 5	CBX5	133.3	120.4	123.8	131.8	123.7	126.9	125.8	127.5	0.740	1.013
Thymidine kinase, cytosolic	TK1	237.2	213.3	227.3	251.9	214.6	220.3	225.9	228.9	0.837	1.013
C-reactive protein	CRP	80.2	86.3	76.8	84.6	76	86	81.1	82.2	0.806	1.014

Leukocyte immunoglobulin-like receptor subfamily B member 2	LILRB2	37.7	48.9	39.2	43.8	45.1	38.7	41.9	42.5	0.890	1.014
Angiopoietin-4	ANGPT4	83.1	83.2	78.8	85.1	84.3	79.4	81.7	82.9	0.621	1.015
Fibroblast growth factor 8 isoform B	FGF8	418.1	409.1	419.2	405.5	405.3	454.7	415.5	421.8	0.738	1.015
Annexin A2	ANXA2	3623	3683.2	3738.6	3647.4	3657.8	3911.1	3681.6	3738.8	0.586	1.016
Fibroblast growth factor 19	FGF19	186.9	120.8	125.5	180.3	127.8	132	144.4	146.7	0.937	1.016
SPARC	SPARC	157677.2	111205.8	142089.9	134781.6	136946.5	145912.6	136991.0	139213.6	0.888	1.016
Tumor necrosis factor ligand superfamily member 18	TNFSF18	209	203.9	219.4	207	216.1	219.5	210.8	214.2	0.593	1.016
Brain-derived neurotrophic factor	BDNF	147.4	148.3	138.6	143.6	148.6	149.3	144.8	147.2	0.547	1.017
Dual 3',5'-cyclic-AMP and -GMP phosphodiesterase 11A	PDE11A	618.7	817.1	804.6	659.8	896.2	722.2	746.8	759.4	0.901	1.017
FACT complex subunit SSRP1	SSRP1	47.7	49.3	49.2	48.9	48.6	51.2	48.7	49.6	0.447	1.017
Platelet glycoprotein Ib alpha chain	GP1BA	66.5	62.7	62.7	71.5	58.9	64.8	64.0	65.1	0.797	1.017
Cytokine receptor-like factor 1:Cardiotrophin-like cytokine factor 1 Complex	CRLF1 CLCF1	160.3	137	143	157.4	143.5	147.1	146.8	149.3	0.771	1.017
Tyrosine-protein kinase HCK	HCK	88.8	82.8	82.9	87.9	82	89.3	84.8	86.4	0.628	1.018
X-linked interleukin-1 receptor accessory protein-like 2	IL1RAPL2	222.9	210.4	216.2	220.8	223.8	217	216.5	220.5	0.397	1.019
Plasmin	PLG	154	157.5	155.4	165.3	154.1	156.2	155.6	158.5	0.492	1.019
A disintegrin and metalloproteinase with thrombospondin motifs 1	ADAMTS1	84.2	93.4	88.6	83.9	93.8	93.5	88.7	90.4	0.712	1.019
Cadherin-1	CDH1	224	218.8	215.6	207.4	220.7	242.7	219.5	223.6	0.730	1.019
Proteasome activator complex subunit 3	PSME3	74.8	74.8	72.7	79.3	76.5	70.7	74.1	75.5	0.641	1.019
RNA-binding protein 39	RBM39	140.7	144.1	128.4	155.1	142.6	123.6	137.7	140.4	0.811	1.020
Pituitary adenylate cyclase-activating polypeptide 38	ADCYAP1	127.8	183.1	137.6	166	157.5	133.8	149.5	152.4	0.890	1.020
Calcium-dependent phospholipase A2	PLA2G5	88.9	95.8	94.4	94.1	92.2	98.3	93.0	94.9	0.545	1.020
Lymphotoxin-alpha	LTA	166.3	172.8	174.5	171.9	176.6	175.6	171.2	174.7	0.306	1.020
Kunitz-type protease inhibitor 1	SPINT1	282.2	260.3	266.6	282.6	289.6	253.7	269.7	275.3	0.689	1.021
G2/mitotic-specific cyclin-B1	CCNB1	56.2	72.1	58.5	75.7	58.1	56.9	62.3	63.6	0.877	1.021
Stromelysin-1	MMP3	131.8	122.2	136.5	123.4	130.1	145.3	130.2	132.9	0.741	1.021
Mitogen-activated protein kinase 13	MAPK13	58.6	54.9	55.4	62.4	52.9	57.2	56.3	57.5	0.717	1.021

Endothelial monocyte-activating polypeptide 2	AIMP1	9574.4	8060.4	10362	8370.2	9034.6	11192.8	9332.3	9532.5	0.863	1.021
Mitochondrial glutamate carrier 2	SLC25A18	548.4	542.1	538.4	480	595	589	543.0	554.7	0.784	1.022
Nidogen-2	NID2	12745.1	10847.3	12092.8	11208.5	11246.5	14013.7	11895.1	12156.2	0.824	1.022
Cysteine-rich secretory protein 3	CRISP3	57.2	61.8	54.8	62.2	60.8	54.8	57.9	59.3	0.686	1.023
Nucleoside diphosphate kinase B	NME2	33	28.2	29.3	30.7	30.4	31.5	30.2	30.9	0.681	1.023
Serine/threonine-protein kinase PLK1	PLK1	60.3	59.9	59.4	64.4	60.5	58.9	59.9	61.3	0.483	1.023
Insulin	INS	51.2	43.7	31.9	43	43.3	43.5	42.3	43.3	0.875	1.024
Plasminogen activator inhibitor 1	SERPINE1	39.1	34.1	42.9	39.4	40.1	39.4	38.7	39.6	0.750	1.024
Interleukin-17B	IL17B	64.3	28.5	27.4	57.5	32	33.6	40.1	41.0	0.951	1.024
Alpha-1-antitrypsin	SERPINA1	54.4	77.8	52.7	67.5	64.1	57.8	61.6	63.1	0.874	1.024
MHC class I polypeptide-related sequence B	MICB	42.3	42.4	41.8	42.3	44.8	42.5	42.2	43.2	0.326	1.025
Amyloid beta A4 protein	APP	73.1	73.2	76.3	79.3	76.1	72.7	74.2	76.0	0.459	1.025
Epiregulin	EREG	154.9	154.8	152.9	161.9	155.1	157.1	154.2	158.0	0.190	1.025
Interleukin-6 receptor subunit beta	IL6ST	137.9	136.1	136.3	146.3	135.1	139.1	136.8	140.2	0.409	1.025
CD5 antigen-like	CD5L	55	51.5	53.7	55.1	54.8	54.3	53.4	54.7	0.321	1.025
Tissue Factor	F3	175.7	178.5	177.3	177.2	174.9	192.8	177.2	181.6	0.511	1.025
Mitogen-activated protein kinase 8	MAPK8	373.2	455.6	310.9	320.4	417.8	430.3	379.9	389.5	0.869	1.025
cAMP-dependent protein kinase catalytic subunit alpha	PRKACA	404.4	762.4	444	606.6	668.9	376.1	536.9	550.5	0.930	1.025
NKG2D ligand 2	ULBP2	58	55.4	55	62.5	54.6	55.6	56.1	57.6	0.633	1.026
Protein disulfide-isomerase	P4HB	58.7	58.9	58.6	60.4	59.8	60.6	58.7	60.3	0.015	1.026
Plasminogen	PLG	24.6	22.8	23.8	23.5	25.6	24	23.7	24.4	0.484	1.027
NADPH--cytochrome P450 reductase	POR	73.7	68.7	70	75.4	66.9	76	70.8	72.8	0.593	1.028
Fibroblast growth factor 4	FGF4	72.6	76.1	76.1	72.1	78.6	80.5	74.9	77.1	0.505	1.028
Alkaline phosphatase, tissue-nonspecific isozyme	ALPL	719.2	304	285.6	271.5	265.6	809	436.3	448.7	0.959	1.028
Myeloperoxidase	MPO	100	99.5	87.6	102.7	93.3	99.3	95.7	98.4	0.610	1.029
Interleukin-4 receptor subunit alpha	IL4R	52.1	54.7	49.5	50.6	55	55.3	52.1	53.6	0.512	1.029
Hepatocyte growth factor activator	HGFAC	196137.5	156323.2	181305.2	176590.9	181546.6	191503.5	177922.0	183213.7	0.703	1.030
Tryptase gamma	TPSG1	108.2	90.9	98.4	107	98.3	101.1	99.2	102.1	0.635	1.030
Iduronate 2-sulfatase	IDS	221.2	213.9	206.7	211.4	227.9	221.8	213.9	220.4	0.371	1.030
Placenta growth factor	PGF	116	116.3	117.2	125.2	114.2	120.8	116.5	120.1	0.381	1.031
Angiotensinogen	AGT	33.6	34.8	32	36.4	35	32.1	33.5	34.5	0.536	1.031

Alpha-2-antiplasmin	SERPINF2	40.4	28.2	27.7	43	26.9	29.4	32.1	33.1	0.885	1.031
Annexin A1	ANXA1	445.7	440.5	452.9	377	496	508.2	446.4	460.4	0.770	1.031
Prothrombin	F2	222246.4	174046.2	207772.3	208100.1	197013.7	218111.7	201355.0	207741.8	0.711	1.032
Bone morphogenetic protein 7	BMP7	664.9	503.4	633.1	569.7	530.3	758.9	600.5	619.6	0.836	1.032
Interleukin-20 receptor subunit alpha	IL20RA	31.4	31.7	30.8	32.2	32.7	32.1	31.3	32.3	0.039	1.033
Complement C1r subcomponent	C1R	17.9	16.1	16.7	16.7	17.4	18.3	16.9	17.5	0.466	1.034
Macrophage-stimulating protein receptor	MST1R	236.4	216.9	224.8	255.9	223	222.1	226.0	233.7	0.584	1.034
Activin receptor type-1B	ACVR1B	108.2	182	103.7	110.4	185.4	111.5	131.3	135.8	0.906	1.034
Killer cell immunoglobulin-like receptor 3DL2	KIR3DL2	57.6	60.1	56.9	64.3	58.3	58	58.2	60.2	0.446	1.034
CD70 antigen	CD70	218.4	248.6	235.2	232	254.9	239.8	234.1	242.2	0.502	1.035
Leukemia inhibitory factor receptor	LIFR	35.3	29.5	29.6	33.4	28.6	35.7	31.5	32.6	0.718	1.035
Tumor-associated calcium signal transducer 2	TACSTD2	122.1	133.4	133.2	127.8	139.4	135.2	129.6	134.1	0.417	1.035
Glucose-6-phosphate isomerase	GPI	41.4	34.8	33.7	42.9	35.1	35.8	36.6	37.9	0.726	1.035
[Pyruvate dehydrogenase (acetyl-transferring)] kinase isozyme 1, mitochondrial	PDK1	624.5	574.5	575.1	627.1	597.7	612.7	591.4	612.5	0.339	1.036
Cadherin-2	CDH2	311	302	317.5	309.8	308.6	345.5	310.2	321.3	0.462	1.036
C-type mannose receptor 2	MRC2	43.9	52.2	42.6	51.2	47.9	44.6	46.2	47.9	0.668	1.036
EGF-like module-containing mucin-like hormone receptor-like 2	EMR2	50.4	45.4	45	47.1	47.8	51	46.9	48.6	0.471	1.036
Platelet glycoprotein VI	GP6	104.6	108.1	109.4	109	112.7	112.2	107.4	111.3	0.103	1.037
Aurora kinase A	AURKA	505.5	480.1	490.9	521.4	508.3	501.5	492.2	510.4	0.128	1.037
Persephin	PSPN	69.9	63.3	63.5	69.4	65.3	69.4	65.6	68.0	0.400	1.038
Aromatic-L-amino-acid decarboxylase	DDC	47.6	37	36.5	47.2	39.1	39.4	40.4	41.9	0.751	1.038
Interleukin-6	IL6	70.3	76.1	65.3	77.1	73	69.7	70.6	73.3	0.520	1.038
Gremlin-1	GREM1	78.1	82.8	77.6	83.6	88.3	75.8	79.5	82.6	0.503	1.039
Histidine-rich glycoprotein	HRG	110.6	112	111.5	123.9	110.3	112.8	111.4	115.7	0.412	1.039
Fibrinogen	FGA FGB FGG	208245.4	165637.2	194427.7	187576.5	192637	210089	189436.8	196767.5	0.642	1.039
Superoxide dismutase [Mn], mitochondrial	SOD2	21602	21504.4	23070.3	23992.3	22169	22624.9	22058.9	22928.7	0.309	1.039
Baculoviral IAP repeat-containing protein 3	BIRC3	72.7	65.7	66.6	79.4	66.9	66.8	68.3	71.0	0.607	1.040
A disintegrin and metalloproteinase with thrombospondin motifs 5	ADAMTS5	142.6	132.7	136.6	143.3	134.3	150.6	137.3	142.7	0.392	1.040

Interleukin-12 receptor subunit beta-1	IL12RB1	129.1	123.6	119.4	135.8	126.2	124.9	124.0	129.0	0.331	1.040
Inhibin beta A chain:Inhibin beta B chain heterodimer	INHBA INHBB	39.9	51.3	49	45.5	52.7	47.6	46.7	48.6	0.676	1.040
Cystatin-SN	CST1	106.2	84.4	73.6	78.5	76	120.5	88.1	91.7	0.847	1.041
Asialoglycoprotein receptor 1	ASGR1	57	59.5	55.4	61.5	57.1	60.4	57.3	59.7	0.255	1.041
Interstitial collagenase	MMP1	127.6	120.8	125.8	137.5	124.1	128.1	124.7	129.9	0.331	1.041
Megakaryocyte-associated tyrosine-protein kinase	MATK	104.1	102.4	96.5	100.1	102.2	113.3	101.0	105.2	0.434	1.042
Ephrin-B3	EFNB3	426.6	421.1	382.8	424.8	405.3	452	410.2	427.4	0.424	1.042
Carbonic anhydrase 2	CA2	44.5	46.1	40.3	49.9	43.1	43.4	43.6	45.5	0.552	1.042
Pancreatic hormone	PPY	114.4	124.5	111.5	128.7	121.2	115.3	116.8	121.7	0.423	1.042
N-acylethanolamine-hydrolyzing acid amidase	NAAA	118.4	114.4	124	121.3	118.8	131.9	118.9	124.0	0.365	1.043
Ficolin-3	FCN3	34.3	87.2	30.6	46.3	81.2	31.1	50.7	52.9	0.931	1.043
Insulin-like growth factor-binding protein 6	IGFBP6	143.7	115	112	149.8	117.9	118.9	123.6	128.9	0.734	1.043
Eukaryotic translation initiation factor 4E-binding protein 2	EIF4EBP2	93	94.1	91.4	93.3	93.5	103.7	92.8	96.8	0.364	1.043
Pleiotrophin	PTN	19735.4	15671.5	16571.9	17223.8	16939.8	20056	17326.3	18073.2	0.663	1.043
Scavenger receptor class F member 2	SCARF2	77	80.1	70.1	91.8	75.8	69.6	75.7	79.1	0.679	1.044
Immunoglobulin D	IGHD IGK@ IGL@	42.5	39.9	38	41.5	40.4	43.8	40.1	41.9	0.347	1.044
Protein Rev_HV2BE	Human-virus	30.5	30	27.5	30	29.7	32.2	29.3	30.6	0.347	1.044
Interleukin-17D	IL17D	74.4	84	82	85.6	86.5	79.1	80.1	83.7	0.393	1.045
Matrilin-3	MATN3	149.3	147.5	145.2	158.1	157.7	146.2	147.3	154.0	0.224	1.045
Contactin-5	CNTN5	72.6	68.8	72.6	70.2	82	71.6	71.3	74.6	0.479	1.046
ATP-dependent RNA helicase DDX19B	DDX19B	159	154.8	141.5	172.5	145.8	157.9	151.8	158.7	0.503	1.046
Carboxypeptidase B2	CPB2	61.4	64.1	63.3	63.5	66.8	67.3	62.9	65.9	0.121	1.047
Growth hormone receptor	GHR	123.3	119.5	127.5	135.4	120.7	131.7	123.4	129.3	0.326	1.047
Complement factor B	CFB	37.1	26.1	23.1	36.6	26.9	26.9	28.8	30.1	0.812	1.048
Leucine-rich repeats and immunoglobulin-like domains protein 3	LRIG3	94.9	94.5	98.4	99.4	103.1	99.1	95.9	100.5	0.062	1.048
C-C motif chemokine 14	CCL14	32.6	32.9	30	34.7	32.6	32.8	31.8	33.4	0.255	1.048
Homeodomain-interacting protein kinase 3	HIPK3	438.7	377.2	409.8	438.6	409.4	437.8	408.6	428.6	0.393	1.049
Neuropilin-1	NRP1	2607.2	2331.1	2376.8	2582.5	2584	2508.9	2438.4	2558.5	0.293	1.049
CD209 antigen	CD209	243.9	221.4	207.7	230.7	242.4	233.1	224.3	235.4	0.408	1.049

Leukocyte immunoglobulin-like receptor subfamily B member 1	LILRB1	47.8	64.7	50.8	50.6	65.6	55.2	54.4	57.1	0.714	1.050
Thrombospondin-4	THBS4	8298.1	7383	7923.1	9139.4	6392.8	9246.5	7868.1	8259.6	0.721	1.050
Ciliary Neurotrophic Factor	CNTF	95.6	86.2	87.1	98.5	89.2	94.7	89.6	94.1	0.328	1.050
Complement C3	C3	57	61.5	55.4	58.2	60.1	64.4	58.0	60.9	0.320	1.051
Galactoside 3(4)-L-fucosyltransferase	FUT3	63.2	60	60.5	69.8	62.7	60.5	61.2	64.3	0.388	1.051
Nicotinamide phosphoribosyltransferase	NAMPT	132.8	86.9	85.8	127.3	98.9	94.8	101.8	107.0	0.796	1.051
A disintegrin and metalloproteinase with thrombospondin motifs 4	ADAMTS4	100.8	94.9	97.5	103.2	99.8	105.1	97.7	102.7	0.098	1.051
Carbonic anhydrase 9	CA9	710.2	633.2	683	614.2	674.3	841.8	675.5	710.1	0.669	1.051
Small nuclear ribonucleoprotein F	SNRPF	605.5	677.7	732.7	722.6	738.9	657.9	672.0	706.5	0.486	1.051
3-hydroxyisobutyrate dehydrogenase, mitochondrial	HIBADH	191.6	188.2	188.5	198.7	189.4	209.5	189.4	199.2	0.232	1.052
Tyrosine-protein kinase Fgr	FGR	50.3	60	50.6	52	58	59.2	53.6	56.4	0.520	1.052
Protein FAM107B	FAM107B	159.7	155.5	156.4	162.4	161.3	172.5	157.2	165.4	0.137	1.052
Tumor necrosis factor receptor superfamily member 4	TNFRSF4	56.4	61.6	54.3	63.2	63	55.2	57.4	60.5	0.426	1.053
Mitogen-activated protein kinase 14	MAPK14	1104.9	1265.2	1073.3	1275.3	1275.8	1074.8	1147.8	1208.6	0.534	1.053
6-phosphogluconate dehydrogenase, decarboxylating	PGD	42036.8	45899.4	44175.7	50723.2	46269.7	42224.6	44037.3	46405.8	0.449	1.054
Stem Cell Growth Factor-beta	CLEC11A	121.4	118.2	114.3	124.6	123.9	124.5	118.0	124.3	0.089	1.054
Reticulon-4	RTN4	51.1	56	51.4	56.6	53.4	57.2	52.8	55.7	0.222	1.055
Complement factor H	CFH	66.9	72.1	69.3	68.6	74.7	76.6	69.4	73.3	0.258	1.056
S-formylglutathione hydrolase	ESD	753.5	778	723.2	777.4	946.1	657.2	751.6	793.6	0.668	1.056
T-cell surface glycoprotein CD4	CD4	117.1	109.3	116.5	120.4	117.9	123.8	114.3	120.7	0.112	1.056
Pyruvate kinase PKM	PKM2	159655.4	126351.2	142337.2	146603.4	142287	163476.3	142781.3	150788.9	0.533	1.056
Ephrin-A4	EFNA4	81.6	71.5	78.5	86.1	78.9	79.6	77.2	81.5	0.318	1.056
Tumor necrosis factor ligand superfamily member 9	TNFSF9	93	85.1	85.8	90.6	91.9	96.3	88.0	92.9	0.189	1.056
Apolipoprotein E (isoform E4)	APOE	108.9	107.7	110	118.7	113.6	112.8	108.9	115.0	0.066	1.057
Serine/threonine-protein kinase pim-1	PIM1	179.1	187.1	250	194.9	194.6	261.9	205.4	217.1	0.730	1.057
Immunoglobulin M	IGHM IGJ IGK@ IGL@	161.9	172.4	161.8	178.2	172.4	173.9	165.4	174.8	0.097	1.057
Fibroblast growth factor receptor 1	FGFR1	35241.9	28770.8	30291.7	35898.7	30555.2	33260.7	31434.8	33238.2	0.511	1.057
Lactotransferrin	LTF	158.4	85.9	66.4	72.2	67	189.4	103.6	109.5	0.909	1.058
Metalloproteinase inhibitor 2	TIMP2	92612.1	68125.7	85303	89501.6	84161.2	86605.3	82013.6	86756.0	0.583	1.058

High affinity cGMP-specific 3',5'-cyclic phosphodiesterase 9A	PDE9A	124	122.4	128.2	120.3	138.2	138	124.9	132.2	0.344	1.058
Endothelial cell-selective adhesion molecule	ESAM	241.2	214	226.7	250.9	226.4	244.5	227.3	240.6	0.284	1.059
X-ray repair cross-complementing protein 6	XRCC6	35.7	35.7	32.7	35.6	37.2	37.4	34.7	36.7	0.170	1.059
Fibroblast growth factor 17	FGF17	53.7	48.4	50.3	51.8	54.4	55.2	50.8	53.8	0.193	1.059
Contactin-2	CNTN2	124.9	121.8	115.4	132.3	125.6	125.7	120.7	127.9	0.119	1.059
Receptor tyrosine-protein kinase erbB-2	ERBB2	167.2	141.2	175	163.5	159.2	189.5	161.1	170.7	0.529	1.060
BDNF/NT-3 growth factors receptor	NTRK2	41.2	40.4	39	44.2	41.3	42.3	40.2	42.6	0.093	1.060
C-X-C motif chemokine 6	CXCL6	86.1	75.1	76.1	85.6	79.1	86.8	79.1	83.8	0.335	1.060
Granzyme A	GZMA	76.9	70.1	71.6	81.8	73.7	76.2	72.9	77.2	0.241	1.060
Fibrinogen gamma chain	FGG	201718.6	172902.2	191518.4	194367.5	194898.2	211063.1	188713.1	200109.6	0.330	1.060
Heparan-sulfate 6-O-sulfotransferase 1	HS6ST1	79.7	64.5	75.9	79.2	75	79.2	73.4	77.8	0.438	1.060
Cytotoxic T-lymphocyte protein 4	CTLA4	44.5	42.4	46.7	45.8	44.1	51.8	44.5	47.2	0.381	1.061
Galectin-2	LGALS2	154.3	143.9	143.8	152.1	147.4	169.3	147.3	156.3	0.319	1.061
Interleukin-20	IL20	61.6	57.1	57.4	61.9	61.8	63.1	58.7	62.3	0.124	1.061
Human Chorionic Gonadotropin	CGA CGB	90.2	79.3	83.3	90.7	88.3	89.2	84.3	89.4	0.245	1.061
Collectin-11	COLEC11	13235.2	11891.5	12063.4	9531.5	12990	16935.6	12396.7	13152.4	0.760	1.061
Osteomodulin	OMD	35	39	35.9	40.2	38.4	38	36.6	38.9	0.202	1.061
Somatostatin-28	SST	172.5	168.8	165.1	181.6	171.1	184.7	168.8	179.1	0.112	1.061
Complement C3d fragment	C3	64.4	58.6	58.2	68.1	59.2	65.1	60.4	64.1	0.324	1.062
Intercellular adhesion molecule 2	ICAM2	232	218.9	221.8	222.5	239.6	252.3	224.2	238.1	0.246	1.062
gp41 C34 peptide, HIV	Human-virus	213.7	213.5	217.4	220	211.4	253.3	214.9	228.2	0.405	1.062
Tumor necrosis factor ligand superfamily member 6, soluble form	FASLG	181.2	169.5	173.9	179.8	184.8	192.8	174.9	185.8	0.099	1.063
Tyrosine-protein phosphatase non-receptor type 2	PTPN2	148.7	140.2	142.8	151.1	153.1	154.5	143.9	152.9	0.055	1.063
Complement component C9	C9	36.4	38.2	41.7	42.4	38.4	42.8	38.8	41.2	0.311	1.063
Sialic acid-binding Ig-like lectin 7	SIGLEC7	34.2	36.7	34.1	37.1	37.6	36.9	35.0	37.2	0.115	1.063
Calcineurin	PPP3CA PPP3R1	838.2	1166.3	806.2	1113.6	909.5	964.5	936.9	995.9	0.681	1.063
C-type lectin domain family 1 member B	CLEC1B	36	29.4	31.4	36.4	32	34.5	32.3	34.3	0.440	1.063
Lactoperoxidase	LPO	57.8	64.3	53.8	63.8	57.5	65.7	58.6	62.3	0.403	1.063
Seprase	FAP	70.8	73.2	69.7	77.4	78.1	71.7	71.2	75.7	0.143	1.063

Clusterin	CLU	40.5	40.3	47	46.7	43.4	45.8	42.6	45.3	0.350	1.063
Interleukin-5 receptor subunit alpha	IL5RA	161.3	149.9	155.5	168.9	168.4	159.1	155.6	165.5	0.097	1.064
Low affinity immunoglobulin gamma Fc region receptor III-B	FCGR3B	54.5	58.3	58.4	57.9	60.8	63.5	57.1	60.7	0.154	1.064
Dual specificity mitogen-activated protein kinase kinase 4	MAP2K4	8213.9	7379.2	7526.7	8410.9	8399.2	7799.6	7706.6	8203.2	0.207	1.064
Cerebral dopamine neurotrophic factor	CDNF	95	89.1	88.9	104	88.8	97.9	91.0	96.9	0.317	1.065
Protein NOV homolog	NOV	376	337.4	340.9	448.6	367.8	306.3	351.4	374.2	0.642	1.065
Proprotein convertase subtilisin/kexin type 7	PCSK7	162.4	152.2	157.5	168.5	158.8	175.5	157.4	167.6	0.160	1.065
Dipeptidyl peptidase 1	CTSC	301.3	258	291.6	302.6	289.4	314.3	283.6	302.1	0.302	1.065
Complement C5	C5	49.9	46.6	51.9	57.5	51.7	48.9	49.5	52.7	0.349	1.065
C-C motif chemokine 25	CCL25	84	76.4	81	87.5	80.6	89.1	80.5	85.7	0.200	1.065
Fibronectin Fragment 4	FN1	164676.4	123673	146561.1	146157.7	139699.7	177534.5	144970.2	154464.0	0.599	1.065
Complement C4	C4A C4B	24.5	25.5	27.6	26.6	27.4	28.7	25.9	27.6	0.207	1.066
Protein DJ-1	PARK7	224.6	192	201	253.8	191	213.4	205.9	219.4	0.561	1.066
Granulocyte colony-stimulating factor	CSF3	120	121.6	119.8	126.5	136.8	122	120.5	128.4	0.209	1.066
Aflatoxin B1 aldehyde reductase member 2	AKR7A2	39.1	37.9	34.7	39.8	42.3	37	37.2	39.7	0.290	1.066
Hepatocyte growth factor receptor	MET	80.8	69.6	74.4	78.3	78.1	83.3	74.9	79.9	0.268	1.066
SLAM family member 6	SLAMF6	45.5	48.8	44.1	58.6	44.6	44.4	46.1	49.2	0.587	1.066
Platelet-derived growth factor C	PDGFC	98.3	83.6	142.9	105.8	88.1	152.5	108.3	115.5	0.797	1.067
Cathepsin Z	CTSZ	64.3	71.1	64.1	75.2	72	65.7	66.5	71.0	0.287	1.067
Tumor necrosis factor	TNF	59	56.9	57.8	65.1	64.9	55.4	57.9	61.8	0.347	1.067
Immunoglobulin alpha Fc receptor	FCAR	60.5	59.6	58	64.6	59.7	65.8	59.4	63.4	0.154	1.067
High affinity immunoglobulin gamma Fc receptor I	FCGR1A	130.8	122.3	120.7	124.1	130.2	144.7	124.6	133.0	0.309	1.067
Protein E7_HPV16	Human-virus	38.2	35	36.1	37.1	37.6	42	36.4	38.9	0.261	1.068
Trypsin-3	PRSS3	98.2	93	95.1	103.6	98.3	103.8	95.4	101.9	0.053	1.068
Kunitz-type protease inhibitor 2	SPINT2	107.3	105.9	107	108.9	110.9	122.1	106.7	114.0	0.219	1.068
Neutrophil collagenase	MMP8	12039.6	10037.2	10250.8	11167.7	10885	12505.5	10775.9	11519.4	0.412	1.069
Cystatin-D	CST5	71.4	57.3	55.7	65.2	60.7	71.3	61.5	65.7	0.514	1.069
Heterogeneous nuclear ribonucleoprotein K	HNRNPK	75.2	72	68.8	78.4	74.9	77.8	72.0	77.0	0.094	1.070
Protein kinase C delta type	PRKCD	99	116.5	125.4	94.7	140.1	130.3	113.6	121.7	0.644	1.071
Glutathione S-transferase A3	GSTA3	34.8	62.5	33.6	33.3	42.6	64.4	43.6	46.8	0.824	1.072
Roundabout homolog 2	ROBO2	27290.3	21612.7	23471.3	24487.4	24806.1	28295	24124.8	25862.8	0.452	1.072

Coactosin-like protein	COTL1	1514.1	1393.5	1396.4	1729.8	1665.6	1220.7	1434.7	1538.7	0.586	1.073
VPS10 domain-containing receptor SorCS2	SORCS2	51.3	47.1	50	53.1	51.1	55.1	49.5	53.1	0.099	1.073
Macrophage migration inhibitory factor	MIF	297.2	328.4	339.4	324.4	399.9	313.5	321.7	345.9	0.481	1.075
Serotransferrin	TF	123	89	103.6	125.4	102.1	112	105.2	113.2	0.546	1.076
Sphingosine kinase 2	SPHK2	153.1	141.5	145.1	156.1	155.6	161.9	146.6	157.9	0.060	1.077
Cryptic protein	CFC1	825.2	834.9	793.1	894.1	850	899.3	817.7	881.1	0.037	1.078
72 kDa type IV collagenase	MMP2	11470.7	8972	9689.2	10717	10012.5	11749	10044.0	10826.2	0.439	1.078
Neurogenic locus notch homolog protein 3	NOTCH3	55.5	58.3	53.8	66.6	58	56.1	55.9	60.2	0.310	1.078
Ectonucleotide pyrophosphatase/phosphodiesterase family member 7	ENPP7	58.8	54	54.1	58.8	60.7	60.5	55.6	60.0	0.096	1.078
Cation-independent mannose-6-phosphate receptor	IGF2R	106965.4	79146.3	88476.2	85920.8	82337.4	127946	91529.3	98734.7	0.695	1.079
Glypican-5	GPC5	62.3	57.7	61.6	70.5	60.5	64.9	60.5	65.3	0.239	1.079
A disintegrin and metalloproteinase with thrombospondin motifs 15	ADAMTS15	99.9	89.1	92.8	103.8	100.4	99.8	93.9	101.3	0.132	1.079
Complement C2	C2	41.7	43.1	39.5	48.2	43.5	42.4	41.4	44.7	0.205	1.079
Group IIE secretory phospholipase A2	PLA2G2E	142.7	117.5	128	146	127	145.9	129.4	139.6	0.350	1.079
Diablo homolog, mitochondrial	DIABLO	627.8	586.9	600.9	651.2	681.6	626.4	605.2	653.1	0.080	1.079
Myeloid cell surface antigen CD33	CD33	37.6	31	33.3	35.1	36	38.9	34.0	36.7	0.310	1.079
Thrombopoietin Receptor	MPL	31	32.6	29.3	34	32.7	33.6	31.0	33.4	0.108	1.080
Alpha-(1,3)-fucosyltransferase 5	FUT5	57.2	46.9	50.1	58.5	53.4	54.7	51.4	55.5	0.313	1.080
Mitogen-activated protein kinase 9	MAPK9	1014	774.6	998.3	980.2	979	1054.3	929.0	1004.5	0.436	1.081
Carbohydrate sulfotransferase 6	CHST6	66.5	65.3	63.7	67.1	69.3	75	65.2	70.5	0.142	1.081
Sialic acid-binding Ig-like lectin 9	SIGLEC9	76.9	69.3	74.3	82.7	74.2	81.6	73.5	79.5	0.162	1.082
Caspase-2	CASP2	45.7	44.5	43.9	53.7	48.7	42.8	44.7	48.4	0.361	1.083
Renin	REN	56.5	55.5	53.1	62.2	57	59.7	55.0	59.6	0.073	1.084
Serine/threonine-protein kinase Chk2	CHEK2	103.3	92.3	97.8	108.1	103	106.9	97.8	106.0	0.106	1.084
Protein-tyrosine kinase 6	PTK6	162.6	156.1	171.1	159.6	165.3	206.1	163.3	177.0	0.451	1.084
Proteasome subunit alpha type-1	PSMA1	197.6	223.3	210.8	223.4	262.9	198.8	210.6	228.4	0.449	1.085
T-lymphocyte surface antigen Ly-9	LY9	34.8	31	36.9	37.4	33.8	40.2	34.2	37.1	0.316	1.085
C-C motif chemokine 4-like	CCL4L1	43.9	45.8	44.7	50.6	46.8	48.4	44.8	48.6	0.055	1.085

Granzyme B	GZMB	57.6	58.1	56.3	57.3	63.4	66	57.3	62.2	0.194	1.085
Secretin	SCT	40.5	40.6	37.9	45.5	40.3	43.4	39.7	43.1	0.141	1.086
C-C motif chemokine 22	CCL22	53.8	52.8	49.7	56	54.9	58.8	52.1	56.6	0.058	1.086
Interleukin-17A	IL17A	88.1	78.9	82.7	87.8	88.7	94.7	83.2	90.4	0.108	1.086
Fibroblast growth factor 23	FGF23	67.8	64.8	61.2	77.4	65.8	67.3	64.6	70.2	0.268	1.086
C3a anaphylatoxin des Arginine	C3	67.6	60.3	65.1	66.6	73.4	69.8	64.3	69.9	0.127	1.087
Epidermal growth factor receptor	EGFR	138551.8	104710.8	121421	122574.4	121700.7	152162.4	121561.2	132145.8	0.491	1.087
Leucine-rich repeat transmembrane neuronal protein 1	LRRTM1	23.7	23.9	22.4	25.9	24.6	25.6	23.3	25.4	0.031	1.087
Tumor necrosis factor receptor superfamily member 21	TNFRSF21	79.5	43.9	43.7	87.6	46.6	47.5	55.7	60.6	0.801	1.087
Brain natriuretic peptide 32	NPPB	95.7	113.3	94	109.9	108.8	110.9	101.0	109.9	0.287	1.088
Resistin	RETN	128.5	139	123.3	149.1	137.8	138.3	130.3	141.7	0.128	1.088
Interleukin-17 receptor A	IL17RA	73.5	79.2	78.6	86.6	86.7	78.4	77.1	83.9	0.119	1.088
Prostate-specific antigen	KLK3	44.6	40.4	41.7	46.8	43.2	47.9	42.2	46.0	0.120	1.088
Neurotrophin-4	NTF4	78.5	72	71.9	79.7	78.1	84.3	74.1	80.7	0.086	1.089
Dynein light chain 1, cytoplasmic	DYNLL1	102.6	94.9	119.5	107.7	104.4	133	105.7	115.0	0.466	1.089
Lymphocyte antigen 86	LY86	6474.5	5806.8	6360.1	6370.9	7389.1	6534.8	6213.8	6764.9	0.229	1.089
Sialoadhesin	SIGLEC1	24.4	22.3	21.7	23.2	25.4	25.9	22.8	24.8	0.156	1.089
Complement C4b	C4A C4B	45.9	48.2	48.3	49	51.7	54.4	47.5	51.7	0.095	1.089
interleukin-17 receptor B	IL17RB	120.7	104.7	115.4	128.2	118.8	124.2	113.6	123.7	0.153	1.089
C3a anaphylatoxin	C3	16.3	15.1	13.4	17.2	15.6	16	14.9	16.3	0.258	1.089
Cell adhesion molecule 1	CADM1	491.4	425	434.6	539.9	453.1	478.9	450.3	490.6	0.292	1.089
Contactin-1	CNTN1	4510.4	3814.7	4032.7	4661.2	4204.3	4606.9	4119.3	4490.8	0.221	1.090
Tyrosine-protein kinase Fer	FER	18.9	27.7	20.1	23.3	26.3	23.2	22.2	24.3	0.547	1.091
Metalloproteinase inhibitor 1	TIMP1	35.3	32.6	33.5	38.8	35.1	36.8	33.8	36.9	0.086	1.092
Heparin-binding EGF-like growth factor	HBEGF	86	81	83.4	86.3	90.8	96.4	83.5	91.2	0.101	1.092
Beta-2-microglobulin	B2M	21.3	20.9	20.2	24	21.9	22.4	20.8	22.8	0.071	1.095
Serine/threonine-protein kinase PAK 6	PAK6	228.2	216.8	237.6	224.1	239.2	284.2	227.5	249.2	0.355	1.095
C5a anaphylatoxin	C5	52.5	48.3	49.9	50.8	58.3	56	50.2	55.0	0.151	1.096
E-Selectin	SELE	95791.5	84481.2	90063.8	106297.3	80183.7	109748.8	90112.2	98743.3	0.459	1.096
Glypican-2	GPC2	41.7	38.6	38.5	45.2	41.5	43.5	39.6	43.4	0.064	1.096
Galectin-3-binding protein	LGALS3BP	29.7	26.6	28.1	30	30.3	32.2	28.1	30.8	0.079	1.096
C-C motif chemokine 18	CCL18	37	40.4	35.1	45.9	40.7	36.7	37.5	41.1	0.322	1.096
Endothelial cell-specific molecule 1	ESM1	146	138.3	143.2	166.8	148.4	153.4	142.5	156.2	0.116	1.096
Serine/threonine-protein kinase Chk1	CHEK1	200	199.2	205.1	210	222.2	230.3	201.4	220.8	0.070	1.096

Lymphatic vessel endothelial hyaluronic acid receptor 1	LYVE1	74.1	70.2	72.2	79.9	78.7	78.9	72.2	79.2	0.017	1.097
Scavenger receptor class F member 1	SCARF1	74.2	79.1	72.6	90.8	80.1	77	75.3	82.6	0.215	1.097
Interleukin-24	IL24	82.2	82.4	82.1	87.7	92.9	90.5	82.2	90.4	0.032	1.099
Interferon gamma receptor 1	IFNGR1	64.2	64.5	62.3	74.6	66.9	68.4	63.7	70.0	0.106	1.099
Ephrin type-A receptor 3	EPHA3	62.1	54.9	53.8	61.9	59.6	66.3	56.9	62.6	0.163	1.100
Thrombin	F2	179.9	164.4	155.4	177.4	185.5	186.6	166.6	183.2	0.133	1.100
Glyceraldehyde-3-phosphate dehydrogenase	GAPDH	316	385.9	292.7	297.1	337.7	460.2	331.5	365.0	0.593	1.101
Elafin	PI3	100.1	105.7	94.9	111.4	103.8	116.3	100.2	110.5	0.100	1.102
Plasma kallikrein	KLKB1	26.6	27.7	26.7	30	28.6	30.7	27.0	29.8	0.027	1.102
Thyroglobulin	TG	74.9	72.2	71.9	80.9	74.8	85.9	73.0	80.5	0.134	1.103
Fetuin-B	FETUB	35.2	34.6	35.5	41.3	36.7	38.2	35.1	38.7	0.110	1.104
Macrophage metalloelastase	MMP12	29.8	27.7	29.1	32.5	30.2	32.9	28.9	31.9	0.050	1.104
Calpastatin	CAST	5879.1	5254.8	5448	5848.7	5577.6	6884	5527.3	6103.4	0.286	1.104
Sex hormone-binding globulin	SHBG	34.1	33	31.1	41.4	34.5	32.6	32.7	36.2	0.328	1.105
Carbonic anhydrase 6	CA6	43	36.7	37.2	42.5	41.6	45.1	39.0	43.1	0.170	1.105
Protein S100-A9	S100A9	320.1	338.3	318.2	385.1	354.4	339.9	325.5	359.8	0.107	1.105
C-C motif chemokine 20	CCL20	122.3	119.2	118.2	119.8	129.3	148.5	119.9	132.5	0.272	1.105
Vitamin K-dependent protein S	PROS1	187195.9	152702.6	173636.8	190617.1	182985.5	194282.4	171178.4	189295.0	0.206	1.106
Sialic acid-binding Ig-like lectin 6	SIGLEC6	46.5	43.7	42.4	48.1	48.7	49.9	44.2	48.9	0.044	1.106
Integrin alpha-I: beta-1 complex	ITGA1 ITGB1	11097.1	9023.1	9390.6	10545.5	11992.3	10111.3	9836.9	10883.0	0.289	1.106
Leucine-rich repeat transmembrane neuronal protein 3	LRRTM3	48.1	44.4	45.7	48.1	47.7	57.1	46.1	51.0	0.247	1.106
Serum paraoxonase/arylesterase 1	PON1	64.6	60.3	62.7	71.2	66.5	69.9	62.5	69.2	0.024	1.107
Natural cytotoxicity triggering receptor 2	NCR2	53.1	45.7	48.1	54.9	53.6	54.4	49.0	54.3	0.130	1.109
Mitogen-activated protein kinase 12	MAPK12	70.7	64.4	69.7	73	77.6	76.7	68.3	75.8	0.041	1.110
Hepatocyte growth factor-like protein	MST1	32.5	34.1	34.4	35.6	38.7	37.9	33.7	37.4	0.036	1.111
Carbonic anhydrase 7	CA7	96.1	94.2	88.1	100	96.9	112.5	92.8	103.1	0.150	1.111
E3 ubiquitin-protein ligase Mdm2	MDM2	44.6	39.7	41	50.9	42.9	45.5	41.8	46.4	0.182	1.112
Prokineticin-1	PROK1	35.4	38.1	34.6	39.3	40.6	40.3	36.0	40.1	0.049	1.112
Interleukin-22 receptor subunit alpha-2	IL22RA2	56.7	48.7	50.3	59.2	52.7	61.3	51.9	57.7	0.177	1.112
C-type lectin domain family 4 member K	CD207	39.1	36.1	39.5	44.3	40.8	42.5	38.2	42.5	0.044	1.112

Tumor necrosis factor receptor superfamily member 9	TNFRSF9	85.8	82.1	84.6	87.4	92.5	101.2	84.2	93.7	0.134	1.113
C-C motif chemokine 8	CCL8	98.1	86.3	93.4	101.5	97.3	110.7	92.6	103.2	0.115	1.114
Arylsulfatase B	ARSB	376.1	350	352.4	424.5	382.7	395.7	359.5	401.0	0.058	1.115
Macrophage colony-stimulating factor 1 receptor	CSF1R	36.2	34.6	32.9	42	36.5	37.2	34.6	38.6	0.132	1.116
Platelet glycoprotein 4	CD36	156.2	155.4	154.5	176.7	162.1	181.4	155.4	173.4	0.089	1.116
Receptor tyrosine-protein kinase erbB-3	ERBB3	32.6	32.5	29.3	36.6	32.4	36.4	31.5	35.1	0.107	1.117
Histone H2A.z	H2AFZ	82.9	98.3	92.2	87.8	134.1	83.7	91.1	101.9	0.580	1.118
Receptor tyrosine-protein kinase erbB-4	ERBB4	54.8	50.2	51.5	57.1	53.9	64	52.2	58.3	0.163	1.118
TATA-box-binding protein	TBP	177.3	185.8	180.1	194.8	206.4	206.6	181.1	202.6	0.014	1.119
Lipopolysaccharide-binding protein	LBP	22.8	23.2	21.2	24.7	24.1	26.4	22.4	25.1	0.045	1.119
Interleukin-11 receptor subunit alpha	IL11RA	196.5	183.1	186.1	204.7	198.9	230	188.6	211.2	0.127	1.120
Erythropoietin	EPO	85.5	81.4	79.2	83.5	94.3	97.9	82.0	91.9	0.137	1.120
WAP, kazal, immunoglobulin, kunitz and NTR domain-containing protein 1	WFIKKN1	82.7	74.3	76	81.4	83	97	77.7	87.1	0.188	1.122
Kallikrein-5	KLK5	31.8	28.6	27.9	30.6	33.1	35.5	29.4	33.1	0.124	1.123
Alpha-2-macroglobulin	A2M	51.2	49.9	46.6	52.9	53.6	59.6	49.2	55.4	0.083	1.125
Interleukin-10	IL10	40.1	38.9	35.8	43.7	38.1	47.4	38.3	43.1	0.211	1.125
Tyrosine-protein kinase Lyn	LYN	189.1	213.6	184.6	246.4	244.8	169.9	195.8	220.4	0.438	1.126
Desmocollin-3	DSC3	48.9	45.3	45.8	57.5	49.2	51	46.7	52.6	0.130	1.126
Cytochrome c	CYCS	2925.4	2309.7	2840	3159.6	3583.1	2355.4	2691.7	3032.7	0.464	1.127
Enteropeptidase	TMPRSS15	66.5	65.2	62.7	76.1	69.1	74	64.8	73.1	0.038	1.128
Transforming growth factor beta-2	TGFB2	83.6	80.2	80.5	89.5	87	99.1	81.4	91.9	0.095	1.128
Interleukin-6 receptor subunit alpha	IL6R	71.6	74	71.2	81.5	83.2	80	72.3	81.6	0.002	1.129
Cathepsin L2	CTSV	84	80.6	81.7	90.9	85.2	101.9	82.1	92.7	0.159	1.129
Kallikrein-13	KLK13	657.7	608	656.7	655.9	751.6	763	640.8	723.5	0.120	1.129
Peptidoglycan recognition protein 1	PGLYRP1	32.5	29	28.3	34.2	31.4	35.8	29.9	33.8	0.102	1.129
C-C motif chemokine 16	CCL16	23.2	27.7	21.2	27.9	27.5	26.3	24.0	27.2	0.234	1.133
Lymphotactin	XCL1	74.5	68.9	71.1	89.1	75.5	78.5	71.5	81.0	0.134	1.133
Cystatin-C	CST3	58.3	31.9	38.6	59.3	41.2	45.6	42.9	48.7	0.585	1.134
COMM domain-containing protein 7	COMMD7	640.1	670	703.5	718.7	899.7	667.7	671.2	762.0	0.325	1.135

Brain-specific serine protease 4	PRSS22	37.3	35.8	35.7	44.8	39.6	39.2	36.3	41.2	0.102	1.136
Homeobox protein NANOG	NANOG	44.2	40.4	41	43.8	45.5	53.4	41.9	47.6	0.185	1.136
Tumor necrosis factor ligand superfamily member 13B	TNFSF13B	91.1	91.8	88.1	99.8	108.1	100.3	90.3	102.7	0.030	1.137
Granzyme H	GZMH	49.6	50.5	47.1	60	53.8	53.7	49.1	55.8	0.064	1.138
Hemopexin	HPX	16.1	13	16.1	18.5	15.9	17.1	15.1	17.2	0.182	1.139
cGMP-specific 3',5'-cyclic phosphodiesterase	PDE5A	1803.1	2303.2	1856.7	2264.2	2931.9	1610.6	1987.7	2268.9	0.550	1.141
Ligand-dependent nuclear receptor corepressor-like protein	LCORL	43.4	40.4	38.6	49.5	44.6	45.8	40.8	46.6	0.046	1.143
Proliferating cell nuclear antigen	PCNA	36.2	33	39.2	42.5	36	45.5	36.1	41.3	0.205	1.144
Heat shock cognate 71 kDa protein	HSPA8	29	23.8	26.7	30.1	27.9	33	26.5	30.3	0.143	1.145
Antileukoproteinase	SLPI	120.5	95.8	88.3	109	104.4	135.5	101.5	116.3	0.343	1.145
ICOS ligand	ICOSLG	172.7	174.6	159	197.8	207.3	175.4	168.8	193.5	0.103	1.147
C-C motif chemokine 19	CCL19	52.1	46.4	47.9	58.8	52.8	56.3	48.8	56.0	0.042	1.147
Thrombospondin-2	THBS2	21785.3	16827.2	19484.2	23608.8	20139	22908.6	19365.6	22218.8	0.191	1.147
Properdin	CFP	52.7	54.5	53.6	56.8	73.4	54.3	53.6	61.5	0.318	1.147
Triosephosphate isomerase	TPI1	8314.1	10152.1	8205.3	9899.5	12084.6	8620.4	8890.5	10201.5	0.344	1.147
Interleukin-23	IL12B IL23A	34.2	31.3	32.5	38.6	37.3	36.6	32.7	37.5	0.012	1.148
Interferon lambda-2	IFNL2	69.3	64.8	67.3	77.1	75	79.1	67.1	77.1	0.005	1.148
Thioredoxin domain-containing protein 12	TXNDC12	779.6	676.8	744.2	827.2	871	829.2	733.5	842.5	0.050	1.149
Granulins	GRN	84.8	85	81.6	92.1	76.1	120.9	83.8	96.4	0.439	1.150
Tyrosine-protein kinase receptor Tie-1, soluble	TIE1	126.6	123	113.2	137.9	136.9	143.6	120.9	139.5	0.026	1.153
Spectrin alpha chain, non-erythrocytic 1	SPTAN1	34.3	39.5	35	48.9	38.6	38	36.3	41.8	0.254	1.153
Semaphorin-6A	SEMA6A	9856.1	7841.8	8165.4	10179.3	9380.1	10313.3	8621.1	9957.6	0.153	1.155
ADP-ribosyl cyclase/cyclic ADP-ribose hydrolase 2	BST1	84.6	72.6	80.7	92.8	86.4	95.6	79.3	91.6	0.055	1.155
Pappalysin-1	PAPPA	45.5	43	44	52.3	50.1	50.8	44.2	51.1	0.002	1.156
Polymeric immunoglobulin receptor	PIGR	74.6	68	65.7	64.8	66.4	110.1	69.4	80.4	0.538	1.158
Granulocyte-macrophage colony-stimulating factor	CSF2	166.8	174.9	197.6	183	221.6	220.6	179.8	208.4	0.149	1.159
Moesin	MSN	135.6	137.7	132.3	171.6	153.1	145.6	135.2	156.8	0.103	1.160
Trypsin-1	PRSS1	63	62.1	60.1	68.4	67.2	79.3	61.7	71.6	0.118	1.160
Neural cell adhesion molecule L1	L1CAM	17.4	14.3	14.7	18.2	16.8	19	15.5	18.0	0.106	1.164
Phosphoglycerate kinase 1	PGK1	1736.7	1775.6	1730.7	1870.1	2402.2	1835	1747.7	2035.8	0.257	1.165

CD166 antigen	ALCAM	7781.2	6514.2	6915.2	8322.9	8078.5	8361.2	7070.2	8254.2	0.080	1.167
Lymphotoxin alpha1:beta2	LTA LTB	17.7	14.8	14.5	17.3	18.6	19	15.7	18.3	0.106	1.168
Xaa-Pro aminopeptidase 1	XPNPEP1	3807.6	7393.3	5423.5	5715.4	8724.3	5018.4	5541.5	6486.0	0.573	1.170
Lysozyme C	LYZ	812.1	912.5	1010.6	1119.1	883.9	1199.1	911.7	1067.4	0.246	1.171
Scavenger receptor cysteine-rich type 1 protein M130	CD163	46.6	44.2	44.5	60	49.8	48.7	45.1	52.8	0.160	1.171
Neurexin-1-beta	NRXN1	218.5	715.5	199.8	299.5	765.4	264.6	377.9	443.2	0.794	1.173
Importin subunit alpha-1	KPNA2	115.1	107.3	102.2	134.1	124.5	123.3	108.2	127.3	0.020	1.177
Connective tissue-activating peptide III	PPBP	33	31.9	31.8	35.3	38.5	40.1	32.2	38.0	0.047	1.178
Interleukin-7	IL7	22.6	22.8	21.6	28.6	23.1	27.3	22.3	26.3	0.131	1.179
Plasma protease C1 inhibitor	SERPING1	60.9	58.8	58.9	67.4	76.7	66.5	59.5	70.2	0.076	1.179
Cystatin-M	CST6	44	35.9	36.4	45.3	36.4	55.6	38.8	45.8	0.341	1.181
Nidogen-1	NID1	16382.6	13564.2	13344.2	17906.4	15891.2	17331.3	14430.3	17043.0	0.099	1.181
Phosphatidylethanolamine-binding protein 1	PEBP1	32.7	29.1	32	38.2	33.1	39.5	31.3	36.9	0.082	1.181
Complement C3b	C3	17.5	16.7	15.8	19.2	19.4	20.5	16.7	19.7	0.010	1.182
14-3-3 protein family	YWHAB,YWHAE,YWHAG,YWHAH,YWHAQ,YWHAZ,SFN	16556.7	15528.5	15009.7	20512.1	18077.5	17151.2	15698.3	18580.3	0.085	1.184
26S proteasome non-ATPase regulatory subunit 7	PSMD7	166.1	141.5	150.9	174.6	186.7	181.9	152.8	181.1	0.040	1.185
Lactadherin	MFGE8	20.4	19.8	17.2	23.1	21.8	23.2	19.1	22.7	0.050	1.186
Spondin-1	SPON1	3049.8	2562.3	2711	3361.1	3020	3517.2	2774.4	3299.4	0.063	1.189
15-hydroxyprostaglandin dehydrogenase [NAD(+)]	HPGD	1929	2126.8	2178.9	2301	2929.7	2193.7	2078.2	2474.8	0.220	1.191
Mannan-binding lectin serine protease 1	MASP1	3305.1	3088.2	3039.6	3761.3	3599.7	3885.3	3144.3	3748.8	0.007	1.192
Vascular endothelial growth factor A	VEGFA	4202.4	3497.3	4006.3	4612.2	3809.2	5592.6	3902.0	4671.3	0.272	1.197
P-Selectin	SELP	33.1	31.5	32.3	43	36.8	36.3	32.3	38.7	0.091	1.198
Interleukin-1 receptor-like 1	IL1RL1	15.9	16.3	15.5	20.2	17.7	19.3	15.9	19.1	0.039	1.199
Interleukin-19	IL19	437.2	398.2	368.2	475.7	471.8	498.7	401.2	482.1	0.040	1.202
Serum albumin	ALB	29.3	41.6	29.4	36.3	34.2	50.3	33.4	40.3	0.355	1.204
A disintegrin and metalloproteinase with thrombospondin motifs 13	ADAMTS13	18.3	19.4	17.2	20.4	21.1	24.7	18.3	22.1	0.088	1.206
Netrin receptor UNC5D	UNC5D	65.1	41	49.5	73.6	54.8	59.3	51.9	62.6	0.305	1.206

MHC class I polypeptide-related sequence A	MICA	18.8	18.7	18.1	21.4	22.6	23.1	18.5	22.4	0.008	1.207
Tyrosine-protein phosphatase non-receptor type 6	PTPN6	176.5	188.8	182.4	238.1	222.3	202.6	182.6	221.0	0.052	1.211
Ephrin type-A receptor 10	EPHA10	121	110.6	113.6	147.9	113.6	156.8	115.1	139.4	0.201	1.212
Endostatin	COL18A1	7867.4	6312.4	6066.8	10135.5	6567.1	7868.5	6748.9	8190.4	0.309	1.214
Galectin-3	LGALS3	12411.2	10213.9	10627.7	14354.6	11967.5	14105.8	11084.3	13476.0	0.079	1.216
Collagen alpha-1(XXIII) chain	COL23A1	59.4	56.5	55.6	73.7	71.5	63.4	57.2	69.5	0.045	1.216
Baculoviral IAP repeat-containing protein 7 Isoform beta	BIRC7	28.4	27.2	26.9	34	31.5	34.9	27.5	33.5	0.015	1.217
Neuroblastoma suppressor of tumorigenicity 1	NBL1	398.1	295.2	307.8	542.7	323.7	360.8	333.7	409.1	0.392	1.226
Tyrosine-protein kinase Lyn, isoform B	LYN	37.9	37.2	35.5	46.9	44.9	43.9	36.9	45.2	0.002	1.227
Aminoacylase-1	ACY1	3559	3045.7	3019.7	4049.1	4703	3068.9	3208.1	3940.3	0.259	1.228
C-C motif chemokine 7	CCL7	1126.2	754.5	801.2	1310	1022.8	980.1	894.0	1104.3	0.250	1.235
Macrophage-capping protein	CAPG	419.5	236.1	366.7	452.6	310.7	501.1	340.8	421.5	0.365	1.237
Annexin A6	ANXA6	747.7	993.9	825.1	1073.4	1148.9	970.2	855.6	1064.2	0.087	1.244
Vascular endothelial growth factor A, isoform 121	VEGFA	105.1	99.7	96.7	125.1	113.9	136.5	100.5	125.2	0.049	1.245
Tumor necrosis factor receptor superfamily member 19	TNFRSF19	251.7	210.8	225.1	330.4	232	295.6	229.2	286.0	0.177	1.248
Tumor necrosis factor receptor superfamily member EDAR	EDAR	287.9	282	295.7	378.9	343.9	360.4	288.5	361.1	0.011	1.251
Dual specificity mitogen-activated protein kinase kinase 2	MAP2K2	229.5	247.4	220.4	277.5	359.6	236.5	232.4	291.2	0.243	1.253
Chloride intracellular channel protein 1	CLIC1	541.4	595.3	642.1	745.1	786	700.2	592.9	743.8	0.018	1.254
Neutrophil gelatinase-associated lipocalin	LCN2	57.3	55.1	50.4	62.1	59.2	83.3	54.3	68.2	0.202	1.257
NudC domain-containing protein 3	NUDCD3	35.8	35.9	34.4	47.3	46.9	40.5	35.4	44.9	0.044	1.270
Phosphoglycerate mutase 1	PGAM1	113.6	95	92.5	142.9	104.6	135.2	100.4	127.6	0.132	1.271
Proteasome activator complex subunit 1	PSME1	717.7	733.2	688.2	817	1345.7	558	713.0	906.9	0.491	1.272
Stem Cell Growth Factor-alpha	CLEC11A	7532.7	6348.8	7816.2	8743.5	8060.3	10921.8	7232.6	9241.9	0.130	1.278
Periostin	POSTN	325.3	292.2	315.5	392.3	342.6	465	311.0	400.0	0.121	1.286
Protein Wnt-7a	WNT7A	13077.4	10630.3	10883.3	18844.5	13222.1	12491.5	11530.3	14852.7	0.234	1.288
Testican-1	SPOCK1	3494.4	3261	3410.8	4133.6	4654.3	4330.5	3388.7	4372.8	0.012	1.290
Ciliary neurotrophic factor receptor subunit alpha	CNTFR	993.1	884.1	852	1390.8	1049.5	1125.6	909.7	1188.6	0.099	1.307
Fibroblast growth factor 12	FGF12	43.5	42.7	40.8	51.2	52.4	62.6	42.3	55.4	0.063	1.309

Ribosomal protein S6 kinase alpha-3	RPS6KA3	306.7	396.8	288.7	446.5	511.8	345.4	330.7	434.6	0.161	1.314
Integrin alpha-V: beta-5 complex	ITGAV ITGB5	8060.2	4181.6	6389.6	6293.2	7369.9	10849.1	6210.5	8170.7	0.334	1.316
Bcl-2-related protein A1	BCL2A1	1068.6	1052.6	1024.1	1384.4	1523.4	1232.5	1048.4	1380.1	0.055	1.316
14-3-3 protein sigma	SFN	6187.4	3284.9	6179.2	6854.9	5480.8	8434.9	5217.2	6923.5	0.257	1.327
Legumain	LGMN	9020.1	9715.5	9973.3	12316.7	15610.7	10179	9569.6	12702.1	0.182	1.327
Growth/differentiation factor 9	GDF9	308.3	291	297.5	385.6	383.1	425.8	298.9	398.2	0.011	1.332
Interleukin-2	IL2	1948.3	1676.4	1843	2485.9	1890.4	2932.7	1822.6	2436.3	0.173	1.337
Serine protease HTRA2, mitochondrial	HTRA2	467.4	533.9	421.2	665.5	815.1	428.2	474.2	636.3	0.284	1.342
Interleukin-1 alpha	IL1A	2731.4	2266.8	2487	3145.8	3583.2	3317.9	2495.1	3349.0	0.010	1.342
Melanoma-derived growth regulatory protein	MIA	3475.3	2888.1	3106.6	4758.8	3596.1	4542.4	3156.7	4299.1	0.067	1.362
Neural cell adhesion molecule 1, 120 kDa isoform	NCAM1	58.7	78.7	72.2	59.1	168.4	60.8	69.9	96.1	0.545	1.375
Adenylosuccinate lyase	ADSL	194.8	194.5	212.3	261.4	300.4	268.2	200.5	276.7	0.012	1.380
Brother of CDO	BOC	5334.3	3825.5	4723.3	7000.8	6267	6170.6	4627.7	6479.5	0.031	1.400
Caspase-10	CASP10	7512.7	6468.7	7156.6	9428.9	10130	10136.6	7046.0	9898.5	0.002	1.405
Ras-related C3 botulinum toxin substrate 1	RAC1	15513.8	21133.2	18394	27295	28189.4	22098.7	18347.0	25861.0	0.041	1.410
Cathepsin B	CTSB	416.7	356.1	372.8	447.7	619.6	564.1	381.9	543.8	0.072	1.424
Tumor necrosis factor receptor superfamily member 27	EDA2R	592.4	561.1	561.9	839.7	761.4	851.6	571.8	817.6	0.007	1.430
Tumor necrosis factor-inducible gene 6 protein	TNFAIP6	63	56.1	60.6	88.3	93	76.8	59.9	86.0	0.020	1.436
Proteasome subunit alpha type-2	PSMA2	98.3	101.1	104.7	158.8	148	132.4	101.4	146.4	0.023	1.444
Macrophage mannose receptor 1	MRC1	11890.9	10861.4	9494.5	16115.3	18102.2	14367.8	10748.9	16195.1	0.018	1.507
Carbohydrate sulfotransferase 15	CHST15	20965.1	17680.5	17591.8	28672.1	25333	31040.1	18745.8	28348.4	0.012	1.512
Follistatin-related protein 3	FSTL3	13398.3	10132.6	11357.2	20231	14381	18352	11629.4	17654.7	0.052	1.518
Eukaryotic translation initiation factor 4 gamma 2	EIF4G2	278.6	351.2	286.2	444.6	599.5	348.7	305.3	464.3	0.152	1.521
Interleukin-18-binding protein	IL18BP	12916	11683.8	14529.8	13125.1	32393.2	14119.4	13043.2	19879.2	0.389	1.524
NT-3 growth factor receptor	NTRK3	913.9	851.7	775.1	1391.8	1224.5	1283.7	846.9	1300.0	0.002	1.535
Glucokinase regulatory protein	GCKR	241.5	188.6	162	257.6	446.8	207.4	197.4	303.9	0.279	1.540
Glial fibrillary acidic protein	GFAP	448.4	424.2	388.3	692.1	622.3	634.3	420.3	649.6	0.001	1.545
Carbonic anhydrase 3	CA3	1543.1	618.5	460.9	2066.9	1013.8	1009	874.2	1363.2	0.373	1.559
Cell adhesion molecule-related/down-regulated by oncogenes	CDON	53.9	65.2	58.6	66.9	152.2	58.5	59.2	92.5	0.382	1.562
Sorting nexin-4	SNX4	263.9	247.5	233.9	401.3	376.2	397.2	248.4	391.6	0.0003	1.576

Atrial natriuretic factor	NPPA	3748.2	2829.5	2331.8	3842.4	3973.1	6348.2	2969.8	4721.2	0.152	1.590
Antithrombin-III	SERPINC1	77501.5	57791.1	77095.7	116339.7	100274.8	124653.9	70796.1	113756.1	0.012	1.607
Thymidylate synthase	TYMS	314.4	199	304	527.5	340.9	467.8	272.5	445.4	0.068	1.635
Agouti-related protein	AGRP	260.3	229.2	244.5	473.3	348.7	383.1	244.7	401.7	0.045	1.642
Insulin-like growth factor 1 receptor	IGF1R	2063.6	1726.7	1792	3207.8	2779.3	3195.2	1860.8	3060.8	0.003	1.645
Insulin receptor	INSR	955	813.4	778	1377.9	1400.8	1410	848.8	1396.2	0.008	1.645
Angiopoietin-2	ANGPT2	119.6	111.2	107.7	196.6	197.4	164.2	112.8	186.1	0.015	1.649
Angiopoietin-related protein 3	ANGPTL3	58449.3	47212.2	51275.1	86120.6	78408.9	96159.2	52312.2	86896.2	0.008	1.661
Trypsin-2	PRSS2	157.3	166.9	117.4	270.5	240.3	225	147.2	245.3	0.009	1.666
SPARC-like protein 1	SPARCL1	66241	50782.9	56343.3	106329.4	91602.2	96343.2	57789.1	98091.6	0.003	1.697
von Willebrand factor	VWF	47989.2	46539.8	45649.1	72161.1	81840.2	84740.6	46726.0	79580.6	0.011	1.703
Olfactomedin-4	OLFM4	46.8	62.3	45.7	51	158.3	55.1	51.6	88.1	0.408	1.708
Thyroid Stimulating Hormone	CGA TSHB	80.3	52.8	51.2	164.7	77.5	86.9	61.4	109.7	0.216	1.786
Neurexin-3-beta	NRXN3	613.9	475.6	528.6	1032.1	880.3	987.7	539.4	966.7	0.002	1.792
Glutathione S-transferase P	GSTP1	1070.6	388.3	244.9	714.6	1940.6	426.6	567.9	1027.3	0.448	1.809
Protein-glutamine gamma-glutamyltransferase E	TGM3	129.2	124.5	129.5	238	101.6	356.3	127.7	232.0	0.292	1.816
Neuroligin-4, X-linked	NLGN4X	615.3	450.4	656.3	1053.2	867.2	1428.9	574.0	1116.4	0.067	1.945
Heme oxygenase 2	HMOX2	198	139.4	135.7	290.8	377.8	259.9	157.7	309.5	0.030	1.963
Stanniocalcin-1	STC1	10585.7	7683.7	8998.7	17194.9	15341.4	21352	9089.4	17962.8	0.023	1.976
Dual specificity protein phosphatase 3	DUSP3	365.5	391.3	329.6	855.4	732.6	623.4	362.1	737.1	0.024	2.036
Mitochondrial import inner membrane translocase subunit TIM14	DNAJC19	132.3	134.8	134.1	191.2	557	139.9	133.7	296.0	0.342	2.214
Tumor necrosis factor receptor superfamily member 12A	TNFRSF12A/ TWEAKR	334.8	250.9	247.3	808.5	618.4	491.3	277.7	639.4	0.049	2.303
WAP, Kazal, immunoglobulin, Kunitz and NTR domain-containing protein 2	WFIKKN2/GA SP2	1921.4	1530.5	1837.7	4562.2	3457.2	4539.7	1763.2	4186.4	0.015	2.374
Heat shock 70 kDa protein 1A/1B	HSPA1A	1873.1	1105.5	1482	3345.3	3760.5	3581.1	1486.9	3562.3	0.003	2.396
Peptide YY	PYY	462.9	471.5	461.4	1091.9	1054.1	1221	465.3	1122.3	0.006	2.412
Growth/differentiation factor 2/BMP9	GDF2/BMP9	1410.6	990.8	826.3	4269.6	2071.4	1745.5	1075.9	2695.5	0.173	2.505
Insulin-like growth factor-binding protein 2	IGFBP2	11210.1	9592.3	10057	27217.8	17678.4	35037.5	10286.5	26644.6	0.081	2.590
Myoglobin	MB	384.1	145.7	105.4	511.8	471.9	810.3	211.7	598.0	0.051	2.824
Glucagon	GCG	178.2	196.3	177	788.2	428.1	463	183.8	559.8	0.081	3.045
Muellerian-inhibiting factor	AMH	1419.7	2428.2	1306.8	1742	3872.7	11434.4	1718.2	5683.0	0.309	3.307

Glypican-3	GPC3	1618.4	1104.1	1246.7	5245.7	4879.4	5428.6	1323.1	5184.6	0.0001	3.919
alpha-1-antichymotrypsin complex	SERPINA3	31.1	28.1	31.1	32.9	33.9	378.7	30.1	148.5	0.412	4.934
60 kDa heat shock protein, mitochondrial	HSPD1	1935.7	2295.6	1945.9	7875.9	23162.8	2815.4	2059.1	11284.7	0.270	5.480
Insulin-like growth factor-binding protein 1	IGFBP1	2138.8	1553.4	730.9	33004.5	32952.6	45645.8	1474.4	37201.0	0.013	25.232

Appendix Table S2. Genes encoding secreted proteins with altered expression in 16-day-old αKOγKO mouse hearts compared to littermate control mouse hearts by RNA-Seq (3 mice per sequencing sample, total of 6 mice per genotype). The proteins are ordered based on fold change. The proteins labeled in blue fonts were tested in Fig 3A based on their selective cardiac expression.

		αHetγWT RPKM		αHetγKO RPKM		αKOγWT RPKM		αKOγKO RPKM		Fold (αKOγKO /αHetγWT)		
Gene ID	Symbol	#1	#2	#1	#2	#1	#2	#1	#2		P-value	FDR
23886	Gdf15	0.4748715	0.997886	1.3095189	0.90588	1.3821645	1.442862	52.784284	19.685112	49.2	2E-173	5E-172
21828	Thbs4	2.4328687	3.296331	6.0846005	6.672508	7.1481602	5.067814	80.599456	71.382332	26.5	0	0
18158	Nppb	74.361504	79.00695	112.34144	121.902	98.99381	206.3011	1952.2222	1393.3965	21.8	0	0
22403	Wisp2	1.2888254	1.359669	1.2930031	1.317705	1.2865563	1.15069	43.951836	11.670889	21.0	2E-118	4E-117
14219	Ctgf	46.579672	60.59649	61.670973	76.32406	57.915667	69.75104	749.12833	650.98171	13.1	0	0
68588	Cthrc1	1.7394549	1.295392	1.493909	1.968447	3.1220728	1.651626	27.425871	9.4353384	12.1	3E-48	2E-47
338417	Scgb1c1	3.3480373	4.50621	7.2392293	5.410324	5.6546353	4.768481	30.361942	41.331863	9.1	7E-119	1E-117
230899	Nppa	2313.1298	2621.314	3367.0254	3175.973	2304.1302	4241.753	22181.396	20368.714	8.6	0	0
19215	Ptgds	16.221988	13.78672	24.39247	30.79052	34.686119	36.91037	118.38455	132.77958	8.4	0	0
20319	Sfrp2	6.0196907	7.437124	6.4733163	7.182672	6.9140704	7.327876	71.378339	33.653565	7.8	2E-293	8E-292
16007	Cyr61	14.366596	16.68046	15.259123	17.29943	14.995867	15.23186	68.57925	173.12288	7.8	0	0
21825	Thbs1	5.2286394	3.92648	3.5903884	4.29786	4.5163257	7.564889	17.176203	30.610852	5.2	1E-271	4E-270
77794	Adamtsl2	19.03228	23.75014	26.019397	26.93898	25.948815	20.96592	142.43255	64.987238	4.8	0	0
67177	Cdt1	31.305857	25.9891	28.969764	28.84586	24.363905	40.06579	133.65543	110.20554	4.3	5E-241	2E-239
21809	Tgfb3	9.8482108	10.63078	12.500611	12.66916	11.079037	13.58571	54.54594	27.524886	4.0	3E-207	9E-206
14314	Fstl1	95.65887	92.46069	97.810682	118.4005	122.69809	107.1257	418.58811	215.07455	3.4	0	0
20720	Serpine2	18.989725	19.13562	22.156414	24.23935	28.168398	31.67206	62.327611	61.08442	3.2	4E-268	1E-266
50781	Dkk3	39.449144	41.66463	46.51386	47.15701	44.868508	59.43272	115.96042	121.9906	2.9	0	0
21857	Timp1	4.8158094	6.012509	6.1172618	5.885596	6.3051527	6.732955	20.654534	10.84075	2.9	1E-16	5E-16
68797	Pdgfrl	7.5298333	8.359186	9.3026695	11.01675	10.502204	10.46082	27.837356	18.362325	2.9	5E-52	5E-51
15200	Hbegf	9.0384409	9.907712	10.147895	9.703299	11.127983	9.440277	31.519358	22.729357	2.9	3E-103	4E-102
12759	Clu	156.70592	152.5458	159.14623	161.5556	123.2628	136.7365	412.15012	390.77409	2.6	0	0
12154	Bmp10	49.534809	50.72414	59.22744	49.63983	31.393906	49.73052	125.94341	125.52264	2.5	1E-220	5E-219
18188	Nrtn	17.510922	24.22381	33.267796	33.94542	37.424718	31.31054	40.634166	55.890149	2.3	3E-151	6E-150
20377	Sfrp1	7.2559878	7.625291	8.368658	9.159584	9.3186335	8.634294	17.32039	16.796048	2.3	1E-120	2E-119
20347	Sema3b	6.437754	6.684743	7.0868546	5.924346	5.6907788	5.994387	16.317912	13.754031	2.3	2E-64	3E-63
22339	Vegfa	153.1366	137.4003	121.68159	124.7486	129.97455	122.1809	85.475104	75.049859	0.6	0	0
22340	Vegfb	139.70188	149.1219	134.92534	134.3411	146.86478	150.2959	55.301087	61.706414	0.4	1E-290	4E-289
239126	C1qtnf9	37.256811	35.70728	37.800366	37.13734	34.658747	27.70463	13.563144	15.45212	0.4	5E-129	9E-128
54612	Sfrp5	3.8652209	3.019122	3.7542527	2.270912	2.5670184	4.3389	0.7435759	1.6351465	0.3	2E-14	9E-14
233813	Vwa3a	5.2057406	4.9079	4.522291	4.800111	3.8811038	4.494185	1.1995982	1.9895772	0.3	6E-51	6E-50
17329	Cxcl9	1.8664876	1.083232	1.7591279	0.952627	0.8998267	0.706654	0.4115116	0.3940112	0.3	1E-23	6E-23
22370	Vtn	19.134422	19.91285	16.405382	17.31733	16.020371	11.57004	2.6198243	4.0963681	0.2	4E-137	8E-136

Appendix Table S3. Sequences of qPCR primers used.

Mouse primer	Sequence
Esrra For	CTCAGCTCTCTACCCAAACGC
Esrra Rev	CCGCTTGGTGATCTCACACTC
Esrrg For	GAATCTTTTTCCCTGCACTACGA
Esrrg Rev	GCTGGAATCAATGTGTCGATCTT
Ghrh For	GGTGCTCTTTGTGATCCTCATC
Ghrh Rev	GTTTCCTGTAGTTGGTGGTGAAG
Gh For	GCTACAGACTCTCGGACCTC
Gh Rev	CGGAGCACAGCATTAGAAAACAG
Npy For	ATGCTAGGTAACAAGCGAATGG
Npy Rev	TGTCGCAGAGCGGAGTAGTAT
Pomc For	ATGCCGAGATTCTGCTACAGT
Pomc Rev	CCACACATCTATGGAGGTCTGAA
Igf1 (class II) For	CCTGGGTGTCCAAATGTAACTA
Igf1 (class II) Rev	TTTACACAGCAGGTCAGAGTG
Igfbp3 For	CCAGGAAACATCAGTGAGTCC
Igfbp3 Rev	GGATGGAACTTGGAATCGGTCA
Igfals For	CTGCCCGATAGCATCCCAG
Igfals Rev	GAAGCCAGACTTGGTGTGTGT
Gdf15 For	GAGAGGACTCGAACTCAGAAC
Gdf15 Rev	GACCCCAATCTCACCTCTG
36b4 For	AGATGCAGCAGATCCGCAT
36b4 Rev	GTTCTTGCCCATCAGCACC

Appendix Table S4. Information of human plasma samples used in Fig 6A.
There are 4 tabs in this file. Mean weight percentage is based on standard body weight chart with 50% as the median BW.

GDF15 (pg/ml)	Control	HD normal BW	HD FTT
mean	176	304	538
median	148	216	357
Standard deviation (SD)	108	300	560
Standard error of the mean (SEM)	16	52	84
% of samples outside of 2 SD	4.5%	5.9%	4.5%
t-test (control vs HD normal BW)	0.02		
t-test (control vs HD FTT)	0.00012		
t-test (HD normal BW vs HD FTT)	0.02		

Group 1: control

Sample #	Age (yrs)	Gender	% BW	Heart disease diagnosis
1	3	F	64.4%	None
2	3	M	62.5%	None
3	2	F	62.9%	None
4	3	M	64.1%	None
5	2	F	46.6%	None
6	2	M	52.8%	None
7	3	F	50.4%	None
8	3	F	68.9%	None
9	3	M	51.0%	None
10	3	F	68.3%	None
11	2	M	40.1%	None
12	2	F	42.9%	None
13	2	F	69.9%	None
14	2	F	62.3%	None
15	2	M	47.4%	None
16	2	F	66.3%	None
17	3	M	57.5%	None
18	2	M	68.8%	None
19	2	M	65.4%	None
20	2	F	58.4%	None
21	3	F	44.0%	None
22	3	M	53.8%	None
23	2	F	57.8%	None
24	3	F	50.0%	None
25	3	M	48.6%	None
26	2	F	65.0%	None
27	3	F	55.9%	None
28	3	F	68.0%	None
29	2	M	58.5%	None
30	3	M	61.6%	None
31	2	M	59.6%	None
32	3	M	45.9%	None
33	3	M	69.5%	None
34	2	M	61.6%	None
35	3	F	47.4%	None
36	3	M	46.2%	None
37	3	F	50.8%	None
38	2	M	62.9%	None
39	2	F	57.2%	None
40	3	M	44.4%	None
41	2	M	65.9%	None
42	2	F	54.9%	None
43	3	F	63.4%	None
44	3	M	52.8%	None
45	2	M	65.9%	None

Group 2: children with heart disease and normal body weight

Sample #	Age (yrs)	Gender	% BW	Heart disease diagnosis
46	2	M	69.7%	PDA, PFO, VSD
47	3	M	69.5%	TGV, DORV
48	3	F	69.3%	PPS
49	3	M	68.4%	ASD (Ostium secundum)
50	2	F	67.1%	Muscular VSD
51	2	F	66.8%	Congenital anomaly of aortic arch, PDA
52	3	F	62.1%	AVC
53	3	M	61.6%	Heart abnormality
54	3	M	59.0%	PPS
55	3	F	58.4%	Acyanotic congenital heart disease
56	2	F	57.1%	Congenital malposition of heart and cardiac apex, Mesocardia, Scimitar
57	3	M	56.8%	PPS
58	2	F	55.5%	PPS
59	3	M	55.3%	Complete common AVC, Other congenital ECD, Partial anomalous
60	3	F	55.2%	PPS
61	2	F	55.0%	ASD (Ostium secundum), VSD, Aortic arch hypoplasia
62	3	M	53.6%	Congenital anomaly of aortic arch, Congenital malposition of heart and
63	2	M	53.1%	Muscular VSD, ASD (Ostium secundum), PDA, PFO
64	3	M	53.1%	ASD (Ostium secundum), PDA
65	2	M	52.8%	Persistent left SVC
66	2	F	52.6%	ASD (Ostium secundum)
67	3	F	52.4%	PDA
68	2	M	52.4%	VSD
69	2	M	52.0%	HLHS, Pulmonary atresia, Right ventricular aorta with pulmonary atresia
70	3	F	51.6%	VSD (ventricular septal defect)
71	3	F	51.6%	VSD
72	2	M	51.1%	PPS
73	3	F	48.9%	ASD
74	2	F	48.5%	PDA
75	2	M	48.3%	PDA
76	3	F	44.5%	PFO
77	2	F	41.9%	PFO
78	3	F	41.6%	Congenital anomaly of aortic arch
79	3	F	40.9%	Other primary cardiomyopathies
80	3	F	40.2%	Anomalies of aortic arch, CoA (preductal, postductal), Congenital AVI

ASD: atrial septal defect
AVC: atrioventricular canal
AVI: aortic valve insufficiency
CoA: coarctation of the aorta
DORV: double outlet right ventricle
ECD: endocardial cushion defect
HLHS: hypoplastic left heart syndrome
PDA: patent ductus arteriosus
PFO: patent foramen ovale
PPS: peripheral pulmonic stenosis
PVS: pulmonary vein stenosis
SAS: subvalvar aortic stenosis
SVC: superior vena cava
TAPVC: total anomalous pulmonary venous connection
TAPVR: total anomalous pulmonary venous return
TGV: transposition of the great vessels
VSD: ventricular septal defect

Group 3: children with heart disease and FTT

Sample #	Age (yrs)	Gender	% BW	Heart disease diagnosis
81	2	M	8.4%	PFO
82	3	M	8.2%	PDA
83	2	M	8.0%	Congenital stenosis of pulmonary valve, Dysplastic pulmonary valve, PDA
84	3	F	7.9%	Congenital anomalies of pulmonary artery, Congenital malposition of heart and cardiac apex, Heart dextroposition, PDA
85	3	M	7.9%	ASD (Ostium secundum), VSD
86	2	M	7.8%	ASD (Ostium secundum), PDA, Other specified congenital anomaly of the heart
87	3	M	7.8%	TAPVC, TAPVR
88	2	M	7.2%	Bulbus cordis anomalies and anomalies of cardiac septal closure, Congenital mitral stenosis, Congenital stenosis of aortic valve, Congenital stenosis of pulmonary valve, HLHS, PVS, Other congenital anomalies of great veins, Other specified congenital anomaly of heart
89	3	M	6.6%	ASD
90	3	F	6.4%	PFO
91	3	F	6.1%	PFO
92	2	F	6.0%	CoA (preductal, postductal), Unspecified congenital anomaly of heart
93	3	M	5.9%	ASD (Ostium secundum), PFO
94	3	M	5.8%	Other primary cardiomyopathies
95	3	F	5.2%	ASD (Ostium secundum), PDA
96	3	M	5.0%	PDA
97	2	M	5.0%	PDA
98	2	F	4.8%	ASD (Ostium secundum), PFO
99	2	F	4.7%	ASD (Ostium secundum), PDA,VSD
100	3	M	4.6%	ASD (Ostium secundum)
101	2	M	3.8%	PDA
102	3	F	3.4%	PDA
103	3	F	3.4%	CoA (preductal, postductal), TGV, DORV, VSD, Other specified congenital anomaly of heart
104	2	F	3.3%	Complete common AVC, Congenital AVI, ECD, PDA, VSD
105	2	M	3.3%	ASD (Ostium secundum), Congenital malposition of heart and cardiac apex, Other congenital anomalies of pulmonary valve, PDA, Other specified congenital anomaly of heart
106	2	M	3.2%	ASD (Ostium secundum), VSD
107	3	F	2.8%	Congenital anomalies of pulmonary artery, ASD (Ostium secundum)
108	2	M	2.8%	Congenital anomaly of aortic arch
109	2	M	2.5%	TGV (D-loop, intact ventricular septum), ASD (Ostium secundum)
110	2	M	2.4%	Persistent left SVC, ASD (Ostium secundum), PFO
111	3	F	2.1%	Patent ductus arteriosus
112	2	F	1.5%	ASD (Ostium Secundum), PFO
113	3	M	1.5%	VSD
114	3	F	1.5%	Abnormality of aortic valve, Complete common AVC, Complete ECD, Congenital bilateral SVC, Congenital subaortic stenosis, SAS
115	2	F	1.3%	Congenital anomalies of pulmonary artery
116	2	M	1.3%	Muscular VSD, PDA
117	2	F	1.1%	PDA
118	2	F	1.0%	PDA, PFO
119	3	F	1.0%	ASD (Ostium secundum), Other congenital anomalies of great veins, Unspecified congenital anomaly of heart

120	3	M	0.7%	VSD
121	3	M	0.5%	PDA
122	3	M	0.3%	ASD (Ostium Secundum)
123	2	M	0.3%	ASD (Ostium secundum), Common (single) atrium, PFO
124	2	F	0.3%	ASD (Ostium secundum), PDA, Persistent left SVC
125	3	F	0.2%	PDA

ASD: atrial septal defect
AVC: atrioventricular canal
AVI: aortic valve insufficiency
CoA: coarctation of the aorta
DORV: double outlet right ventricle
ECD: endocardial cushion defect
HLHS: hypoplastic left heart syndrome
PDA: patent ductus arteriosus
PFO: patent foramen ovale
PVS: pulmonary vein stenosis
SAS: subvalvar aortic stenosis
SVC: superior vena cava
TAPVC: total anomalous pulmonary venous connection
TAPVR: total anomalous pulmonary venous return
TGV: transposition of the great vessels
VSD: ventricular septal defect

Appendix Table S5. Statistical analysis information.

Figure	Groups	p value
1A	Body weight of αKOγKO vs αHetγWT or αHetγKO or αWTγKO (biggest p value presented)	p = 0.02 (d5), 0.003 (d6), 0.016 (d7), $8x10^{-5}$ (d8), $3x10^{-5}$ (d9), $3x10^{-6}$ (d10), $2x10^{-7}$ (d11), $9x10^{-8}$ (d12), $2x10^{-8}$ (d13), $3x10^{-9}$ (d14), $3x10^{-9}$ (d15), $3x10^{-7}$ (d16)
1C	Plasma IGF1 of P10 αKOγKO vs αHetγWT or αHetγKO or αWTγKO (biggest p value presented)	p = 0.04
1D	Plasma IGF1 of P16 αKOγKO vs αHetγWT or αHetγKO or αWTγKO (biggest p value presented)	p = 0.04
1F	Liver p-STAT5 between αKOγKO and αHetγWT	p = 0.0013
1G	Liver gene expression in αKOγKO vs αHetγWT or αHetγKO or αWTγKO (biggest p value presented)	p = 0.011 for Igf1, p = 0.0015 for Igfbp3, p = 0.006 for Igfals
1H	Liver/plasma IGFBP3 between αKOγKO and αHetγWT	p = 0.000009 for liver IGFBP3, p = 0.000007 for plasma IGFBP3
3A	Plasma IGF1 between GDF15 and PBS injected mice	p = 0.004
3C	Liver gene expression between GDF15 and PBS injected mice	p = 0.004 for Igf1, p = 0.02 for Igfbp3, p = 0.0013 for Igfals
3D	Plasma IGF1 between GDF15 and PBS injected mice	p = 0.006
3E	Plasma IGFBP3 between GDF15 and PBS injected mice	p = 0.04
3G	Body weight between GDF15 and PBS injected mice	p = 0.03 (d8), 0.004 (d9), 0.0008 (d10), 0.003 (d11)
4A	Cardiac Gdf15 mRNA level between αKOγKO and αHetγWT	p = 0.007 (P7), 0.00016 (P10), 0.0009 (P13)
4C	Plasma GDF15 between αKOγKO and αHetγWT	p = 0.02 (P7), 0.0012 (P10)
5B	Cardiac Gdf15 mRNA in AAV-shRNA injected mice	p = 0.004 (αHetγWT shControl vs αKOγKO shControl), p = 0.006 (αKOγKO shControl vs αKOγKO shGdf15)
5C	Plasma GDF15 in AAV-shRNA injected mice	p = 0.02 (αHetγWT shControl vs αKOγKO shControl), p = 0.04 (αKOγKO shControl vs αKOγKO shGdf15)
5D	Cardiac Bnp mRNA in AAV-shRNA injected mice	p = 0.0011 (αHetγWT shControl vs αKOγKO shControl), p = 0.0008 (αHetγWT shControl vs αKOγKO shGdf15)
5E	Liver p-STAT5 in AAV-shRNA injected mice	p = 0.0009 (αHetγWT shControl vs αKOγKO shControl), p = 0.03 (αKOγKO shControl vs αKOγKO shGdf15)
5F	Plasma IGF1 in AAV-shRNA injected mice	p = 0.0005 (αHetγWT shControl vs αKOγKO shControl), p = 0.03 (αKOγKO shControl vs αKOγKO shGdf15), p = 0.0019 (αHetγWT shControl vs αKOγKO shGdf15)
6A	Plasma GDF15 in children	p = 0.02 (control vs HD normal BW), p = 0.00012 (control vs HD FTT), p = 0.02 (HD normal BW vs HD FTT)

EMBO Molecular Medicine

GDF15 is a heart-derived hormone that regulates body growth

Ting Wang, Jian Liu, Caitlin McDonald, Katherine Lupino, Xiandun Zhai, Benjamin J Wilkins, Hakon Hakonarson, Liming Pei

Corresponding author: Liming Pei, Children's Hospital of Philadelphia/University of Pennsylvania

Review timeline:

Submission date:	18 January 2017
Editorial Decision:	15 February 2017
Revision received:	23 April 2017
Editorial Decision:	03 May 2017
Revision received:	06 May 2017
Accepted:	11 May 2017

Transaction Report:

(Note: With the exception of the correction of typographical or spelling errors that could be a source of ambiguity, letters and reports are not edited. The original formatting of letters and referee reports may not be reflected in this compilation.)

Editor: Céline Carret

1st Editorial Decision 15 February 2017

Thank you for the submission of your manuscript to EMBO Molecular Medicine. We have now heard back from the three referees whom we asked to evaluate your manuscript. Although the referees find the study to be of potential interest, they also raise a number of concerns that must be addressed in the next final version of your article.

You will see from the comments pasted below that while referees 1 and 2 are rather supportive of publication pending better mechanistic details on the role of GDF15 and relevant missing information and discussions are provided, referee 3 is more critical. This referee questions the experimental setting in animals (age), the clinical data (not conclusive) and would like to see a reorganised and more focused article. As all 3 referees are nevertheless in favour of inviting a revision for EMBO Molecular Medicine we would like to do so. We understand that addressing all in vivo experimentations requested might be too much time consuming and/or not readily possible due to high animal lethality. We would still encourage you to address as much as you can, but concentrate in the key assays that would greatly improve the conclusiveness and clinical appeal of the findings.

Revised manuscripts should be submitted within three months of a request for revision; they will otherwise be treated as new submissions, except under exceptional circumstances in which a short extension is obtained from the editor. In this case, as in vivo experiments are requested, let us know as soon as possible should you expect delays.

Please note that it is EMBO Molecular Medicine policy to allow only a single round of revision and that, as acceptance or rejection of the manuscript will depend on another round of review, your

responses should be as complete as possible. EMBO Molecular Medicine has a "scooping protection" policy, whereby similar findings that are published by others during review or revision are not a criterion for rejection. Should you decide to submit a revised version, I do ask that you get in touch after three months if you have not completed it, to update us on the status.

Please also contact us as soon as possible if similar work is published elsewhere. If other work is published we may not be able to extend the revision period beyond three months.

Please read below for important editorial formatting and consult our author's guidelines.

I look forward to receiving your revised manuscript.

***** Reviewer's comments *****

Referee #1 (Remarks):

In this study, ERRα and ERRγ double cardiac muscle specific knockout mice are used as a model to examine how heart defects result in poor development and growth in children with heart disease and FTT. Cardiac ERRα/γ double knockout mice have reduced IGF1 levels despite normal levels of GH. Treatment of hepatocytes with plasma from ERRα/γ double knockout mice led to reduced phosphorylation of STAT5, a downstream effector of GH receptor. Unbiased approaches were used to identify GDF15 as a potential cardiac secreted protein that modulates GH signaling and IGF1 production. Treatment of mice with GDF15 reduced liver STAT5 phosphorylation, IGF1 production, and body weight. Cardiac specific knockdown of GDF15 in cardiac ERRα/γ double knockout mice partially restores GH signaling and plasma IGF1 levels. Lastly, GDF15 levels are increased in children with heart disease, and are further increased in children that fail to thrive.

GDF15 has been identified as a biomarker of various cardiac pathologies. The current study further implicates GDF15 as a cardiac-derived endocrine hormone that mediates the communication between heart and liver during cardiac pathogenesis. In this regard, the authors have provided convincing evidence to support the conclusion. How GDF15 blocks GH signaling remains unresolved, although this might be beyond the scope of the current study.

Specific Comments

1. It's unclear how GDF15 suppress STAT5 phosphorylation without affecting JAK2 phosphorylation. Fig 1E seems to show some reduction in total STAT5 protein, which was not the case in hepatocytes in Fig. 2A. The authors should include phospho- and total protein levels of STAT5 (and JAK2) in all panels to determine whether GDF15 modulates STAT5 protein stability.
2. Along the same line, the authors should treat primary hepatocytes with GH +/- GDF15 to determine its specific and direct action in the liver. One could also examine whether GDF15 increases the activity of potential phosphatases known to de-activate STAT5.
3. Do levels of GDF15 correlate with plasma IGF1 levels in Fig. 6A?

Minor Comments

1. The title should better fit the model proposed by the authors (i.e., GDF15 as a pathological modulator of GH signaling). Based on the data provided, it is unclear whether GDF15 has a normal physiological function in modulating body growth.
2. The effect of cardiac GDF15 knockdown on plasma IGF1 levels is moderate in Fig. 5F, suggesting cardiac GDF15 may not be sufficient to rescue IGF1-related phenotypes in the context of ERRa/r double KO. Perhaps the authors could discuss other potential mechanisms (e.g., based on the serum proteomics and/or RNA-seq results).

Referee #2 (Remarks):

Using gene-targeted mice lacking estrogen-related receptor alpha and cardiac estrogen-related receptor gamma (aKOgKO mice) as a model for congenital heart disease/failure, the authors

propose that heart-derived GDF15 reduces postnatal body growth by inhibiting growth hormone signaling in the liver. This is an interesting paper, but several questions need to be addressed.

aKOgKO mice develop lethal cardiomyopathy with a median life span of 14-15 days. Previous work has shown that GDF-15 acts as a central appetite-suppressing hormone (Johnen et al. Tumor-induced anorexia and weight loss are mediated by the TGF-beta superfamily cytokine MIC-1 (=GDF15). Nat Med 2007;13:1333-40). Pair-feeding is probably not possible in the first two weeks after birth, but the authors need to discuss whether the appetite-suppressant effects of GDF15 may have contributed to the observed phenotype.

Is anything known about estrogen-related receptors in congenital heart disease?

Page 4: I am not aware of any ‚intracellular' functions of GDF15.

Page 4 (and elsewhere): authors should cite the relevant original works and more recent reviews on GDF15 plasma levels in cardiac disease. For example, the publication by Marin & Roldan, 2015 is just a brief comment on a paper. This paper with immediate relevance to the present work should be cited: Baggen et al. Prognostic value of N-terminal pro-B-type natriuretic peptide, troponin-T, and growth-differentiation factor 15 in adult congenital heart disease. Circulation 2017;135:264-79. It is not quite true that 'the organ source and biological function of increased circulating GDF15 in heart disease are unclear'. For a discussion see Wollert et al. Growth differentiation factor 15 as a biomarker in cardiovascular disease. Clin Chem 2017;63:140-51.

Page 9: it is not clear how the '8 top candidates' were selected. Not all of them are listed in Table EV2.

Page 20: the dosing regimens for GDF15 are not clear from the text. Please provide a supplementary figure to illustrate better.

The authors should treat hepatocytes with growth hormone +/- GDF15 in vitro to explore if GDF15 has a direct effect on GH signaling in hepatocytes.

Page 12: the authors propose that 'The heart synthesizes and secretes GDF15 to inhibit body growth, thereby relieving cardiac burden as well as helping the body adapt to decreased cardiac output'. Since neither 'cardiac burden' (e.g. afterload, blood pressure) nor cardiac output have been measured, this statement is very speculative.

Table EV4 is highly unusual. Patient characteristics (e.g. age, gender, diagnoses, NYHA class etc.) need to be presented for all groups. 'ICD codes' need to be removed.

Referee #3 (Remarks):

General comments:
This manuscript utilizes a previously reported mouse model of lethal cardiac dysfunction, the cardiomyocyte-specific estrogen-related receptor α and γ double knockout animal (henceforth ERR double KO), to demonstrate the impact of GDF15 of cardiac origin as a potential endocrine hormone causing growth failure through liver signaling mechanism. The data suggest an exciting and potentially novel role of the heart as an endocrine organ in growth. The results do demonstrate that GDF15, almost certainly of cardiac origin, does signal hepatic IGF-mediated pathways. The authors then measure plasma GDF15 levels in children with heart disease and suggest that elevated GDF15 is the mechanism underlying failure to thrive (FTT) in these children. However, there are many limitations to the experiments presented that cloud the interpretation making them insufficient to support this conclusion.
First, the manuscript is difficult to read. The huge amount of data presented includes far too much detail, minimally relevant, or completely extraneous information that detracts from the key points to be made. For example, in Figure 1, all data from the α-het/γKO and αKO/γHet are unnecessary and should be deleted. Only the data from the double KO are necessary in panels C-J. Panels C, F, and G can be deleted. Selection and presentation of the key and relevant results would allow the reader to focus on that information.

Second, because the double KO animals died at a median of "14-15 days" of age (page 7, lines 13-14 and Wang et al, 2015b) indicating severe morbidity at that age, inclusion of data from the surviving minority of 16 day old animals is problematic in terms on causative mechanisms. Double KO animals began to fall off the growth curves much earlier. Was SOMA analysis and data from, for example, more healthy, but with slowed growth, 10 and 13 day old animals obtained?
Third, the SOMA analysis (Table EV1, another example of excessive presentation of results) indicates substantial differences in more than 45 proteins increased by more than 1.5 fold in doubleKO animals versus "controls", including several that may reflect significant morbidity in these very ill animals, such as glucagon (consistent with hypoglycemia), IGFBF2, peptide YY, myoglobin (consistent with rhabdomyolysis), and ANF, and that were not tested in the primary hepatocyte assay and that may have influenced the FTT phenotype. What was the rationale for their exclusion? These other proteins may well have been those causing slowed growth, rather than just GDF15. A key experiment not reported would be to deplete the HMW double KO plasma of GDF15 only and assess impact in the p-STAT5 readout assay. Other increased intracellular and not normally secreted proteins, such as TIM14, may indicate substantial cell damage.
Fourth, the data shown in Figure 4 are compelling evidence that cardiac GDF15 mRNA expression increases dramatically by post-natal day 10 in the double KO animals at the time that growth failure is accelerating in these animals, whereas expression at post-natal day 3 is not statistically increased. The plasma GDF15 increase by day 10 is also impressive. The manuscript would be strengthened if cardiac mRNA, cardiac pro-GDF15 and mature GDF (by immunoblot and immunohistochemistry), and plasma GDF15 levels were all measured at multiple time points during days 3-14 (e.g. every other day) to demonstrate the correlation, kinetics, and time association with changes in growth.
Fifth, the shRNA knockdown results (Figure 5 and assessed in 10 day old animals) strongly support the critical conclusion that increased cardiac GDF15 synthesis and secretion do result in an endocrine effect in the liver, the exciting and key conclusion of this work. Improvement in weight gain was apparently not observed, however, a result which tempers the concept that increased cardiac GDF15 secretion alone is responsible for FTT. Because knockdown vectors were injected in 2 day old animals, the lack of impact on growth is surprising, especially in light of the authors comments (discussion, data not shown) that plasma GDF levels normalize by day 9. To adequately interpret this experiment, it is essential to know the kinetics of mRNA knockdown, GDF15 synthesis and secretion, and reduction on plasma GDF levels, results that are not provided. In addition, because the vector likely entered the circulation and not just the myocardium, systemic effects may have occurred, including knockdown of GDF15 synthesis in other tissues. No assessment of this possibility is provided. A further weakness of this experiment is that details of "intrapericardial" injection, a technically demanding or impossible task, and the success rate for actual knockdown are not given because all animals with "unsuccessful" knockdown are excluded. These data should be given.
The results in children with "heart disease" are problematic, given the lack of any description of the severity of heart disease and the huge scatter in the results, with several outliers that skew the results. The means, medians, and standard deviations are not given, and the figure does not provide the number or percentage of patients with values above two standard deviations. In fact, even the vast majority of patients with poor growth overlap with normal. That is, only 7/45 appear to exceed the normal range. This might suggest that, in fact, elevated plasma GDF15 is not associated with poor growth. Review of the ICD9 codes suggest that almost all have congenital heart disease (CHD) (codes 745, 746, 747) and not cardiomyopathy (425.4, only 3 patients among 70 total) and that the entire spectrum of anomalies, from trivial to life-threatening is included. Cardiac patients with other causes of FTT, such as chromosomal anomalies which are common in CHD, are not excluded. Therefore, the conclusion that GDF15 levels may be a useful biomarker in children cannot be justified by these data.
The discussion contains some inappropriate comments and does not focus on the key points. For example, the statement (page 12, lines 2-3), "However, pediatric heart disease results in decreased cardiac function that fails to match these increased demands" is far too broad and factually incorrect. Actually, most pediatric heart disease, especially CHD, does not cause symptoms and does not have decreased cardiac function/output.

Similarly, the statement (page 13, last two lines) "This is in contrast to most other heart disease animal models whose late-onset nature or early embryonic/neonatal lethality prohibited the chance to study the pediatric period." Is also incorrect. There are many mouse models that would allow examination in this same time frame.

These limitations detract from the key conclusions, which are reasonably well supported. First, GDF15 is synthesized in the heart, induced in this mouse model, and does serve an endocrine role to signal hepatocytes. Second, this pathway may play a role in overall growth. These are important and exciting.

However, the data do not support the authors' conclusion that cardiac GDF15 is the only factor altering growth in the mouse model and certainly not in children with heart disease.

Specific comments:
1. Introduction, page 3, line 6. A key endocrine organ to add to the list is the intestine.
2. Figure EV 1A, a "cartoon" of growth hormone signaling is superfluous, but could be part of a concluding figure to emphasize role of GDF15 in growth, e.g. Figure 6B
3. The key component of the data is hepatic phosphorylated stat-5 levels, as shown in figure 1E (10 day old) and Figure EV1, panel E (16 days).
4. All other panels in Figure EV1 are adequately described in the text and can be deleted.

1st Revision - authors' response 23 April 2017

Referee #1 (Remarks):

In this study, ERRα and ERRγ double cardiac muscle specific knockout mice are used as a model to examine how heart defects result in poor development and growth in children with heart disease and FTT. Cardiac ERRα/γ double knockout mice have reduced IGF1 levels despite normal levels of GH. Treatment of hepatocytes with plasma from ERRα/γ double knockout mice led to reduced phosphorylation of STAT5, a downstream effector of GH receptor. Unbiased approaches were used to identify GDF15 as a potential cardiac secreted protein that modulates GH signaling and IGF1 production. Treatment of mice with GDF15 reduced liver STAT5 phosphorylation, IGF1 production, and body weight. Cardiac specific knockdown of GDF15 in cardiac ERRα/γ double knockout mice partially restores GH signaling and plasma IGF1 levels. Lastly, GDF15 levels are increased in children with heart disease, and are further increased in children that fail to thrive.

GDF15 has been identified as a biomarker of various cardiac pathologies. The current study further implicates GDF15 as a cardiac-derived endocrine hormone that mediates the communication between heart and liver during cardiac pathogenesis. In this regard, the authors have provided convincing evidence to support the conclusion. How GDF15 blocks GH signaling remains unresolved, although this might be beyond the scope of the current study.

Response: We thank the reviewer for his/her valuable suggestions and positive comment that we have provided convincing evidence to support the conclusion.

Specific Comments
1. It's unclear how GDF15 suppress STAT5 phosphorylation without affecting JAK2 phosphorylation. Fig 1E seems to show some reduction in total STAT5 protein, which was not the case in hepatocytes in Fig. 2A. The authors should include phospho- and total protein levels of STAT5 (and JAK2) in all panels to determine whether GDF15 modulates STAT5 protein stability.

Response: We appreciate the reviewer's point. We have included new data of phospho- and total levels of STAT5 and JAK2 (via Western blot or ELISA) in our revised manuscript as suggested. The Western blot in Fig 1E included only 3-4 mice per genotype due to PAGE gel space limit. The ELISA-based measurement allowed us to include all samples available and determine statistical significance. This new result shows that there is no significant difference in total liver STAT5, phospho JAK2 and total JAK2 in αKOγKO mice (new Fig 1F). Similar results are seen in another age of αKOγKO mice (new Fig EV1C) and in GDF15 treated mice (new Fig 3B).

2. Along the same line, the authors should treat primary hepatocytes with GH +/- GDF15 to determine its specific and direct action in the liver. One could also examine whether GDF15 increases the activity of potential phosphatases known to de-activate STAT5.

Response: We agree with the reviewer and performed the experiment in mouse primary hepatocytes as suggested (new Fig 3H). The results show that GDF15 inhibits GH signaling in mouse primary hepatocytes, suggesting that GDF15 directly acts on the liver.
STAT5 is known to be dephosphorylated by several protein tyrosine phosphatases (PTP) (https://www.ncbi.nlm.nih.gov/pubmed/12615921, https://www.ncbi.nlm.nih.gov/pubmed/14637146). We therefore measured PTP family phosphatases activities in mouse primary hepatocytes as suggested. Our results suggest that GDF15 does not directly change PTP activity in this experimental condition (new Fig EV3H).

3. Do levels of GDF15 correlate with plasma IGF1 levels in Fig. 6A?

Response: We thank the reviewer for this comment. Following the reviewer's suggestion, we measured plasma IGF1 concentrations in the same clinical samples. The children with both heart disease and FTT have about 10% lower average plasma IGF1 levels (2684±247 pg/ml) compared to those with heart disease and normal body weight (2978±850 pg/ml). This is consistent with our finding that GDF15 inhibits IGF1 production, although we note that this difference is not statistically significant, potentially due to small sample size and relatively large variation among samples (IGF1 is known to be sensitive to many other factors such as nutritional status, https://www.ncbi.nlm.nih.gov/pubmed/26844335).

Minor Comments

1. The title should better fit the model proposed by the authors (i.e., GDF15 as a pathological modulator of GH signaling). Based on the data provided, it is unclear whether GDF15 has a normal physiological function in modulating body growth.

Response: We appreciate the reviewer's comment. We respectfully point out that GDF15 can modulate WT mice body growth (Fig 3G) in normal, physiological growing conditions. Our findings support GDF15 as a heart-derived hormone based on hormone definition from both professional endocrine organizations (http://www.endocrine.org/news-room/glossary/g-to-hypoglycemia, https://www.endocrinology.org/about-us/what-is-endocrinology) and esteemed dictionaries (https://www.merriam-webster.com/dictionary/hormone).
We therefore respectfully suggest that we keep our current title because it best summarizes the most important and novel findings of this study, that GDF15 is a heart-derived hormone and it regulates body growth.

2. The effect of cardiac GDF15 knockdown on plasma IGF1 levels is moderate in Fig. 5F, suggesting cardiac GDF15 may not be sufficient to rescue IGF1-related phenotypes in the context of ERRa/r double KO. Perhaps the authors could discuss other potential mechanisms (e.g., based on the serum proteomics and/or RNA-seq results).

Response: We thank the reviewer for the suggestion. We have included discussion of other potential mechanisms in our revised manuscript as suggested (page 15, highlighted).

Referee #2 (Remarks):

Using gene-targeted mice lacking estrogen-related receptor alpha and cardiac estrogen-related receptor gamma (aKOgKO mice) as a model for congenital heart disease/failure, the authors propose that heart-derived GDF15 reduces postnatal body growth by inhibiting growth hormone signaling in the liver. This is an interesting paper, but several questions need to be addressed.

Response: We thank the reviewer for his/her insightful suggestions and comment that our paper is interesting.

aKOgKO mice develop lethal cardiomyopathy with a median life span of 14-15 days. Previous work has shown that GDF-15 acts as a central appetite-suppressing hormone (Johnen et al. Tumor-induced anorexia and weight loss are mediated by the TGF-beta superfamily cytokine MIC-1 (=GDF15). Nat Med 2007;13:1333-40). Pair-feeding is probably not possible in the first

two weeks after birth, but the authors need to discuss whether the appetite-suppressant effects of GDF15 may have contributed to the observed phenotype.

Response: Johnen et al showed that GDF15 suppressed appetite at least partially by reducing NPY and increasing POMC expression in adult mouse hypothalami. We measured hypothalamic NPY and POMC expression in our cardiac αKOγKO mice and in GDF15-injected young WT mice, and observed no change (new Fig EV1B and Fig EV3C). Of note the appetite-regulating neural circuits in the hypothalamus in these young mice (1-2 weeks old) are still developing and remain functionally immature compared to those in adult mice (https://www.ncbi.nlm.nih.gov/pubmed/15804403). We think this is probably why we did not observe NPY and POMC expression changes in young mice upon GDF15 treatment. We therefore believe that the appetite-suppressant effects of GDF15 in adult mice are unlikely to contribute to the slow body growth of cardiac αKOγKO mice. We have included these discussions and new data in our revised manuscript (page 13-14 highlighted, new Fig EV1B and EV3C).

Is anything known about estrogen-related receptors in congenital heart disease?

Response: Although decreased expression of ERRα and its target genes have been associated with heart failure (https://www.ncbi.nlm.nih.gov/pubmed/19061896), to our knowledge there are no mutations of ERR associated with human congenital heart disease. We previously demonstrated that only loss of all 4 alleles of ERRα and ERRγ results in heart failure (http://www.ncbi.nlm.nih.gov/pubmed/25624346), which is presumably rare.

Page 4: I am not aware of any ‚intracellular' functions of GDF15.

Response: There is one recent report of possible intracellular function of GDF15 (https://www.ncbi.nlm.nih.gov/pubmed/25893289). We agree with the reviewer that GDF15 most likely functions in the autocrine/paracrine fashion in the context cited in page 4. We therefore removed “intracellular” in our revised manuscript.

Page 4 (and elsewhere): authors should cite the relevant original works and more recent reviews on GDF15 plasma levels in cardiac disease. For example, the publication by Marin & Roldan, 2015 is just a brief comment on a paper. This paper with immediate relevance to the present work should be cited: Baggen et al. Prognostic value of N-terminal pro-B-type natriuretic peptide, troponin-T, and growth-differentiation factor 15 in adult congenital heart disease. Circulation 2017;135:264-79. It is not quite true that 'the organ source and biological function of increased circulating GDF15 in heart disease are unclear'. For a discussion see Wollert et al. Growth differentiation factor 15 as a biomarker in cardiovascular disease. Clin Chem 2017;63:140-51.

Response: We thank the reviewer for pointing out these two references, which we have added in our revised manuscript. We apologize for the confusion regarding “the organ source and biological function of increased circulating GDF15 in heart disease are unclear”. We meant that their organ source was not rigorously determined using organ/cell type-specific GDF15 knockdown approaches as we did. The cited review (Wollert et al, Clin Chem 2017) stated that “So far, little is known about the tissues that produce GDF-15 in patients with CV disease”. We therefore rephrased this sentence accordingly to “the organ source and biological function of increased circulating GDF15 in heart disease are little known” (page 4, highlighted).

Page 9: it is not clear how the '8 top candidates' were selected. Not all of them are listed in Table EV2.

Response: We appreciate the reviewer’s point. The RNA-Seq data (Table EV2) included differentially expressed genes encoding secreted proteins in the ERRα/γ double KO hearts. However, this list may not account for candidates that affect the secretion or maturation of putative heart-derived factors. We therefore combined data from both RNA-Seq (Table EV2) and SOMAscan (Table EV1) studies. Because we were looking for heart-derived factors, we next narrowed the list to those genes that showed significantly higher expression in the heart than in other tissues such as the liver. In case of proteins with close sequence/structure/functions such as BNP

and ANP, we chose to prioritize testing one of them (BNP) first *in vivo*. We have provided these additional details in our revised manuscript (page 8-9).

Page 20: the dosing regimens for GDF15 are not clear from the text. Please provide a supplementary figure to illustrate better.

Response: We thank the reviewer for the suggestion. We have provided an illustration of the GDF15 dosing regimen (new Fig EV3A) in the revised manuscript as suggested.

The authors should treat hepatocytes with growth hormone +/- GDF15 in vitro to explore if GDF15 has a direct effect on GH signaling in hepatocytes.

Response: We agree with the reviewer and performed the experiment as suggested (new Fig 3H). The results show that GDF15 inhibits GH signaling in mouse primary hepatocytes, suggesting a direct effect. This result is included and discussed in the revised manuscript (new Fig 3H, page 9-10, highlighted).

Page 12: the authors propose that 'The heart synthesizes and secretes GDF15 to inhibit body growth, thereby relieving cardiac burden as well as helping the body adapt to decreased cardiac output'. Since neither 'cardiac burden' (e.g. afterload, blood pressure) nor cardiac output have been measured, this statement is very speculative.

Response: We thank the reviewer for the comment. We respectively point out that we have previously shown that ERRα/γ double KO mice have significantly decreased cardiac output (only 1/4 of control, measured by echocardiography, http://www.ncbi.nlm.nih.gov/pubmed/25624346). The small size and young age of ERRα/γ double KO mice make direct measurement of cardiac burden (such as blood pressure) technically challenging. Because this is the Discussion section we intended to offer our thoughts of the physiological rationale of GDF15 in coordinating body growth and pediatric heart function. We have revised this sentence to "The heart synthesizes and secretes GDF15 to inhibit body growth, thereby relieving potential extra cardiac burden as well as helping the body adapt to decreased cardiac output" following the reviewer's suggestion (page 13, highlighted).

Table EV4 is highly unusual. Patient characteristics (e.g. age, gender, diagnoses, NYHA class etc.) need to be presented for all groups. 'ICD codes' need to be removed.

Response: We apologize for this oversight. We have revised Table EV4 following the reviewer's suggestion and included information of age, gender and diagnosis in our revised manuscript. We apologize that NYHA codes for these samples are not available (most were collected a while ago), but we have included the actual underlying heart disease diagnosis for each of the child in the revised Table EV4 and hope this is acceptable.

Referee #3 (Remarks):

General comments:
This manuscript utilizes a previously reported mouse model of lethal cardiac dysfunction, the cardiomyocyte-specific estrogen-related receptor α and γ double knockout animal (henceforth ERR double KO), to demonstrate the impact of GDF15 of cardiac origin as a potential endocrine hormone causing growth failure through liver signaling mechanism. The data suggest an exciting and potentially novel role of the heart as an endocrine organ in growth. The results do demonstrate that GDF15, almost certainly of cardiac origin, does signal hepatic IGF-mediated pathways. The authors then measure plasma GDF15 levels in children with heart disease and suggest that elevated GDF15 is the mechanism underlying failure to thrive (FTT) in these children. However, there are many limitations to the experiments presented that cloud the interpretation making them insufficient to support this conclusion.

Response: We thank the reviewer for his/her valuable suggestions and comment that our data suggest an exciting and potentially novel role of the heart as an endocrine organ in growth.

First, the manuscript is difficult to read. The huge amount of data presented includes far too much detail, minimally relevant, or completely extraneous information that detracts from the key points to be made. For example, in Figure 1, all data from the α-het/γKO and αKO/γHet are unnecessary and should be deleted. Only the data from the double KO are necessary in panels C-J. Panels C, F, and G can be deleted. Selection and presentation of the key and relevant results would allow the reader to focus on that information.

Response: We appreciate the suggestions and have accordingly reorganized the data. We removed as many data as possible as suggested (except those requested by other reviewers). We respectfully point out that the livers of ERRα/γ double KO mice are genotypically ERRα KO, so it is essential to include αKOγWT mice as controls in liver studies to exclude the impact of different liver genetic backgrounds, at least when certain data (weight, gene expression, etc) were presented for the first time. We followed the reviewer's suggestion and made every effort to limit presenting these controls to minimum unless absolutely necessary (removed from later figures).

Second, because the double KO animals died at a median of "14-15 days" of age (page 7, lines 13-14 and Wang et al, 2015b) indicating severe morbidity at that age, inclusion of data from the surviving minority of 16 day old animals is problematic in terms on causative mechanisms. Double KO animals began to fall off the growth curves much earlier. Was SOMA analysis and data from, for example, more healthy, but with slowed growth, 10 and 13 day old animals obtained?

Response: We thank the reviewer for the comment. We used plasma from 16 days old mice due to technical reasons. The SOMAscan assay requires at least 75 µl plasma per sample. Only older mice allowed collection of such volume of plasma. We were very careful and made sure those 16-day-old mice used for SOMAscan analysis were not losing weight at the time (still growing but gaining less weight than controls).

Third, the SOMA analysis (Table EV1, another example of excessive presentation of results) indicates substantial differences in more than 45 proteins increased by more than 1.5 fold in double KO animals versus "controls", including several that may reflect significant morbidity in these very ill animals, such as glucagon (consistent with hypoglycemia), IGFBF2, peptide YY, myoglobin (consistent with rhabdomyolysis), and ANF, and that were not tested in the primary hepatocyte assay and that may have influenced the FTT phenotype. What was the rationale for their exclusion? These other proteins may well have been those causing slowed growth, rather than just GDF15. A key experiment not reported would be to deplete the HMW double KO plasma of GDF15 only and assess impact in the p-STAT5 readout assay. Other increased intracellular and not normally secreted proteins, such as TIM14, may indicate substantial cell damage.

Response: We thank the reviewer for the comment. We have provided additional details in the revised manuscript regarding the rationale of the selection of candidate proteins (page 8-9). Change in plasma TIM14 of cardiac ERRα/γ double KO mice was not statistically significant (Table EV1). We did not test IGFBP2 and ANF because we already tested IGFBP1 and BNP (Fig 3A), proteins with close sequence/structure/functions that exhibited even greater changes in cardiac ERRα/γ double KO mice. We did not test glucagon and peptide YY because they were barely expressed in the hearts of ERRα/γ double KO mice. Following the reviewer's suggestions we performed experiments which show that peptide YY and myoglobin does not impact GH signaling in mouse primary hepatocytes. These data are presented below for the reviewer, to keep the paper focused and concise as suggested by the reviewer.

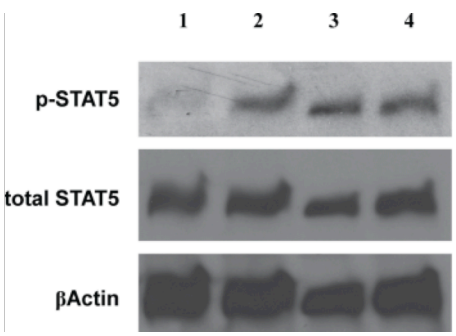

WT mouse primary hepatocytes were first treated with control, 500ng/ml myoglobin o 10ng/ml PYY for 30 min, then with 20ng/ml GH for 15 min. Phosphorylated and total STAT5 and βActin (loading control) were determined by western blot.

We agree with the reviewer that it is important to determine whether depletion of GDF15 from ERRα/γ double KO plasma would pare reduced GH signaling. We demonstrated that we can use a GDF15 antibody to specifically deplete GDF15 in ERRα/γ double KO plasma, and this GDF15 depleted ERRα/γ double KO plasma largely lost its ability to inhibit GH signaling (new Fig EV4B and C). These new data strongly support the conclusion that GDF15 is a major GH-inhibiting factor in ERRα/γ double KO plasma.

Fourth, the data shown in Figure 4 are compelling evidence that cardiac GDF15 mRNA expression increases dramatically by post-natal day 10 in the double KO animals at the time that growth failure is accelerating in these animals, whereas expression at post-natal day 3 is not statistically increased. The plasma GDF15 increase by day 10 is also impressive. The manuscript would be strengthened if cardiac mRNA, cardiac pro-GDF15 and mature GDF (by immunoblot and immunohistochemistry), and plasma GDF15 levels were all measured at multiple time points during days 3-14 (e.g. every other day) to demonstrate the correlation, kinetics, and time association with changes in growth.

Response: We agree with the reviewer that such kinetic studies would strengthen the current manuscript, and we have now generated enough mice of additional ages and performed the suggested experiments. These new data from multiple ages (about every 3 days) are now included in the revised manuscript (new Fig 4). The results show that the time course of increased heart-derived GDF15 strongly correlates with the body growth inhibition observed in ERRα/γ double KO mice.

Fifth, the shRNA knockdown results (Figure 5 and assessed in 10 day old animals) strongly support the critical conclusion that increased cardiac GDF15 synthesis and secretion do result in an endocrine effect in the liver, the exciting and key conclusion of this work. Improvement in weight gain was apparently not observed, however, a result which tempers the concept that increased cardiac GDF15 secretion alone is responsible for FTT. Because knockdown vectors were injected in 2 day old animals, the lack of impact on growth is surprising, especially in light of the authors comments (discussion, data not shown) that plasma GDF levels normalize by day 9. To adequately interpret this experiment, it is essential to know the kinetics of mRNA knockdown, GDF15 synthesis and secretion, and reduction on plasma GDF levels, results that are not provided. In addition, because the vector likely entered the circulation and not just the myocardium, systemic effects may have occurred, including knockdown of GDF15 synthesis in other tissues. No assessment of this possibility is provided.

Response: We agree with the reviewer that a kinetics study of GDF15 shRNA knockdown *in vivo* would be informative. We respectfully point out that a huge number of mice will be needed for such a kinetics study which makes it practically impossible to complete within the time allowed for the revision. To put this into perspective, it took us more than 6 months to complete such a study of one time point (10 days). For this reason we prioritized available ERRα/γ double KO mice for other critical studies suggested by the reviewers, including those addressing the 3rd and 4th points above which required many litters of mice and effectively exhausted all the mice we had during the revision period. We hope that this is acceptable.
We designed several strategies to ensure the cardiac-specific knockdown of Gdf15. First, because Gdf15 is exclusively expressed in αKOγKO mouse cardiomyocytes, we designed the AAV vector to ensure that Gdf15 shRNA is solely expressed in Cre+ cells (αKOγKO mouse cardiomyocytes, Fig 5A). Second, we used AAV9 serotype which was previously shown to achieve stable and relatively cardiac-specific expression of transgenes (http://www.ncbi.nlm.nih.gov/pubmed/18795839). Last, we directly measured Gdf15 expression in non-cardiac tissues including liver and subcutaneous fat as suggested by the reviewer, and observed no change (new Fig EV4D). These new data are included in the revised manuscript.

A further weakness of this experiment is that details of "intrapericardial" injection, a technically demanding or impossible task, and the success rate for actual knockdown are not given because all animals with "unsuccessful" knockdown are excluded. These data should be given.

Response: We thank the reviewer for this comment. We largely followed procedures previously described for mouse pericardial injection and have cited this paper which provides detailed

illustrations of the procedures. (https://www.ncbi.nlm.nih.gov/pubmed/23250337), adapting the technique to young mice without using ultrasound guidance. As quality control and based upon pre-established criteria, mice dead before 9 days of age or with unsuccessful cardiac Gdf15 knockdown (presumably due to unsuccessful injection or ineffective AAV infection) were excluded from the analysis. With these criteria, 2 of 10 αKOγKO mice that received AAV9-shGDF15 and survived to 9-10 days of age in the experiment in Fig 5 were excluded from the study (one mouse showed little change in cardiac Gdf15 expression; the other mouse has been losing weight since 6 days of age and looked very sick/dying by day 9). Similar success rate was observed in control groups. These details are now included in the Materials and Methods section of the revised manuscript.

The results in children with "heart disease" are problematic, given the lack of any description of the severity of heart disease and the huge scatter in the results, with several outliers that skew the results. The means, medians, and standard deviations are not given, and the figure does not provide the number or percentage of patients with values above two standard deviations. In fact, even the vast majority of patients with poor growth overlap with normal. That is, only 7/45 appear to exceed the normal range. This might suggest that, in fact, elevated plasma GDF15 is not associated with poor growth. Review of the ICD9 codes suggest that almost all have congenital heart disease (CHD) (codes 745, 746, 747) and not cardiomyopathy (425.4, only 3 patients among 70 total) and that the entire spectrum of anomalies, from trivial to life-threatening is included. Cardiac patients with other causes of FTT, such as chromosomal anomalies which are common in CHD, are not excluded. Therefore, the conclusion that GDF15 levels may be a useful biomarker in children cannot be justified by these data.

Response: We appreciate the reviewer's comment. We have included the means, medians, standard deviations and % of patients outside of 2 standard deviations in a revised Table EV4 as requested. When we analyze data excluding samples that fall outside of 2 standard deviations as the reviewer suggested, the conclusion remains that children with heart disease and FTT have statistically higher plasma GDF15 than controls or heart disease and normal body weight. In fact, the difference becomes more statistically significant (the numbers are shown below). We removed descriptions of GDF15 as a potential biomarker following the reviewer's suggestion.

The discussion contains some inappropriate comments and does not focus on the key points. For example, the statement (page 12, lines 2-3), "However, pediatric heart disease results in decreased cardiac function that fails to match these increased demands" is far too broad and factually incorrect. Actually, most pediatric heart disease, especially CHD, does not cause symptoms and does not have decreased cardiac function/output.

Response: We thank the reviewer for this comment and have removed this sentence in the revised manuscript.

All samples

GDF15 (pg/ml)	Control	HD normal BW	HD FTT
mean	176	304	538
median	148	216	357
Standard deviation (SD)	108	300	560
Standard error of the mean (SEM)	16	52	84
% of samples outside of 2 SD	4.5%	5.9%	4.5%
t-test (control vs HD normal BW)	0.02		
t-test (control vs HD FTT)	0.00012		
t-test (HD normal BW vs HD FTT)	0.02		

Exclude samples outside of 2 SD

GDF15 (pg/ml)	Control	HD normal BW	HD FTT
mean	159	236	445
median	145	201	335
Standard deviation (SD)	73	127	318
Standard error of the mean (SEM)	11	23	49
t-test (control vs HD normal BW)	0.002		
t-test (control vs HD FTT)	0.0000007		
t-test (HD normal BW vs HD FTT)	0.0002		

Similarly, the statement (page 13, last two lines) "This is in contrast to most other heart disease animal models whose late-onset nature or early embryonic/neonatal lethality prohibited the chance to study the pediatric period." Is also incorrect. There are many mouse models that would allow examination in this same time frame.

Response: We thank the reviewer for the comment and have removed this sentence in our revised manuscript.

These limitations detract from the key conclusions, which are reasonably well supported. First, GDF15 is synthesized in the heart, induced in this mouse model, and does serve an endocrine role to signal hepatocytes. Second, this pathway may play a role in overall growth. These are important and exciting.

Response: We thank the reviewer for his/her positive comments that our studies are important and exciting.

However, the data do not support the authors' conclusion that cardiac GDF15 is the only factor altering growth in the mouse model and certainly not in children with heart disease.

Response: We thank the reviewer for this comment and have expanded in discussion about other potential mechanisms (page 15, highlighted):

Specific comments:
1. Introduction, page 3, line 6. A key endocrine organ to add to the list is the intestine.

Response: We thank the reviewer for pointing out this oversight. We have added intestine with relevant reference in our revised manuscript (page 3, highlighted).

2. Figure EV 1A, a "cartoon" of growth hormone signaling is superfluous, but could be part of a concluding figure to emphasize role of GDF15 in growth, e.g. Figure 6B

Response: We removed the cartoon (original Fig EV1A) in our revised manuscript following the reviewer's suggestion.

3. The key component of the data is hepatic phosphorylated stat-5 levels, as shown in figure 1E (10 day old) and Figure EV1, panel E (16 days).

Response: We made every effort to reorganize Fig EV1 and it now contains only essential data or those requested by other reviewers.

4. All other panels in Figure EV1 are adequately described in the text and can be deleted.

Response: We removed as much as possible the other data (except those requested by other reviewers).

2nd Editorial Decision 03 May 2017

Thank you for the submission of your revised manuscript to EMBO Molecular Medicine. We have now received the enclosed reports from the referees that were asked to re-assess it. As you will see the reviewers are now globally supportive and I am pleased to inform you that we will be able to accept your manuscript pending the following final editorial amendments:

1) Please carefully check the authors guidelines for formatting your supplemental information: Expanded view and/or Appendix (see: http://embomolmed.embopress.org/authorguide#expandedview)

You provided a single pdf file including 4 supplemental figures and 3 supplemental tables. The simpler option would be to relabeling all as "Appendix" and within the Appendix, add a Table of Content as the 1st page, then "Appendix Figure S1" and so on, "Appendix Table S1" and so on.

Please do not forget to update the callouts in the main article file.

2) GEO accession number: please make ensure that the data is publicly available upon acceptance of the article (it is now private until 2019)

We are looking forward to receiving the revised article within 2 weeks.

***** Reviewer's comments *****

Referee #1 (Comments on Novelty/Model System):

Authors have made an effort to answer questions raised by myself and reviewer 3 (which I was asked to take a look). I think their responses are very reasonable and appropriate. I don't have additional comments.

Referee #1 (Remarks):

The authors have addressed my comments. Majority of reviewer 3' concerns have also been addressed with new experiments and/or revised data interpretation.

Referee #2 (Remarks):

The authors have adequately responded to all my previous comments. As requested by the editorial office, I also had a look at their responses to reviewer #3; here, they also responded appropriately. I feel that this manuscript can now be published.

EMBO PRESS

YOU MUST COMPLETE ALL CELLS WITH A PINK BACKGROUND ↓

PLEASE NOTE THAT THIS CHECKLIST WILL BE PUBLISHED ALONGSIDE YOUR PAPER

Corresponding Author Name: Liming Pei
Journal Submitted to: EMBO Molecular Medicine
Manuscript Number: EMM-2017-07604

Reporting Checklist For Life Sciences Articles (Rev. July 2015)

This checklist is used to ensure good reporting standards and to improve the reproducibility of published results. These guidelines are consistent with the Principles and Guidelines for Reporting Preclinical Research issued by the NIH in 2014. Please follow the journal's authorship guidelines in preparing your manuscript.

A- Figures

1. Data

The data shown in figures should satisfy the following conditions:

- the data were obtained and processed according to the field's best practice and are presented to reflect the results of the experiments in an accurate and unbiased manner.
- figure panels include only data points, measurements or observations that can be compared to each other in a scientifically meaningful way.
- graphs include clearly labeled error bars for independent experiments and sample sizes. Unless justified, error bars should not be shown for technical replicates.
- if n< 5, the individual data points from each experiment should be plotted and any statistical test employed should be justified
- Source Data should be included to report the data underlying graphs. Please follow the guidelines set out in the author ship guidelines on Data Presentation.

2. Captions

Each figure caption should contain the following information, for each panel where they are relevant:

- a specification of the experimental system investigated (eg cell line, species name).
- the assay(s) and method(s) used to carry out the reported observations and measurements
- an explicit mention of the biological and chemical entity(ies) that are being measured.
- an explicit mention of the biological and chemical entity(ies) that are altered/varied/perturbed in a controlled manner.

- the exact sample size (n) for each experimental group/condition, given as a number, not a range;
- a description of the sample collection allowing the reader to understand whether the samples represent technical or biological replicates (including how many animals, litters, cultures, etc.).
- a statement of how many times the experiment shown was independently replicated in the laboratory.
- definitions of statistical methods and measures:
  - common tests, such as t-test (please specify whether paired vs. unpaired), simple $\chi 2$ tests, Wilcoxon and Mann-Whitney tests, can be unambiguously identified by name only, but more complex techniques should be described in the methods section;
  - are tests one-sided or two-sided?
  - are there adjustments for multiple comparisons?
  - exact statistical test results, e.g., P values = x but not P values < x;
  - definition of 'center values' as median or average;
  - definition of error bars as s.d. or s.e.m.

Any descriptions too long for the figure legend should be included in the methods section and/or with the source data.

Please ensure that the answers to the following questions are reported in the manuscript itself. We encourage you to include a specific subsection in the methods section for statistics, reagents, animal models and human subjects.

In the pink boxes below, provide the page number(s) of the manuscript draft or figure legend(s) where the information can be located. Every question should be answered. If the question is not relevant to your research, please write NA (non applicable).

B- Statistics and general methods

Please fill out these boxes ↓ (Do not worry if you cannot see all your text once you press return)

1.a. How was the sample size chosen to ensure adequate power to detect a pre-specified effect size?	page 17
1.b. For animal studies, include a statement about sample size estimate even if no statistical methods were used.	page 17
2. Describe inclusion/exclusion criteria if samples or animals were excluded from the analysis. Were the criteria pre-established?	pages 18, 24
3. Were any steps taken to minimize the effects of subjective bias when allocating animals/samples to treatment (e.g. randomization procedure)? If yes, please describe.	page 17
For animal studies, include a statement about randomization even if no randomization was used.	page 17
4.a. Were any steps taken to minimize the effects of subjective bias during group allocation or/and when assessing results (e.g. blinding of the investigator)? If yes please describe.	page 17
4.b. For animal studies, include a statement about blinding even if no blinding was done	page 17
5. For every figure, are statistical tests justified as appropriate?	page 24
Do the data meet the assumptions of the tests (e.g., normal distribution)? Describe any methods used to assess it.	NA
Is there an estimate of variation within each group of data?	page 24
Is the variance similar between the groups that are being statistically compared?	page 24

C- Reagents

USEFUL LINKS FOR COMPLETING THIS FORM

http://www.antibodypedia.com
http://1degreebio.org
http://www.equator-network.org/reporting-guidelines/improving-bioscience-research-repo

http://grants.nih.gov/grants/olaw/olaw.htm
http://www.mrc.ac.uk/Ourresearch/Ethicsresearchguidance/Useofanimals/index.htm
http://ClinicalTrials.gov
http://www.consort-statement.org
http://www.consort-statement.org/checklists/view/32-consort/66-title

http://www.equator-network.org/reporting-guidelines/reporting-recommendations-for-tun

http://datadryad.org

http://figshare.com

http://www.ncbi.nlm.nih.gov/gap

http://www.ebi.ac.uk/ega

http://biomodels.net/

http://biomodels.net/miriam/
http://jjj.biochem.sun.ac.za
http://oba.od.nih.gov/biosecurity/biosecurity_documents.html
http://www.selectagents.gov/

6. To show that antibodies were profiled for use in the system under study (assay and species), provide a citation, catalog number and/or clone number, supplementary information or reference to an antibody validation profile. e.g., Antibodypedia (see link list at top right), 1DegreeBio (see link list at top right).	pages 18, 20
7. Identify the source of cell lines and report if they were recently authenticated (e.g., by STR profiling) and tested for mycoplasma contamination.	NA

* for all hyperlinks, please see the table at the top right of the document

D- Animal Models

8. Report species, strain, gender, age of animals and genetic modification status where applicable. Please detail housing and husbandry conditions and the source of animals.	page 17
9. For experiments involving live vertebrates, include a statement of compliance with ethical regulations and identify the committee(s) approving the experiments.	page 17
10. We recommend consulting the ARRIVE guidelines (see link list at top right) (PLoS Biol. 8(6), e1000412, 2010) to ensure that other relevant aspects of animal studies are adequately reported. See author guidelines, under 'Reporting Guidelines'. See also: NIH (see link list at top right) and MRC (see link list at top right) recommendations. Please confirm compliance.	page 17

E- Human Subjects

11. Identify the committee(s) approving the study protocol.	NA
12. Include a statement confirming that informed consent was obtained from all subjects and that the experiments conformed to the principles set out in the WMA Declaration of Helsinki and the Department of Health and Human Services Belmont Report.	NA
13. For publication of patient photos, include a statement confirming that consent to publish was obtained.	NA
14. Report any restrictions on the availability (and/or on the use) of human data or samples.	NA
15. Report the clinical trial registration number (at ClinicalTrials.gov or equivalent), where applicable.	NA
16. For phase II and III randomized controlled trials, please refer to the CONSORT flow diagram (see link list at top right) and submit the CONSORT checklist (see link list at top right) with your submission. See author guidelines, under 'Reporting Guidelines'. Please confirm you have submitted this list.	NA
17. For tumor marker prognostic studies, we recommend that you follow the REMARK reporting guidelines (see link list at top right). See author guidelines, under 'Reporting Guidelines'. Please confirm you have followed these guidelines.	NA

F- Data Accessibility

18. Provide accession codes for deposited data. See author guidelines, under 'Data Deposition'. Data deposition in a public repository is mandatory for: a. Protein, DNA and RNA sequences b. Macromolecular structures c. Crystallographic data for small molecules d. Functional genomics data e. Proteomics and molecular interactions	page 19
19. Deposition is strongly recommended for any datasets that are central and integral to the study; please consider the journal's data policy. If no structured public repository exists for a given data type, we encourage the provision of datasets in the manuscript as a Supplementary Document (see author guidelines under 'Expanded View' or in unstructured repositories such as Dryad (see link list at top right) or Figshare (see link list at top right).	NA
20. Access to human clinical and genomic datasets should be provided with as few restrictions as possible while respecting ethical obligations to the patients and relevant medical and legal issues. If practically possible and compatible with the individual consent agreement used in the study, such data should be deposited in one of the major public access-controlled repositories such as dbGAP (see link list at top right) or EGA (see link list at top right).	NA
21. As far as possible, primary and referenced data should be formally cited in a Data Availability section. Please state whether you have included this section. Examples: **Primary Data** Wetmore KM, Deutschbauer AM, Price MN, Arkin AP (2012). Comparison of gene expression and mutant fitness in Shewanella oneidensis MR-1. Gene Expression Omnibus GSE39462 **Referenced Data** Huang J, Brown AF, Lei M (2012). Crystal structure of the TRBD domain of TERT and the CR4/5 of TR. Protein Data Bank 4O26 AP-MS analysis of human histone deacetylase interactions in CEM-T cells (2013). PRIDE PXD000208	NA
22. Computational models that are central and integral to a study should be shared without restrictions and provided in a machine-readable form. The relevant accession numbers or links should be provided. When possible, standardized format (SBML, CellML) should be used instead of scripts (e.g. MATLAB). Authors are strongly encouraged to follow the MIRIAM guidelines (see link list at top right) and deposit their model in a public database such as Biomodels (see link list at top right) or JWS Online (see link list at top right). If computer source code is provided with the paper, it should be deposited in a public repository or included in supplementary information.	NA

G- Dual use research of concern

23. Could your study fall under dual use research restrictions? Please check biosecurity documents (see link list at top right) and list of select agents and toxins (APHIS/CDC) (see link list at top right). According to our biosecurity guidelines, provide a statement only if it could.	No